5-2022

Developing Implantable Hydrogel-Based Sensors to Measure Biomarkers in Synovial Joint Fluid Using Plain Radiography

Uthpala N. Wijayaratna
Clemson University, uwijaya@clemson.edu

DEVELOPING IMPLANTABLE HYDROGEL-BASED SENSORS TO MEASURE BIOMARKERS IN SYNOVIAL JOINT FLUID USING PLAIN RADIOGRAPHY

A Dissertation
Presented to
the Graduate School of
Clemson University

In Partial Fulfillment
of the Requirements for the Degree
Doctor of Philosophy
Chemistry

---

by
Uthpala Nawamali Wijayaratna
May 2022

Accepted by:
Dr. Jeffrey N. Anker, Committee Chair
Dr. Stephen Creager
Dr. Jason D. McNeill
Dr. Daniel Whitehead

ABSTRACT

The goal of my dissertation research is to develop implantable sensors that attaches to prosthesis prior to implantation and measures biomarkers of infection in joint fluid in order to detect, monitor and study infection using plain radiography. Joint replacement surgeries are common procedures improving the mobility and lives of millions of people worldwide. Although the surgeries are generally successful, about 1% of prosthetic hips become infected. If the infections are not detected and treated promptly with antibiotics and surgical debridement, device removal is almost always required to treat the infections. Therefore, it's important to detect post-surgery infections early and monitor the effect of therapies for effective treatment. The sensors developed in this report can be attached to prosthetic joints and enable analysis of synovial fluid biomarkers for local infection in vivo using plain radiography. The biomarkers of infection focused here are pH, carbon dioxide and viscosity of synovial fluid. The pH and carbon dioxide sensors are based on a pH responsive hydrogel, whereas the viscosity sensor is based on the velocity of a falling bead. Radiopaque markers are incorporated into the sensor to enable biochemical measurements, radiographically. The sensors can be expanded to other biomarkers of infections, as well as other disease conditions. The sensors developed provide noninvasive local chemical measurements using plain radiography which are simple, rapid, and already acquired as part of the standard of care for early detection of prosthetic joint infections.

DEDICATION

To my beloved parents

Sisira Wijayaratna and Reka Dissanayake

for their endless love and support.

ACKNOWLEDGMENTS

I would like to acknowledge the guidance, support and patience of my PhD advisor, Dr. Jeffrey Anker throughout my PhD journey. He gave me this valuable opportunity to explore interesting topics and develop my research with freedom and enthusiasm, along with his thoughtful guidance and support. I wish to thank all the people whose assistance was a milestone in the completion of this project especially my PhD committee, Drs. Stephen Creager, Jason D. McNeill, and Daniel Whitehead.

I wish to thank my friend and colleague, Sachindra Kiridena, from Dr. Anker's lab for the collaborative work we did together throughout these past few years. I would also like to thank Dr. Jeremy Tzeng for his collaborative support and valuable insight on our research over the years. I am very thankful to my fellow graduate students at Dr. Anker's group and Dr. Tzeng's group. I would also like to thank the faculty and staff in the Chemistry Department. I wish to show my gratitude to the wonderful staff at the Godley-Snell Research Center, especially Travis Pruitt, Cindy Smoak, Jessica Privett, Tina Parker for all their support and Dr. John Parish for performing the animal surgeries.

I am very thankful to my fellow graduate students at Clemson University for their support, encouragement, and friendship. I would like to extend many thanks to my parents, family and friends for their unconditional love, sacrifice, guidance, and support; without them, I wouldn't be able to accomplish this great milestone in my life.

TABLE OF CONTENTS

LIST OF FIGURES

CHAPTER ONE

INTRODUCTION

We designed implantable sensors that can be attached to hip prosthesis to detect and monitor biomarkers of infections for prosthetic joint infections using standard of care X-ray imaging. Hip replacement surgeries are performed on millions of people worldwide each year. In the United States alone, there were 450,000 total hip arthroplasties performed annually. Most of these surgeries are successful with no complications. However, infections are a leading cause of failure, with an incidence of about ~0.5-2% of total hip replacement surgeries. If detected early, these infections can be treated promptly with antibiotics and surgical debridement. However, mature biofilms usually require implant removal to treat the infection, followed by revision surgery with associated risks of morbidity, mortality, and large cost. Therefore, it's important to detect post-surgery infections early and monitor the effect of therapies for effective treatment.

X-ray imaging is ubiquitously available in hospitals, easy to use, and is part of the standard of care for many medical conditions, to show anatomical changes, especially orthopedics. Radiographs are also routinely used in preclinical research as well. However, they are usually blind to chemical concentrations, which are measured only after invasive aspiration or biopsy procedures. Alternatively, molecular imaging approaches can detect some relevant disease features, but are expensive, not available everywhere, slow compared to plain radiography. We developed implantable X-ray visualized sensors to measure local biomarkers of synovial fluid infections. The X-ray based implantable sensors

used in our studies are based on the pH responsive swelling mechanism of polyacrylic-acid hydrogels, where the hydrogel swelling moves an embedded tantalum bead relative to a scale for simple readout on X-ray. The sensors are small enough to be incorporated into various biomedical implants on the market. Unlike other implantable sensors, these devices do not use any electronics, battery, or telemetry which greatly improves reliability and makes it much easier to develop, manufacture, and integrate into clinical applications. This technology has the potential to transform biomedical research and clinical practice.

I worked in close collaboration with my colleague, Sachindra Kiridena, on developing unique X-ray based sensors for different applications including synovial fluid pH sensor for early detection of hip infections (co-first author in journal article published in Advanced Functional Materials), peritoneal fluid pH sensor for early detection of peritonitis, injectable tumor pH sensor to determine tumor acidosis, and miniaturized the sensor for imaging tumor pH heterogeneity using an array of hydrogel pillars using ultrasound and micro-computed tomography. We also worked on developing sensors based on other biomarkers for different biomedical applications related to infection and cancer including sensors for measuring carbon dioxide, C-reactive protein, glucose, viscosity, moisture, matrix metalloproteinases.

This dissertation focuses on three of the sensors for applications for early detection of prosthetic joint infections by local measurement of synovial fluid biomarkers of infection; hydrogel-based pH sensor; hydrogel-based carbon dioxide sensor; an X-ray interrogated falling bead synovial fluid viscosity sensor. These sensors can be easily attached to the prosthesis and provides useful biochemical information at the site of

infection itself. The sensor design is simple enough to be extended for any implant and can be extended for a broad range of biomarkers for different disease conditions.

The following sections in this chapter cover some background on orthopedic implant infections, it's current challenges in diagnosis and treatment, and the importance in developing X-ray visualized chemical sensors to overcome these challenges, with potential to transform orthopedic applications for detecting, monitoring, and studying implant infection.

1.1. Joint replacement surgeries

Joint replacement surgeries are life-enhancing procedures with the purpose of restoring joint function, relief from pain, and overall improvement in quality of life of patients with joint dysfunctions.[1,2] Patients undergoing joint surgery include people suffering from accidents and joint diseases like osteoarthritis, rheumatoid arthritis.[3,4] In the US alone, more than 450,000 total hip arthroplasties are performed annually.[4] During joint replacement surgeries, the patient's joint is replaced with a prosthetic implant made of a biocompatible material such as metallic alloys, ceramics, and polymers.[3] Currently, it is possible to perform total joint replacement surgeries in most of the major joints in humans, such as hip, knee, shoulder, elbow, wrist, ankle, spine, etc. using a wide range of orthopedic implants.

1.2. Prosthetic joint infections

One of the leading causes of failure following joint replacement surgery are post-surgery infections with an incidence of about ~0.2-3% of primary total hip or knee replacement surgeries.[4,5] Prosthetic joint infection refers to an infection involving the prosthesis and tissues surrounding the implant through direct contamination during surgery, hematogenous spread as a result of bacteremia related to a remote site of infection, or as a contiguous infection due to contact with an adjacent site of infection or open wound.[6,7] Complications of post-surgery infections involve prolonged hospitalization, multiple operations, significant permanent deformity, or loss of the implant. In the elderly it may result in a higher incidence of mortality as well.[5,8] Risk factors for infection include obesity, diabetes mellitus, rheumatoid arthritis, exogenous immunosuppressive medications, and malignancy.[6,9] Occurrence of prosthetic joint infections is a most challenging complication and pose significant risks for patient mobility, other morbidities and mortality (5% 2-month mortality following prosthetic joint infection in 2015),[10] as well as staggering hospital costs (cost of treatment $100,000 per episode,[11] and lifetime treatment cost for a 65-year-old is an estimated $390,806).[12] The projected total direct cost in the US in 2030 for prosthetic joint infections is $1.8 B ($753 M for hip).[13]

Infection associated with prosthetic joints are caused by microbial contamination of the prosthesis.[9,14,15] The most common cases of joint infections are caused by staphylococci species such as *Staphylococci aureus* and coagulase-negative staphylococcus species.[16] The prosthetic implant/ joint provides a surface for the attachment of microbial cells. On initial contact with blood, plasma proteins are adsorbed

onto the surface of the prosthesis forming a "conditioning film" for which microorganisms can adhere.[2,17,18] The microbes grow to form a monolayer, which later develops into a microcolony and eventually a biofilm is formed where the microbes are enclosed in a polymer matrix.[19] The biofilm protects the microbes from conventional antimicrobial agents and the host immune system, thus resulting in increased resistance to antibiotics and host immune responses.[20,21]

Prosthetic joint infections can be classified as early (1-4 weeks), delayed (3 to 24 months after surgery) or late (more than 24 months after surgery), based on the time of infection.[22] Early infections are commonly caused by virulent microorganisms, such as *S. aureus* and gram-negative bacilli, resulting in acute onset of joint pain, effusion, erythema and warmth at implant site, and fever.[23] Delayed infections are caused by less virulent microorganisms, such as coagulase-negative staphylococci and *Propionibacterium acnes*. Patients usually show subtle signs and symptoms, such as implant loosening, persistent joint pain. Early and delayed infections are usually acquired during implantation of the prosthesis. Late infections are caused by low virulence organisms such as *P. acnes* and occur mainly due to hematogenous seeding (from infections in skin, respiratory tract, dental, and urinary tract). If detected early, these infections can be treated promptly with antibiotics and surgical debridement. However, mature biofilms usually require implant removal followed by reinsertion of the medical device after the infection is eradicated. Therefore, it's important to detect post-surgery infections as early as possible for effective treatment.[24,14]

1.3. Current diagnosis of prosthetic joint infections

The diagnosis of post-surgery infections is based upon a combination of clinical findings based on nonspecific symptoms, laboratory results from peripheral blood and synovial fluid, microbiological data, histological evaluation of periprosthetic tissue, intraoperative inspection, and imaging techniques such as X-ray, magnetic resonance imaging (MRI), computed tomography (CT).[25,26] Nonspecific post-surgery infection symptoms include pain, joint swelling (effusion), warmth around the joint (erythema), fever, drainage, or the presence of a sinus tract (narrow opening or passageway underneath the skin that can extend in any direction through soft tissue and results in dead space with potential for abscess formation) communicating with the arthroplasty.[27] Laboratory tests include systemic measures of inflammation: erythrocyte sedimentation rate (ESR) greater than 30 mm/h, serum C-Reactive protein (CRP) levels greater than 10 mg/L; local measure of synovial inflammation: synovial white blood cell (WBC) count greater than 3000 cells/μL, or a synovial neutrophil differential percentage greater than 65%, synovial tissue histology greater than 5 neutrophils per high-power field on frozen section; bacterial isolation techniques including Gram stain and bacterial culture with a pathogen isolated by culture from two separate tissue or fluid samples obtained from the affected prosthetic joint or/and isolation of a microorganism in one periprosthetic tissue or fluid culture; radiographic tests including radiographs, bone scan, MRI, CT, positron emission tomography.[22,28] In order to address inconsistencies in diagnosing joint infections with these tests, the Musculoskeletal Infection Society (MSIS) published a concise definition of a prosthetic infection. It requires either one of two major criteria (sinus tract

communication with a prosthesis or a pathogen isolated by culture from two separate fluid samples), or four of six minor criteria (elevated ESR, elevated CRP, elevated WBC count, elevated synovial neutrophil differential percentage, presence of purulence, and greater than 5 neutrophils per high-power field on frozen section).[29] Although clinically useful, this definition remains complex and time consuming. In addition, there are several drawbacks of the current diagnostic methods. For example, radiographic images may indicate infection via bone erosion, implant loosening, and/or sinus tracts,[30] however, the technique lacks sensitivity and specificity for infection and cannot be used to detect early stages since bacteria are often localized to inaccessible regions on implant surfaces. MRI and CT imaging techniques are able to detect bone resorption and sinus tracts, which relate to local acidosis, but are unhelpful until later stages of infections.[31,8] Research using intraoperative pH electrode measurements have indicated that infected devices develop local acidosis from bacteria and neutrophils during infection.[32] Histological tissue examination provides high sensitivity and specificity, however neutrophil infiltration varies significantly even within the specimen and there is no accepted definition for acute infection.[26, 33] Bacterial culturing from tissue or intraoperative samples typically need at least three "positive" cultures before the area can be considered infected.[33] Therefore, it's imperative to develop more sensitive/specific methods to detect and monitor prosthetic joint infections.

1.4. Synovial fluid analysis for prosthetic joint infections

Synovial fluid is the viscous solution found in the cavities of synovial joints which are joints that allow a large range of motion and encompass wrists, knees, ankles, shoulders, and hips.[34] Synovial fluid is a highly viscous, straw colored, clear fluid which provides lubrication and nutrition to the joint. The amount of synovial fluid in normal joints varies from a few drops in small joints to several milliliters in larger joints (e.g. a normal knee joint may contain up to 3–4 mL of synovial fluid).[35]

Synovial fluid is a combination of a dialysate of blood plasma filtered through the synovial membrane and components secreted by the joint tissues. The main component of synovial fluid is hyaluronic acid (2 and 4 mg/mL in normal synovial fluid)[36,37] which is secreted by the synovial cells and polymerizes with proteins in synovial fluid to form a hyaluronic acid-protein complex that functions as a viscous lubricant within the joint.[3438] The concentrations of small molecules like electrolytes will be similar to those in plasma since it's an ultrafiltrate of plasma. However, larger molecules like proteins are present in low concentrations (25% that of plasma), unless an inflammatory condition alters vasopermeability.[39,40]

Changes in volume and composition of synovial fluid reflect changes within the joint, especially during infection. Some physical changes include change in clarity from clear to opaque (due to increased number of leukocytes), change in color (formation of pus may give an off-white color to synovial fluid), viscosity (decreases due to depolymerization of the hyaluronic acid by polymorphonuclear leukocyte enzymes). Changes in chemical composition may include elevated lactate, lactate dehydrogenase, proteins, decreased pH

and glucose levels. Therefore, synovial fluid is potentially of great diagnostic significance for joint infection diagnosis.

As discussed previously, the current standard of care detection involves systemic markers of inflammation (ESR, CRP) which do not localize the inflammation source and have poor sensitivity/specificity for implant-associated infection. In recent years, researches on post-surgery infection diagnosis have started to focus on synovial fluid instead of serum since synovial fluid is the site of primary infection and it is believed that the diagnosis should be more sensitive than that of serum, theoretically.[41] Arthrocentesis or joint aspiration is a common procedure carried out if infection is suspected. During the procedure, the joint is aspirated using a syringe to collect synovial fluid from a joint capsule. In general clinical practices, the aspirated synovial fluid is then analyzed for synovial fluid WBC count and differential, synovial tissue histology as mentioned previously. Synovial fluid analysis adds further confidence to the diagnostic of infection, avoiding unnecessary surgeries, however, none of these can be considered reliably predictive on its own.[42] Recently, large number of studies have been carried out to determine a suitable biomarker specific for prosthetic joint infections which can be used for infection diagnosis such as glucose, low pH/high lactate concentrations,[43–45] leukocyte counts,[46,47] other biomarkers of infection such as leukocyte esterase,[46,48,49] CRP,[41,46,50] interleukins,[50–52] interferon-γ,[25,50] α defensin.[53–55] However, analysis of these biomarkers also require collection of synovial fluid by arthrocentesis which is not practical for routine screening or serial monitoring during treatment, since the procedure is expensive, painful and needs to be performed by a radiologist under image guidance (such as fluoroscopy,

ultrasound, MRI or CT),[8,22] with reported complications including allergic reactions to the local anesthetic or the contrast agent used.[56] In addition, improper/inadequate fluid aspiration or delayed measurement can confound analysis and substantial dilution of synovial fluid with saline or blood during collection (caused by the presence of a hemarthrosis or a dry tap), result in poor quality synovial fluid specimens with diluted biomarkers, decreasing the sensitivity of the laboratory testing.[57,58] Therefore, there is need for the development of efficient diagnostic methods to measure local synovial fluid biomarkers to determine post-surgery infections as early as possible for effective treatment.

1.5. X-ray visualized chemical sensors for synovial fluid analysis

Physicians routinely use X-ray imaging to image anatomy and associated pathologies because they penetrate through deep tissue and show contrast between air, soft tissue, bone, and metal hardware.[59] An X-ray based sensor inserted during surgery would be painless, rapid, non-invasive, inexpensive, enable serial measurements at the same location (or locations for comparative local analysis) and fit with current standard of care. However, X-rays are usually blind to local biochemical information and insensitive to small biomechanical changes which are critical for studying, detecting, and monitoring pathologies associated with implant-associated infection.[59,60] At late stages of orthopedic-implant-associated infection, bone erosion near the implant is visible radiographically,[30] however, these features are rarely present at early stages and difficult to quantify objectively for infection monitoring. Our approach is to develop simple, passive sensors

that can be easily incorporated into implants on the market and read using plain radiography. These sensors would enable noninvasive local chemical measurements using plain radiography, which is simple, rapid, and already acquired as part of the standard of care.

Two of the sensors discussed in the dissertation are based on a stimuli responsive hydrogel which is a water-swollen biomaterial which can expand or contract in response to various physical and chemical stimuli.[62,63] Hydrogels are cross-linked hydrophilic polymers that contain large amounts of water.[62,64,65] By incorporating functional groups, a hydrogel can be made stimulus sensitive which can undergo volume changes in response to changes in stimuli (pH, temperature, light, ion concentration or electric field, etc.).[62,63] Biomedical applications of stimulus-sensitive hydrogels include controlled drug delivery, sensors, and actuators due to their good biocompatibility.[66–69] Hydrogel-based sensors usually consist of a particular stimulus-sensitive hydrogel, which is used as a sensing element, and a transducer to convert the swelling of the hydrogel.[70,71] In the presented research, a pH responsive hydrogel based on polyacrylic acid[72,73] was used for the studies and radiopaque markers were incorporated in the hydrogel in order to determine length changes radiographically.

1.6. Description of dissertation

Chapter 1 introduces the hypotheses for the research presented in this dissertation and explains the significance of research followed by a brief description of the research explained in each chapter.

Chapter 2 describes the development of an X-ray based synovial fluid pH sensor for the early detection of hip infections. The sensor was characterized in vitro, and the sensor attached to a prosthetic implant was imaged through X-ray imaging.

Chapter 3 describes modification of the pH sensor as a carbon dioxide sensor by separating the pH responsive hydrogel from the external environment by a gas permeable membrane. The sensor was characterized in vitro, and the prototype sensor was imaged through X-ray imaging. The sensor can be used to measure synovial fluid carbon dioxide levels for the early detection of hip infections.

Chapter 4 describes an X-ray based synovial fluid falling bead synovial fluid viscosity sensor for the detection of prosthetic joint infections. The sensor is based on measuring the movement of a radiopaque bead through a series of X-ray images.

Chapter 5 provides an overall summary of the research with the implications of the research. The chapter is concluded with potential directions for future studies including development of implantable sensors responsive to other biomarkers of infection for the early detection of joint infections.

1.7. References

(1) Porrino, J.; Wang, A.; Moats, A.; Mulcahy, H.; Kani, K. Prosthetic Joint Infections: Diagnosis, Management, and Complications of the Two-Stage Replacement Arthroplasty. *Skeletal Radiol.* 2020, *49* (6), 847–859. https://doi.org/10.1007/s00256-020-03389-w.

(2) Song, Z.; Borgwardt, L.; Høiby, N.; Wu, H.; Sørensen, T. S.; Borgwardt, A. Prosthesis Infections after Orthopedic Joint Replacement: The Possible Role of Bacterial Biofilms. *Orthop. Rev.* 2013, *5* (2), 14. https://doi.org/10.4081/or.2013.e14.

(3) Jin, W.; Chu, P. K. Orthopedic Implants. In *Encyclopedia of Biomedical Engineering*; Elsevier, 2019; pp 425–439. https://doi.org/10.1016/B978-0-12-801238-3.10999-7.

(4) Hip Fracture Prevention - OrthoInfo - AAOS https://www.orthoinfo.org/en/staying-healthy/hip-fracture-prevention/ (accessed 2019 -11 -21).

(5) Del Pozo, J. L.; Patel, R. Infection Associated with Prosthetic Joints. *N. Engl. J. Med.* 2009, *361* (8), 787–794. https://doi.org/10.1056/NEJMcp0905029.

(6) Pulido, L.; Ghanem, E.; Joshi, A.; Purtill, J. J.; Parvizi, J. Periprosthetic Joint Infection: The Incidence, Timing, and Predisposing Factors. *Clin. Orthop.* 2008, *466* (7), 1710–1715. https://doi.org/10.1007/s11999-008-0209-4.

(7) Tande, A. J.; Patel, R. Prosthetic Joint Infection. *Clin. Microbiol. Rev.* 2014, *27* (2), 302–345. https://doi.org/10.1128/CMR.00111-13.

(8) Abad, C. L.; Haleem, A. Prosthetic Joint Infections: An Update. *Curr. Infect. Dis. Rep.* 2018, *20* (7), 15. https://doi.org/10.1007/s11908-018-0622-0.

(9) Esposito, S.; Leone, S. Prosthetic Joint Infections: Microbiology, Diagnosis, Management and Prevention. *Int. J. Antimicrob. Agents* 2008, *32* (4), 287–293. https://doi.org/10.1016/j.ijantimicag.2008.03.010.

(10) Berbari, E. F.; Hanssen, A. D.; Duffy, M. C.; Steckelberg, J. M.; Ilstrup, D. M.; Harmsen, W. S.; Osmon, D. R. Risk Factors for Prosthetic Joint Infection: Case-Control Study. *Clin. Infect. Dis.* 1998, *27* (5), 1247–1254. https://doi.org/10.1086/514991.

(11) Kurtz, S. M.; Lau, E. C.; Son, M.-S.; Chang, E. T.; Zimmerli, W.; Parvizi, J. Are We Winning or Losing the Battle With Periprosthetic Joint Infection: Trends in Periprosthetic Joint Infection and Mortality Risk for the Medicare Population. *J. Arthroplasty* 2018, *33* (10), 3238–3245. https://doi.org/10.1016/j.arth.2018.05.042.

(12) Garfield, K.; Noble, S.; Lenguerrand, E.; Whitehouse, M. R.; Sayers, A.; Reed, M. R.; Blom, A. W. What Are the Inpatient and Day Case Costs Following Primary Total Hip Replacement of Patients Treated for Prosthetic Joint Infection: A Matched Cohort Study Using Linked Data from the National Joint Registry and Hospital Episode Statistics. *BMC Med.* 2020, *18* (1), 335. https://doi.org/10.1186/s12916-020-01803-7.

(13) Svensson, K. Diagnosis and Management of Periprosthetic Joint Infections. 2020.

(14) Premkumar, A.; Kolin, D. A.; Farley, K. X.; Wilson, J. M.; McLawhorn, A. S.; Cross, M. B.; Sculco, P. K. Projected Economic Burden of Periprosthetic Joint

Infection of the Hip and Knee in the United States. *J. Arthroplasty* 2021, *36* (5), 1484-1489.e3. https://doi.org/10.1016/j.arth.2020.12.005.

(15) Sendi, P.; Banderet, F.; Graber, P.; Zimmerli, W. Periprosthetic Joint Infection Following Staphylococcus Aureus Bacteremia. *J. Infect.* 2011, *63* (1), 17–22. https://doi.org/10.1016/j.jinf.2011.05.005.

(16) Figueiredo, A.; Ferreira, R.; Alegre, C.; Judas, F.; Fonseca, F. Diagnosis of Periprosthetic Joint Infection from from Novel Synovial Fluid Biomarkers to Identification of the Etiological Agent. *Bone Res.* 2018, *2* (4), 555594.

(17) Berbari, E. F.; Osmon, D. R.; Duffy, M. C. T.; Harmssen, R. N. W.; Mandrekar, J. N.; Hanssen, A. D.; Steckelberg, J. M. Outcome of Prosthetic Joint Infection in Patients with Rheumatoid Arthritis: The Impact of Medical and Surgical Therapy in 200 Episodes. *Clin. Infect. Dis.* 2006, *42* (2), 216–223. https://doi.org/10.1086/498507.

(18) Costerton, J. W.; Lewandowski, Z.; DeBeer, D.; Caldwell, D.; Korber, D.; James, G. Biofilms, the Customized Microniche. *J. Bacteriol.* 1994, *176* (8), 2137–2142. https://doi.org/10.1128/jb.176.8.2137-2142.1994.

(19) Arciola, C. R.; Campoccia, D.; Montanaro, L. Implant Infections: Adhesion, Biofilm Formation and Immune Evasion. *Nat. Rev. Microbiol.* 2018, *16* (7), 397–409. https://doi.org/10.1038/s41579-018-0019-y.

(20) Ribeiro, M.; Monteiro, F. J.; Ferraz, M. P. Infection of Orthopedic Implants with Emphasis on Bacterial Adhesion Process and Techniques Used in Studying

Bacterial-Material Interactions. *Biomatter* 2012, *2* (4), 176–194. https://doi.org/10.4161/biom.22905.

(21) Dunne, W. M. Bacterial Adhesion: Seen Any Good Biofilms Lately? *Clin. Microbiol. Rev.* 2002, *15* (2), 155–166. https://doi.org/10.1128/CMR.15.2.155-166.2002.

(22) Molina-Manso, D.; del Prado, G.; Ortiz-Pérez, A.; Manrubia-Cobo, M.; Gómez-Barrena, E.; Cordero-Ampuero, J.; Esteban, J. In Vitro Susceptibility to Antibiotics of Staphylococci in Biofilms Isolated from Orthopaedic Infections. *Int. J. Antimicrob. Agents* 2013, *41* (6), 521–523. https://doi.org/10.1016/j.ijantimicag.2013.02.018.

(23) Zimmerli, W.; Trampuz, A.; Ochsner, P. E. Prosthetic-Joint Infections. *N. Engl. J. Med.* 2004, *351* (16), 1645–1654. https://doi.org/10.1056/NEJMra040181.

(24) Tsukayama, D. T.; Estrada, R.; Gustilo, R. B. Infection after Total Hip Arthroplasty. A Study of the Treatment of One Hundred and Six Infections*: *J. Bone Jt. Surg.* 1996, *78* (4), 512–523. https://doi.org/10.2106/00004623-199604000-00005.

(25) Rodríguez, D.; Pigrau, C.; Euba, G.; Cobo, J.; García-Lechuz, J.; Palomino, J.; Riera, M.; del Toro, M. D.; Granados, A.; Ariza, X. Acute Haematogenous Prosthetic Joint Infection: Prospective Evaluation of Medical and Surgical Management. *Clin. Microbiol. Infect.* 2010, *16* (12), 1789–1795. https://doi.org/10.1111/j.1469-0691.2010.03157.x.

(26) Deirmengian, C.; Kardos, K.; Kilmartin, P.; Cameron, A.; Schiller, K.; Parvizi, J. Diagnosing Periprosthetic Joint Infection: Has the Era of the Biomarker Arrived?

Clin. Orthop. Relat. Res. 2014, *472* (11), 3254–3262. https://doi.org/10.1007/s11999-014-3543-8.

(27) Osmon, D. R.; Berbari, E. F.; Berendt, A. R.; Lew, D.; Zimmerli, W.; Steckelberg, J. M.; Rao, N.; Hanssen, A.; Wilson, W. R. Diagnosis and Management of Prosthetic Joint Infection: Clinical Practice Guidelines by the Infectious Diseases Society of America. *Clin. Infect. Dis.* 2013, *56* (1), e1–e25. https://doi.org/10.1093/cid/cis803.

(28) Betsch, B. Y.; Eggli, S.; Siebenrock, K. A.; Täuber, M. G.; Mühlemann, K. Treatment of Joint Prosthesis Infection in Accordance with Current Recommendations Improves Outcome. *Clin. Infect. Dis.* 2008, *46* (8), 1221–1226. https://doi.org/10.1086/529436.

(29) Saleh, A.; George, J.; Faour, M.; Klika, A. K.; Higuera, C. A. Serum Biomarkers in Periprosthetic Joint Infections. *Bone Jt. Res.* 2018, *7* (1), 85–93. https://doi.org/10.1302/2046-3758.71.BJR-2017-0323.

(30) Parvizi, J.; Zmistowski, B.; Berbari, E. F.; Bauer, T. W.; Springer, B. D.; Della Valle, C. J.; Garvin, K. L.; Mont, M. A.; Wongworawat, M. D.; Zalavras, C. G. New Definition for Periprosthetic Joint Infection: From the Workgroup of the Musculoskeletal Infection Society. *Clin. Orthop.* 2011, *469* (11), 2992–2994. https://doi.org/10.1007/s11999-011-2102-9.

(31) Cyteval, C.; Bourdon, A. Imaging Orthopedic Implant Infections. *Diagn. Interv. Imaging* 2012, *93* (6), 547–557. https://doi.org/10.1016/j.diii.2012.03.004.

(32) Ehrlich, G. D.; Stoodley, P.; Kathju, S.; Zhao, Y.; McLeod, B. R.; Balaban, N.; Hu, F. Z.; Sotereanos, N. G.; Costerton, J. W.; Stewart, P. S.; Post, J. C.; Lin, Q.

Engineering Approaches for the Detection and Control of Orthopaedic Biofilm Infections: *Clin. Orthop.* 2005, *NA;* (437), 59–66. https://doi.org/10.1097/00003086-200508000-00011.

(33) Wang, F.; Raval, Y.; Chen, H.; Tzeng, T.-R. J.; DesJardins, J. D.; Anker, J. N. Development of Luminescent PH Sensor Films for Monitoring Bacterial Growth Through Tissue. *Adv. Healthc. Mater.* 2014, *3* (2), 197–204. https://doi.org/10.1002/adhm.201300101.

(34) Hughes, H. C.; Newnham, R.; Athanasou, N.; Atkins, B. L.; Bejon, P.; Bowler, I. C. J. W. Microbiological Diagnosis of Prosthetic Joint Infections: A Prospective Evaluation of Four Bacterial Culture Media in the Routine Laboratory. *Clin. Microbiol. Infect.* 2011, *17* (10), 1528–1530. https://doi.org/10.1111/j.1469-0691.2011.03597.x.

(35) Brannan, S. R.; Jerrard, D. A. Synovial Fluid Analysis. *J. Emerg. Med.* 2006, *30* (3), 331–339. https://doi.org/10.1016/j.jemermed.2005.05.029.

(36) Bhuanantanondh, P.; Grecov, D.; Kwok, E. Rheological Study of Viscosupplements and Synovial Fluid in Patients with Osteoarthritis. *CMBES Proc.* 2010, 33.

(37) MacWilliams, P. S.; Friedrichs, K. R. Laboratory Evaluation and Interpretation of Synovial Fluid. *Vet. Clin. North Am. Small Anim. Pract.* 2003, *33* (1), 153–178. https://doi.org/10.1016/S0195-5616(02)00083-9.

(38) Ropes, M. W.; Bennett, G. A.; Bauer, W. The Origin and Nature of Normal Synovial Fluid. *J. Clin. Invest.* 1939, *18* (3), 351–372. https://doi.org/10.1172/JCI101050.

(39) Ogston, A. G.; Stanier, J. E. The Physiological Function of Hyaluronic Acid in Synovial Fluid; Viscous, Elastic and Lubricant Properties. *J. Physiol.* 1953, *119* (2–3), 244–252. https://doi.org/10.1113/jphysiol.1953.sp004842.

(40) More, S.; Kotiya, A.; Kotia, A.; Ghosh, S. K.; Spyrou, L. A.; Sarris, I. E. Rheological Properties of Synovial Fluid Due to Viscosupplements: A Review for Osteoarthritis Remedy. *Comput. Methods Programs Biomed.* 2020, *196*, 105644. https://doi.org/10.1016/j.cmpb.2020.105644.

(41) Tamer, T. M. Hyaluronan and Synovial Joint: Function, Distribution and Healing. *Interdiscip. Toxicol.* 2013, *6* (3), 111–125. https://doi.org/10.2478/intox-2013-0019.

(42) Fink, B.; Makowiak, C.; Fuerst, M.; Berger, I.; Schäfer, P.; Frommelt, L. The Value of Synovial Biopsy, Joint Aspiration and C-Reactive Protein in the Diagnosis of Late Peri-Prosthetic Infection of Total Knee Replacements. *J. Bone Joint Surg. Br.* 2008, *90-B* (7), 874–878. https://doi.org/10.1302/0301-620X.90B7.20417.

(43) Berger, P.; Van Cauter, M.; Driesen, R.; Neyt, J.; Cornu, O.; Bellemans, J. Diagnosis of Prosthetic Joint Infection with Alpha-Defensin Using a Lateral Flow Device: A Multicentre Study. *Bone Jt. J.* 2017, *99-B* (9), 1176–1182. https://doi.org/10.1302/0301-620X.99B9.BJJ-2016-1345.R2.

(44) Brook, I.; Reza, M. J.; Bricknell, K. S.; Bluestone, R.; Finegold, S. M. Synovial Fluid Lactic Acid. a Diagnostic Aid in Septic Arthritis. *Arthritis Rheum.* 1978, *21* (7), 774–779. https://doi.org/10.1002/art.1780210706.

(45) Treuhaft, P. S.; McCarty, D. J. Synovial Fluid PH, Lactate, Oxygen and Carbon Dioxide Partial Pressure in Various Joint Diseases. *Arthritis Rheum.* 1971, *14* (4), 475–484. https://doi.org/10.1002/art.1780140407.

(46) Cummings, N. A.; Nordby, G. L. Measurement of Synovial Fluid PH in Normal and Arthritic Knees. *Arthritis Rheum.* 1966, *9* (1), 47–56. https://doi.org/10.1002/art.1780090106.

(47) De Vecchi, E.; Romanò, C. L.; De Grandi, R.; Cappelletti, L.; Villa, F.; Drago, L. Alpha Defensin, Leukocyte Esterase, C-Reactive Protein, and Leukocyte Count in Synovial Fluid for Pre-Operative Diagnosis of Periprosthetic Infection. *Int. J. Immunopathol. Pharmacol.* 2018, *32*, 1–6. https://doi.org/10.1177/2058738418806072.

(48) Ward, T. T.; Steigbigel, R. T. Acidosis of Synovial Fluid Correlates with Synovial Fluid Leukocytosis. *Am. J. Med.* 1978, *64* (6), 933–936. https://doi.org/10.1016/0002-9343(78)90446-1.

(49) Wyatt, M. C.; Beswick, A. D.; Kunutsor, S. K.; Wilson, M. J.; Whitehouse, M. R.; Blom, A. W. The Alpha-Defensin Immunoassay and Leukocyte Esterase Colorimetric Strip Test for the Diagnosis of Periprosthetic Infection: A Systematic Review and Meta-Analysis. *J. Bone Jt. Surg.* 2016, *98* (12), 992–1000. https://doi.org/10.2106/JBJS.15.01142.

(50) Chen, Y.; Kang, X.; Tao, J.; Zhang, Y.; Ying, C.; Lin, W. Reliability of Synovial Fluid Alpha-Defensin and Leukocyte Esterase in Diagnosing Periprosthetic Joint

Infection (PJI): A Systematic Review and Meta-Analysis. *J. Orthop. Surg.* 2019, *14* (1), 453. https://doi.org/10.1186/s13018-019-1395-3.

(51) Deirmengian, C.; Hallab, N.; Tarabishy, A.; Della Valle, C.; Jacobs, J. J.; Lonner, J.; Booth, R. E. Synovial Fluid Biomarkers for Periprosthetic Infection. *Clin. Orthop. Relat. Res.* 2010, *468* (8), 2017–2023. https://doi.org/10.1007/s11999-010-1298-4.

(52) Lenski, M.; Scherer, M. A. Synovial IL-6 AS Inflammatory Marker in Periprosthetic Joint Infections. *J. Arthroplasty* 2014, *29* (6), 1105–1109. https://doi.org/10.1016/j.arth.2014.01.014.

(53) Keemu, H.; Vaura, F.; Maksimow, A.; Maksimow, M.; Jokela, A.; Hollmén, M.; Mäkelä, K. Novel Biomarkers for Diagnosing Periprosthetic Joint Infection from Synovial Fluid and Serum. *JBJS Open Access* 2021, *6* (2). https://doi.org/10.2106/JBJS.OA.20.00067.

(54) Bonanzinga, T.; Ferrari, M. C.; Tanzi, P.; Vandenbulcke, F.; Zahar, A.; Marcacci, M. The Role of Alpha Defensin in Prosthetic Joint Infection (PJI) Diagnosis: A Literature Review. *EFORT Open Rev.* 2019, *4* (1), 10–13. https://doi.org/10.1302/2058-5241.4.180029.

(55) Deirmengian, C.; Kardos, K.; Kilmartin, P.; Cameron, A.; Schiller, K.; Parvizi, J. Combined Measurement of Synovial Fluid &b.Alpha;-Defensin and C-Reactive Protein Levels: Highly Accurate for Diagnosing Periprosthetic Joint Infection: *J. Bone Jt. Surg.-Am. Vol.* 2014, *96* (17), 1439–1445. https://doi.org/10.2106/JBJS.M.01316.

(56) Bonanzinga, T.; Zahar, A.; Dütsch, M.; Lausmann, C.; Kendoff, D.; Gehrke, T. How Reliable Is the Alpha-Defensin Immunoassay Test for Diagnosing Periprosthetic Joint Infection? A Prospective Study. *Clin. Orthop.* 2017, *475* (2), 408–415. https://doi.org/10.1007/s11999-016-4906-0.

(57) Yee, D. K.; Chiu, K.; Yan, C.; Ng, F. Review Article: Joint Aspiration for Diagnosis of Periprosthetic Infection. *J. Orthop. Surg.* 2013, *21* (2), 236–240. https://doi.org/10.1177/230949901302100225.

(58) Deirmengian, C.; Feeley, S.; Kazarian, G. S.; Kardos, K. Synovial Fluid Aspirates Diluted with Saline or Blood Reduce the Sensitivity of Traditional and Contemporary Synovial Fluid Biomarkers. *Clin. Orthop.* 2020, *478* (8), 1805–1813. https://doi.org/10.1097/CORR.0000000000001188.

(59) Kerolus, G.; Clayburne, G.; Schumacher, H. R. Is It Mandatory to Examine Synovial Fluids Promptly after Arthrocentesis? *Arthritis Rheum.* 1989, *32* (3), 271–278. https://doi.org/10.1002/anr.1780320308.

(60) Chen, H.; Rogalski, M. M.; Anker, J. N. Advances in Functional X-Ray Imaging Techniques and Contrast Agents. *Phys. Chem. Chem. Phys.* 2012, *14* (39), 13469. https://doi.org/10.1039/c2cp41858d.

(61) Gureyev, T. E.; Mayo, S. C.; Myers, D. E.; Nesterets, Ya.; Paganin, D. M.; Pogany, A.; Stevenson, A. W.; Wilkins, S. W. Refracting Röntgen's Rays: Propagation-Based x-Ray Phase Contrast for Biomedical Imaging. *J. Appl. Phys.* 2009, *105* (10), 102005. https://doi.org/10.1063/1.3115402.

(62) Koetting, M. C.; Peters, J. T.; Steichen, S. D.; Peppas, N. A. Stimulus-Responsive Hydrogels: Theory, Modern Advances, and Applications. *Mater. Sci. Eng. R Rep.* 2015, *93*, 1–49. https://doi.org/10.1016/j.mser.2015.04.001.

(63) Ahmed, E. M. Hydrogel: Preparation, Characterization, and Applications: A Review. *J. Adv. Res.* 2015, *6* (2), 105–121. https://doi.org/10.1016/j.jare.2013.07.006.

(64) Bahram, M.; Mohseni, N.; Moghtader, M. An Introduction to Hydrogels and Some Recent Applications. In *Emerging Concepts in Analysis and Applications of Hydrogels*; Majee, S. B., Ed.; InTech, 2016. https://doi.org/10.5772/64301.

(65) Lee, B. K.; Kim, J.-R.; Park, K.; Cho, Y. W. Environment-Responsive Hydrogels for Drug Delivery. *Drug Des.* 22.

(66) Sood, N.; Bhardwaj, A.; Mehta, S.; Mehta, A. Stimuli-Responsive Hydrogels in Drug Delivery and Tissue Engineering. *Drug Deliv.* 2016, *23* (3), 748–770. https://doi.org/10.3109/10717544.2014.940091.

(67) Caló, E.; Khutoryanskiy, V. V. Biomedical Applications of Hydrogels: A Review of Patents and Commercial Products. *Eur. Polym. J.* 2015, *65*, 252–267. https://doi.org/10.1016/j.eurpolymj.2014.11.024.

(68) Aswathy, S. H.; Narendrakumar, U.; Manjubala, I. Commercial Hydrogels for Biomedical Applications. *Heliyon* 2020, *6* (4), e03719. https://doi.org/10.1016/j.heliyon.2020.e03719.

(69) Chai, Q.; Jiao, Y.; Yu, X. Hydrogels for Biomedical Applications: Their Characteristics and the Mechanisms behind Them. *Gels* 2017, *3* (1), 6. https://doi.org/10.3390/gels3010006.

(70) Farhoudi, N.; Leu, H.-Y.; Laurentius, L. B.; Magda, J. J.; Solzbacher, F.; Reiche, C. F. Smart Hydrogel Micromechanical Resonators with Ultrasound Readout for Biomedical Sensing. *ACS Sens.* 2020, *5* (7), 1882–1889. https://doi.org/10.1021/acssensors.9b02180.

(71) Richter, A.; Paschew, G.; Klatt, S.; Lienig, J.; Arndt, K.-F.; Adler, H.-J. Review on Hydrogel-Based PH Sensors and Microsensors. *Sensors* 2008, *8* (1), 561–581. https://doi.org/10.3390/s8010561.

(72) Elliott, J. E.; Macdonald, M.; Nie, J.; Bowman, C. N. Structure and Swelling of Poly(Acrylic Acid) Hydrogels: Effect of PH, Ionic Strength, and Dilution on the Crosslinked Polymer Structure. *Polymer* 2004, *45* (5), 1503–1510. https://doi.org/10.1016/j.polymer.2003.12.040.

(73) Sennakesavan, G.; Mostakhdemin, M.; Dkhar, L. K.; Seyfoddin, A.; Fatihhi, S. J. Acrylic Acid/Acrylamide Based Hydrogels and Its Properties - A Review. *Polym. Degrad. Stab.* 2020, *180*, 109308. https://doi.org/10.1016/j.polymdegradstab.2020.109308.

CHAPTER TWO

X-RAY BASED SYNOVIAL FLUID pH SENSOR FOR EARLY DETECTION OF PROSTHETIC HIP INFECTIONS

2.1. Abstract

Hip replacement surgeries are generally safe and effective, however, about 1% of prosthetic hips become infected. If infections are not detected and treated promptly, the implant must be removed followed by reinsertion of the medical device after the infection is eradicated. During infection, studies show that in a well-mixed synovial joint fluid, pH correlates with white blood cell count and pH decreases from 7.5 to around 6.7 with a threshold around 7. The sensor developed can be used to measure synovial fluid pH in order to detect and monitor hip infections using plain radiography which is already routinely acquired during patient follow up visits. The sensor was made of a pH responsive polyacrylic acid-based hydrogel, which expands at high pH and contracts at low pH. A radiodense tantalum bead and a metal wire were embedded in the two ends of the hydrogel in order to monitor the change in length of the hydrogel sensor in response to pH via plain radiography. The sensor showed a linear response and reversibility in the physiologically relevant pH range of pH 6.5 and 7.5 in both buffer and bovine synovial fluid solutions. The sensor was attached to a hip prosthetic implant and the change in length in response to pH was determined from the X-ray images by measuring the length between the tantalum bead and the radiopaque wire. Therefore, the developed sensor would enable noninvasive

detection and studying of implant hip infection using plain radiography. Much of this chapter is based on work published in Advanced Functional Materials, 2021.[1]

2.2. Introduction

Hip replacement surgeries are performed on millions of people worldwide each year. During these surgeries, the hip is surgically removed and replaced with a prosthetic component **(Figure 1a)**.[1] Successful joint replacement surgeries provide a safe and effective procedure that relieves pain, restores function and independence, thereby improving the quality of life of the patient.[2,3] Most of these joint arthroplasties are complication-free; however, one of the leading causes of failure following joint replacement surgery are post-surgery infections with an incidence of about ~0.5-2% of total hip replacement surgeries.[4,5] If detected early, these infections can potentially be treated with antibiotics and surgical debridement.[6] However, after 3 to 4 weeks, bacteria can produce biofilms that resist antibiotic treatment, which necessitates removal of prosthetic implants and then reimplantation.[2,7,8] As a result, these infections have high morbidity, mortality and financial costs. Revisions typically cost around $50,000 per patient with an estimated total hospital cost of $250 million per year to the healthcare system in USA.[9] Therefore, early detection of infections is very important for patients and the healthcare system in general.

Current diagnosis of post-surgery infections is based on a combination of clinical findings based on nonspecific symptoms, laboratory results from peripheral blood,

microbiological data, histological evaluation of periprosthetic tissue, intraoperative inspection, and imaging techniques (such as X-ray, MRI, CT).[6,10] These procedures include systemic markers of inflammation which do not localize the inflammation source and have poor sensitivity/specificity for implant-associated infection. Infection markers can be more sensitive and specific in synovial fluid (fluid around synovial joint) than in serum because they are localized to the site of infection.[11] The current standard of care involves arthrocentesis when an infection is suspected, where the joint is aspirated using a syringe to collect synovial fluid from the joint capsule and analyzed for white blood cell count and differential,[12,13] crystals, Gram stain, and culture.[14,15] In addition, the synovial fluid is composed of infection biomarkers such as glucose,[16] low pH/high lactate concentrations,[17–19] C-reactive protein,[20–22] interleukins,[23,24] interferon-γ,[10] leukocyte esterase,[25,26] α-defensin,[20,27,28] and cathelicidin[29] which can be useful for the diagnosis of infection.

Several studies show that in a well-mixed synovial joint fluid and during infection, synovial fluid pH decreases from 7.5 in aseptic conditions to 6.7-7.0.[16,30] In addition, pH correlates strongly with white blood cell count,[30,31] as well as lactic acid,[18,32] both of which are used to detect prosthetic joint infection: typical infection thresholds for synovial white blood cell count is >3000 cells/μL (sensitivity of 84% and specificity of 93%)[33] and for lactic acid is >8.3 mmol/L (sensitivity of 71.4% and specificity of 88%).[23] Acidosis results from production of acidic products as a result of metabolic activity of bacterial cells (e.g. short chain fatty acid by-products) and immune cells (e.g. lactic acid and carbon dioxide from anaerobic glycolysis activity).[15,34,35] However, arthrocentesis is not practical for routine screening or serial monitoring during treatment, since the procedure is painful and

needs to be performed by a radiologist under fluoroscopic or ultrasonic image guidance.[36,37] In addition, improper/inadequate fluid aspiration or delayed measurement can confound analysis[38,39] and reported complications include allergic reactions to the local anesthetic or the contrast agent used.[36] Numerous detection methods have been studied to measure pH in tissue during infection using imaging methods such as positron emission tomography (PET) and magnetic resonance imaging (MRI).[40,41] However, the currently available diagnostics have not been used to detect pH in synovial fluid and they lack sufficient sensitivity, specificity, and simplicity for early and effective noninvasive detection of infections.

We report the development of an X-ray based sensor inserted during surgery that could be used as a potential X-ray imaging functional chemical sensor for noninvasive detection and studying of implant infection **(Figure 1b)**. Physicians routinely use X-rays following prosthetic joint surgeries to image anatomy and associated pathologies because they penetrate through deep tissue and show contrast between air, soft tissue, bone, and metal hardware.[42,43] However, X-rays are usually blind to local biochemical information such as pH and insensitive to small biomechanical changes. Our sensor is the first sensor that is being developed to measure synovial fluid, radiographically. The sensor uses a polyacrylic-acid based hydrogel[44,45] with pH-dependent swelling to report pH in a plain radiograph via measuring the position of a radio-dense tantalum bead in the hydrogel relative to a radiodense scale next to the hydrogel (see Figure 2.1). The sensor is attached to or integrated into the prosthesis prior to surgical implantation and would provide a

painless, rapid, non-invasive, inexpensive, measurement using plain radiographs already acquired as part of the current standard of care.

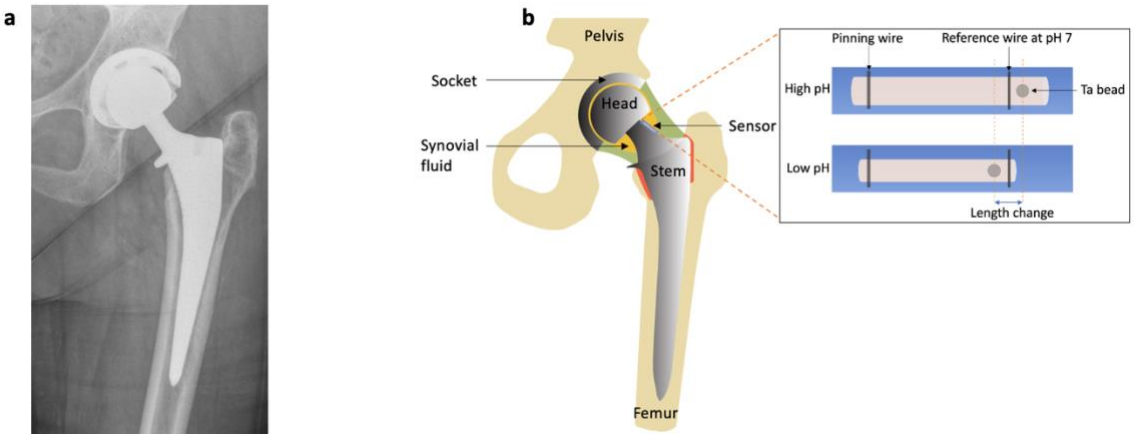

Figure 2.1: a) Radiograph of a patient with a prosthetic hip. b) Schematic diagram of prosthetic hip with attached synovial pH sensor. Inset shows the mechanism of pH sensing**.** Reproduced with permission from Reference 1, Advanced Functional Materials, 2021.

2.3. Materials and Methods

2.3.1. Materials

Acrylic acid 99% (Sigma, USA), n-octyl acrylate containing 400 ppm 4-methoxyphenol as inhibitor (Scientific Polymer Products, USA), anhydrous poly(ethylene glycol) diacrylate with average Mn 700 (Sigma, USA), 2-oxoglutaric acid (Wako Pure Chemical Industries Ltd, USA), N,N-dimethyl formamide (Sigma, USA), phosphate buffered saline (Sigma, USA), reagent alcohol (VWR, Radnor, PA), reference standard pH buffers ranging from 2 to 11 (VWR Analytical, USA) were used as received. Bovine synovial fluid was obtained from Lampire Biological Labs, Pipersville, PA. Tantalum beads (0.394 mm diameter) were

purchased from X-Medics, Frederiksberg, Denmark. Tungsten wire (diameter 0.26 mm) was purchased from McMaster-Carr, US. The polycarbonate casings for the sensor were machined by the Clemson University Machining and Technical Services. The sensor was attached to the prosthesis using Loctite Superglue Gel Control (Rocky Hill, CT).

2.3.2. Synthesis of pH sensing hydrogel

The hydrogel was prepared by free-radical co-polymerization of acrylic acid and n-octyl acrylate as the monomers, poly(ethylene glycol) diacrylate (M_n 700) as the crosslinker and 2-oxoglutaric acid as the photoinitiator, with dimethylformamide as the solvent. The photo-polymerization reaction was performed under an inert nitrogen atmosphere (Cleatech 2100-4-C glove box, Cleatech, LLC, Santa Ana, CA, with attached oxygen analyzer maintained at 0 % oxygen level and a Cleatech A21-HM-OA Nitrogen Purge controller), using UV irradiation (365 nm) from both sides of the reaction cell at a temperature of approximately 45 °C. The resulting polyacrylic acid-based hydrogel films were washed with 70% ethanol to remove any residual monomers, N,N-dimethyl formamide and hydrate the hydrogel. The hydrogel was washed daily for at least 5 days to ensure removal of unreacted monomers and initiators in the hydrogel film. Hydrogel samples of length were transferred to pH 7.4 phosphate buffered saline (PBS).

2.3.3. Calibration of pH sensing hydrogel

Hydrogel samples were fully immersed in a series of standard pH buffers ranging from 2

to 11 at room temperature (25 °C) and their size was measured photographically using the NIH ImageJ software package. Bovine synovial fluid sample (Lampire Biological Labs, Pipersville, PA) was adjusted from pH 5-9 and the response of the hydrogel sensor to pH changes in the bovine synovial fluid was studied. Prior to the experiment, the bovine synovial fluid was thawed and degassed by incubating in a water bath at 60 ˚C for 1 hour. The pH of the bovine synovial fluid was then adjusted by the addition of 1 M HCl, or 1 M NaOH as needed to reach the desired pH to be tested. The pH was measured using a pH meter (Orion™ PerpHecT™ ROSS™ Combination pH Electrode, Thermo Scientific, Beverly, MA). Hydrogel samples were then placed in bovine synovial fluid of each pH and images were taken using camera.

2.3.4. Response rate of pH sensing hydrogel

The hydrogel sensor was alternately placed in bovine synovial fluid adjusted to pH 6.5 to pH 7.5 (by the addition of 1 M HCl, or 1 M NaOH as needed) and images were taken. The size of the hydrogel sensor can be determined with NIH ImageJ software.

2.3.5. Synovial fluid pH sensor fabrication

Hydrogel with a radiodense tantalum bead (0.394 mm diameter) embedded in one end was pinned to the polycarbonate casing/ groove with a tungsten wire (diameter 0.26 mm). The groove with the hydrogel was then filled with pH 7 standard buffer and the hydrogel was

allowed to equilibrate at pH 7. Then, another tungsten wire was glued to the outside of the casing using commercially available adhesive to mark the pH 7 reference position (Loctite Superglue Gel Control, Rocky Hill, CT).

2.3.6. X-ray imaging of synovial fluid pH sensor on prosthetic hip implant

In order to determine the best position to place the sensor on the implant, the sensor (the polycarbonate casing containing the hydrogel with radiopaque markers) was placed on a prosthetic hip implant at different locations and X-ray images were taken at 80 keV using projection X-ray imaging/ plain radiography (NEXT Equine DR II portable digital radiography system, Carlsbad, CA, with a battery powered veterinary X-ray generator, Oberhausen-Germany). The sensor was then placed at the neck of the prosthesis and tested at pH 6.5 and 7.5 by changing the solution in the groove and allowed to equilibrate in the solution for 30 minutes, after which an X-ray image was taken, and length measurements were analyzed using NIH ImageJ software.

2.3.7. Interobserver reliability of synovial fluid pH sensor

Fifteen radiographs of sensor attached to the prosthetic implant in bovine synovial fluid between pH 6 and 8.5 were given to five observers. The order was randomized and each observer measured length of the sensor for each radiograph using NIH ImageJ software. The length measurements were then converted to pH using the developed calibration graph of length of hydrogel versus pH. 2.4.

Results and Discussion

2.4.1. Synthesis of pH sensing hydrogel

Hydrogels are a group of water-swollen polymeric materials that exhibit reversible volume changes in response to environmental changes such as changes in pH, temperature, electric field and light.[46–48] These stimuli-responsive hydrogels are commonly used as smart soft materials in the fabrication of sensors and drug delivery systems. Since we are interested in measuring pH, we selected a hydrogel based on polyacrylic acid due to its pH response and high biocompatibility (e.g. used in diapers, cosmetics, and medical implants).[49–51] Polyacrylic acid is reported to be stable, nontoxic, non-inflammatory, and with the ability to mimic tissues surrounding bone. Polyacrylic acid coatings have been previously studied for use in preventing corrosion on titanium and other metallic implants.[52] Polyethylene glycol (PEG)/polyacrylic acid devices have also been investigated in a rabbit model for use as corneal implants.[53] The hydrogel was prepared by free-radical copolymerization of monomers acrylic acid and n-octyl acrylate (which shifts the effective pK_a and calibration curve closer to neutral pH).[44,45,54] The resulting polymer chains were crosslinked using poly(ethylene glycol) diacrylate as crosslinker and 2-oxoglutaric acid as photoinitiator. Photopolymerization in an inert atmosphere under UV light (365 nm) produced the hydrogel films used for the sensor fabrication.

2.4.2. Calibration of pH sensing hydrogel

In order to determine the pH response and effective pK_a of the hydrogel films, a pH calibration was carried out by placing the hydrogel in a series of pH buffer standards (VWR Analytical, USA) and measuring its length. The results showed that the swelling behavior of the polyacrylic acid-based hydrogel is highly dependent on the pH of the surrounding medium due to the presence of carboxylic acid side groups (**Figure 1**). At low pH, the carboxylic acid (–COOH) groups in the polyacrylic acid hydrogel chains of the network are neutral. At high pH, the carboxylic acid groups get deprotonated and become negatively charged carboxylate ions ($–COO^–$).[55] The increased ionization in more alkaline environments causes the hydrogel to swell due to a combination of increased electrostatic repulsions between bound charges on the polymer chains and increased osmotic pressure.[44,45] A radiodense tantalum bead and a metal wire were embedded in the two ends of the hydrogel to monitor the change in length of the hydrogel sensor in response to pH via plain radiography.

The calibration curve was fitted to a modified Henderson–Hasselbach equation with the degree of swelling assumed to be proportional to the fraction of negatively charged (deprotonated) carboxyl groups (α) (equation 2.1 and 2.2). In the equations, pK_a is the acid dissociation constant of polyacrylic acid, prefactor n is added to account for the distribution of dissociation constants, and α is the fraction of negatively charged (deprotonated) carboxyl groups, d_e is the equilibrium diameter of hydrogel, d_{max} and d_{min} are the maximum and minimum diameters of the hydrogel, respectively. From the calibration graph in Figure 2.2, the pK_a of the synthesized hydrogel was 5.56 and n value of 2.50. Similar results were observed when the experiment was repeated in bovine synovial fluid in the physiologically relevant pH.

$$pH = pK_a + n \log \frac{\alpha}{1-\alpha} \qquad (2.1)$$

$$d_e = \frac{d_{max} \times 10^{(pH-pK_a)/n} + d_{min}}{1 + 10^{(pH-pK_a)/n}} \qquad (2.2)$$

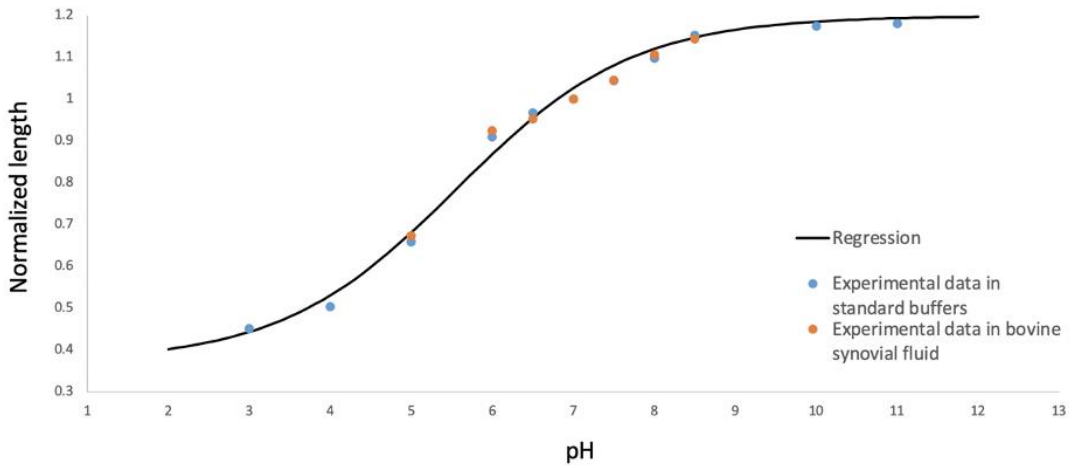

Figure 2.2: pH response of the polyacrylic acid hydrogel pH 2 to 11. Reproduced with permission from Reference 1, Advanced Functional Materials, 2021.

2.4.3. Response rate of pH sensing hydrogel

The sensor response time and reversibility were studied in bovine synovial fluid by adjusting the synovial fluid to pH 6.5 and 7.5, the pH range relevant to infection. As seen in Figure 2.3**,** the sensor showed a high reversibility in bovine synovial fluid under repeated cycles and no significant drift. The lack of drift (here and also after incubation in synovial fluid for days) is expected because it is an equilibrium-based sensor and is in contrast to most pH electrodes, which are highly sensitive to surface biofouling because they measure non-equilibrium current through the surface. The results in bovine synovial fluid were also

similar to that observed in buffers. We also previously showed that the same hydrogel swelling was minimally affected by physiological variation in buffer and tryptic soy broth bacterial culture ionic strength, temperature (25-40 ˚C), or long term incubation in a highly oxidative environment with hydrogen peroxide and copper ions.[56]

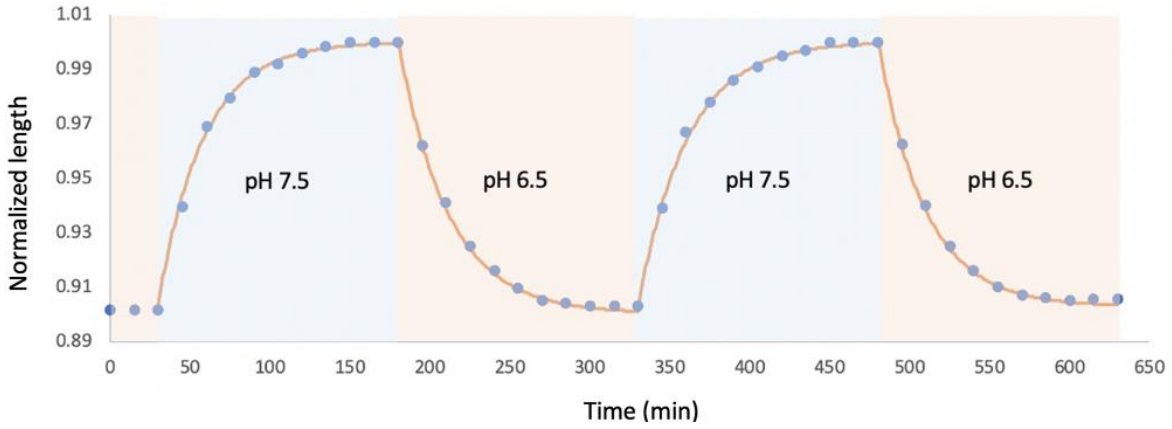

Figure 2.3: Reversibility of polyacrylic acid hydrogel in bovine synovial fluid cyclically varied between pH 6.5 and 7.5. Lines show fit to an exponential (t=30 min). Reproduced with permission from Reference 1, Advanced Functional Materials, 2021.

The swelling and deswelling cycles were fit to an exponential decay and had a time constant of around 30 minutes. Compared to buffer solutions, synovial fluid rates were slower likely due to increase in viscosity; however, since the lateral diffusion rate scales with the diameter squared, we reduced the diameter by half and found 30-minute response time. Although many physiological responses will be slow, on the order or hours or days, a faster rate is important for facilitating in vitro experiments; 30-minute rates would be

appropriate for studying acute changes (e.g., after a glucose spike especially in diabetic patients), while slower response rates find average response.

2.4.4. Synovial fluid pH sensor fabrication

In order for the hydrogel length changes to measured radiographically, radiopaque markers were used to mark the two ends of the hydrogel. Since hydrogels are fragile, in order to prevent damage for in vivo studies, a polycarbonate casing was used to hold the hydrogel (Figure 2.4**)**. Polycarbonate is widely used in biomedical applications such as in blood oxygenators and blood reservoirs in cardiac surgery products, filter cartridges for renal dialysis and surgical instruments due to its biocompatibility, glass like clarity, high strength, and impact resistance.[57,58] A hydrogel with a radiopaque tantalum bead at one end was pinned to the polycarbonate casing using a radiopaque tungsten wire. After equilibrating the sensor at pH 7, the position of the hydrogel at pH 7 was marked by another piece of tungsten wire. The sensor is therefore composed of the pH responsive hydrogel, radiopaque markers (pinning wire, reference wire and bead at end of hydrogel) and the polycarbonate casing.

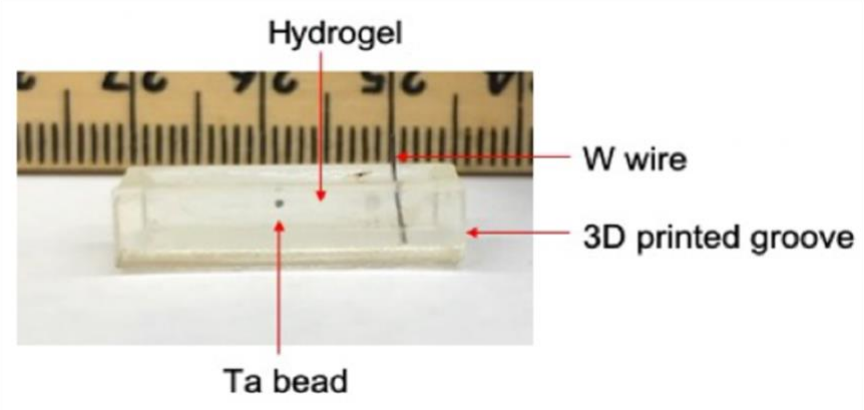

Figure 2.4: Photograph of sensor with hydrogel and radiopaque markers.

2.4.5. X-ray imaging of synovial fluid pH sensor on prosthetic hip implant

The sensor (hydrogel with radiopaque markers in the polycarbonate casing) was attached to the neck of the hip prosthetic implant (Figure 2.5a). so that the sensor would be in contact with synovial fluid but away from pressure bearing surfaces. The radiographs clearly showed the implant and the sensor position (Figure 2.5b). The change in length in response to pH can be determined from the X-ray images by measuring the length between the tantalum bead and the radiopaque wire. At pH 7.5, the bead could clearly be seen passing the pH 7 marker wire, while at pH 6.5, the bead was clearly before the marker (Figure 2.5c).

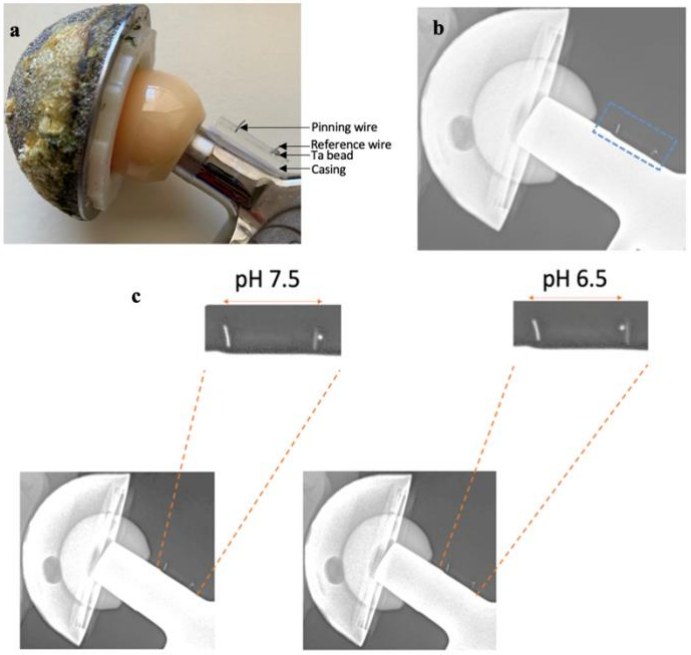

Figure 2.5: a) Photograph of hip prosthesis with attached pH sensor. b) Radiograph of hip prosthesis with attached pH sensor. c) Sensor on implant at 7.5 and 6.5 in bovine synovial

fluid. Reproduced with permission from Reference 1, Advanced Functional Materials, 2021.

2.4.6. Interobserver reliability of synovial fluid pH sensor

To assess inter-observer variability, five-observers were given a randomized series of 15 radiographs in bovine synovial fluid between pH 6 and 8.5 (Figure 2.6a). Each observer measured bead position and distance between pin markers as a calibrant; the relative length and a prior-data calibration curve was used to determine "measured pH." Plot of measured pH versus actual pH is shown in Figure 2.6b. The observers largely agreed with each other and with the values used in the initial calibration fit except at pH 6, where there was a 0.22 pH unit systematic error. Specifically, the average interobserver precision was 0.03 pH units and interobserver accuracy (root mean square difference from calibration fit) was 0.08 pH units (including the pH 6.0 data).

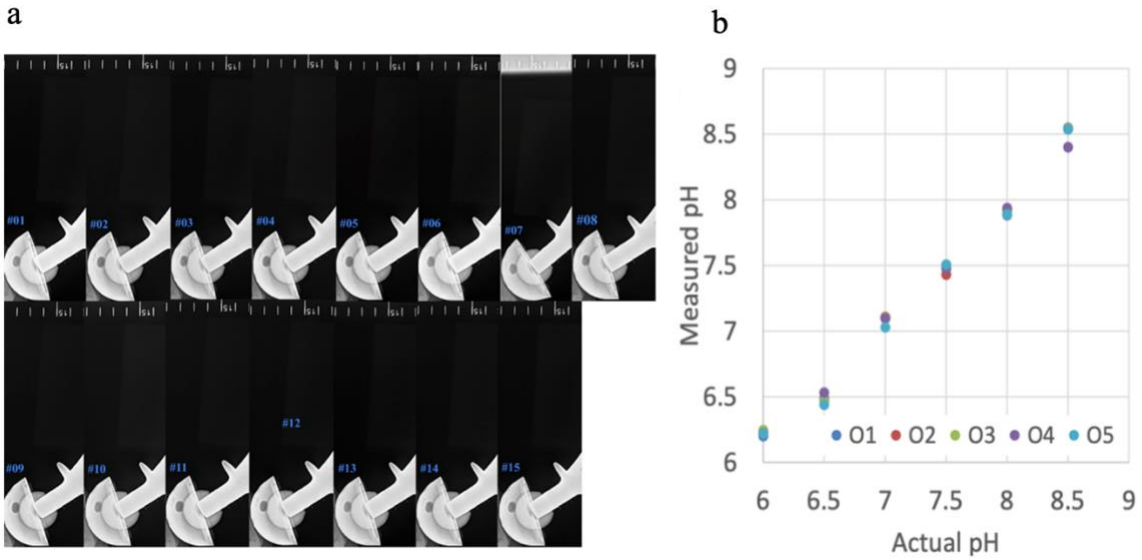

Figure 2.6: a) Randomized series of 15 radiographs in bovine synovial fluid between pH 6 and 8.5 given to five observers. b) Measured pH versus actual pH (reproduced with permission from Reference 1, Advanced Functional Materials, 2021).

2.4.7. Limitations

The study has several limitations especially with respect to ultimate clinical application. First, it was performed only in ex vivo bovine synovial fluid with added HCl and NaOH to adjust the pH (and previously in buffers and bacterial cultures with varying temperature, sodium chloride concentration, and oxidative environment).[56] The in vivo response may be different, especially after long term implantation.

Second, the experiment was performed without tissue and clothing, and with a device at a single orientation, the presence of tissue and orientation mismatch may affect the resolution. That said, the bead position is measured relative to a scale on the device which normalizes for changes in angle. We have consistently observed ≈50–100 μm resolution on several port- able X-ray systems (C-arm and portable X-rays) and with several different devices (pH sensor on orthopedic plate in cadaveric tibia,[56] orthopedic tibial plate bending indicator,[59] orthopedic screw bending sensor,[60] and a fluidic plate bending sensor).[61] This resolution appears to be mostly limited by the X-ray pixel resolution rather than device or sample. Most clinical standing X-rays are taken using equipment that includes anti-scatter grids which give better images than the equipment we are using. Additionally, the sensor resolution could be increased in future by making the

sensor longer, adding mechanical gain,[62] using computer vision algorithms to estimate bead position in place of manual measurements, or changing composition.[63,64]

Third, although there have been many infection studies measuring white blood cell counts and synovial lactate con- centration, which correlate with pH, there have only been a few studies which directly measured pH in synovial fluid after arthrocentesis,[30,32] in part because of pH drift if fluid is improperly stored.[30,38] Consequently, the sensitivity and specificity of pH would need to be evaluated clinically, especially compared to inflammation from aseptic loosening (which is also interesting but would be treated differently).[15,65] Moreover, the threshold and required resolution would depend upon the application, for example in early screening versus confirmation or monitoring.

The developed implantable sensor is expected to remain inside the body indefinitely. Two potential concerns regarding long term implantation involve potential health risks from any toxic degradation products and effect on long-term performance of the sensor. For the development of the sensor, we have selected materials that are designed for long-term implantation. Tantalum, which is used as a bead in the sensor to deter- mine the length changes of the hydrogel, can be toxic if large volumes in the form of microparticles are inhaled or when injected as an intraperitoneal injection as a chloride salt in rats (LD50 of 38 mg/kg body weight).[66] However, the bead used in the sensor is smooth, does not dissolve and has excellent anti-corrosion properties due to the presence of the stable tantalum oxide protective film formed on the surface of the metal.[67,68] Tantalum-based materials have been widely used in clinical applications as radiographic markers, in joint implants, reconstructive surgery, and in dental applications.[67,69] Tantalum containing

medical implants left in the body over long periods have been reported with no adverse health effects.[70] The polyacrylic acid based hydrogel which responds to pH, is expected to have very low degradation as well, thus minimizing the release of any toxic products. Acrylic acid polymers are widely used in drug delivery, biosensors, membrane and separation devices due to their biocompatibility and extended lifespan.[46,71] Even though shorter chain length acrylates can degrade and be excreted easily,[72,73] the hydrogels with their crosslinked polymer networks such as this, is expected to be highly resistant to degradation within the lifetime of the patient.[74,75]

For all implanted chemical sensors, sensor fouling would affect the performance of the sensor, in vivo.[76,77] Fouling is considered less of a concern for an equilibrium sensor as described here, although build-up could slow diffusion and affect the response rate. No fouling effect on the sensor calibration curve, response rate, or sensor degradation was observed in solutions of tryptic soy broth bacterial cell culture, bovine synovial fluid, bovine serum, highly oxidative hydrogen peroxide, and copper ion medium, or storage in pH 7 buffer.[56] Several studies using polyacrylic acid-based hydrogels also demonstrated the stability of these materials in vivo. However, modifications can be made to the sensor to improve the lifetime by encasing the sensor and fluid in a carbon dioxide permeable membrane such as polydimethylsiloxane, which is impermeable to aqueous molecules.[78,79] To better address these issues, we are planning future studies ex vivo in patient samples and in vivo in total hip arthroplasty sheep studies. We also plan to alter the hydrogel composition (e.g., using enzymes,[80] antibodies,[81,82] and selectively permeable

membranes)[78,83] to detect other biomarkers of infection, such as glucose,[80,84] carbon dioxide,[32] and alpha-defensin[27,28] levels.

Physicians diagnose PJI using multiple lines of evidence as mentioned above and a pH sensor to be useful, but values near the threshold around pH 7.1 may be equivocal, particularly in differentiating septic infection from aseptic inflammation. Ongoing antibiotic treatment may also lower pH response and there may be differences among microbial species. Thus, pH measurements will not always avoid arthrocentesis or other imaging techniques. Nonetheless, advantages of the sensor compared to synovial fluid analysis lie in simplicity, speed (radiographs already routinely acquired), and more reliable immersion in synovial fluid with no risk of dilution or drift between fluid removal and analysis, and easier repeated analysis.

2.5. Conclusions

In summary, we describe the first implantable sensor that measures synovial fluid pH using plain radiography. The sensor has a linear response and repeatable response within 30 min in the range of pH 6.5 and 7.5 in bovine synovial fluid solutions and a pH accuracy of 0.08 pH units. The approach is rapid, non-invasive, and uses X-rays that are already taken as part of the postoperative standard of care. Thus, the developed sensor could be used as a potential X-ray imaging functional chemical sensor to detect post-surgery hip infections.

2.6. References

(1) Wijayaratna, U. N.; Kiridena, S. D.; Adams, J. D.; Behrend, C. J.; Anker, J. N. Synovial Fluid PH Sensor for Early Detection of Prosthetic Hip Infections. *Adv. Funct. Mater.* 2021, *31* (37), 2104124. https://doi.org/10.1002/adfm.202104124.

(2) Felson, D. T. Osteoarthritis: New Insights. Part 2: Treatment Approaches. *Ann. Intern. Med.* 2000, *133* (9), 726. https://doi.org/10.7326/0003-4819-133-9-200011070-00015.

(3) Jones, C. A.; Beaupre, L. A.; Johnston, D. W. C.; Suarez-Almazor, M. E. Total Joint Arthroplasties: Current Concepts of Patient Outcomes after Surgery. *Rheum. Dis. Clin. N. Am.* 2007, *33* (1), 71–86. https://doi.org/10.1016/j.rdc.2006.12.008.

(4) Del Pozo, J. L.; Patel, R. Infection Associated with Prosthetic Joints. *N. Engl. J. Med.* 2009, *361* (8), 787–794. https://doi.org/10.1056/NEJMcp0905029.

(5) Pulido, L.; Ghanem, E.; Joshi, A.; Purtill, J. J.; Parvizi, J. Periprosthetic Joint Infection: The Incidence, Timing, and Predisposing Factors. *Clin. Orthop.* 2008, *466* (7), 1710–1715. https://doi.org/10.1007/s11999-008-0209-4.

(6) Osmon, D. R.; Berbari, E. F.; Berendt, A. R.; Lew, D.; Zimmerli, W.; Steckelberg, J. M.; Rao, N.; Hanssen, A.; Wilson, W. R. Diagnosis and Management of Prosthetic Joint Infection: Clinical Practice Guidelines by the Infectious Diseases Society of America. *Clin. Infect. Dis.* 2013, *56* (1), e1–e25. https://doi.org/10.1093/cid/cis803.

(7) Ribeiro, M.; Monteiro, F. J.; Ferraz, M. P. Infection of Orthopedic Implants with Emphasis on Bacterial Adhesion Process and Techniques Used in Studying

Bacterial-Material Interactions. *Biomatter* 2012, *2* (4), 176–194. https://doi.org/10.4161/biom.22905.

(8) Betsch, B. Y.; Eggli, S.; Siebenrock, K. A.; Täuber, M. G.; Mühlemann, K. Treatment of Joint Prosthesis Infection in Accordance with Current Recommendations Improves Outcome. *Clin. Infect. Dis.* 2008, *46* (8), 1221–1226. https://doi.org/10.1086/529436.

(9) Esposito, S.; Leone, S. Prosthetic Joint Infections: Microbiology, Diagnosis, Management and Prevention. *Int. J. Antimicrob. Agents* 2008, *32* (4), 287–293. https://doi.org/10.1016/j.ijantimicag.2008.03.010.

(10) Deirmengian, C.; Hallab, N.; Tarabishy, A.; Della Valle, C.; Jacobs, J. J.; Lonner, J.; Booth, R. E. Synovial Fluid Biomarkers for Periprosthetic Infection. *Clin. Orthop. Relat. Res.* 2010, *468* (8), 2017–2023. https://doi.org/10.1007/s11999-010-1298-4.

(11) Fink, B.; Makowiak, C.; Fuerst, M.; Berger, I.; Schäfer, P.; Frommelt, L. The Value of Synovial Biopsy, Joint Aspiration and C-Reactive Protein in the Diagnosis of Late Peri-Prosthetic Infection of Total Knee Replacements. *J. Bone Joint Surg. Br.* 2008, *90-B* (7), 874–878. https://doi.org/10.1302/0301-620X.90B7.20417.

(12) Deirmengian, C.; Lonner, J. H.; Booth, R. E. The Mark Coventry Award: White Blood Cell Gene Expression: A New Approach toward the Study and Diagnosis of Infection. *Clin. Orthop.* 2005, *440* (NA;), 38–44. https://doi.org/10.1097/01.blo.0000185756.17401.32.

(13) Garcia-Tsao, G.; Conn, H. O.; Lerner, E. The Diagnosis of Bacterial Peritonitis: Comparison of PH, Lactate Concentration and Leukocyte Count. *Hepatology* 1985, *5* (1), 91–96. https://doi.org/10.1002/hep.1840050119.

(14) Trampuz, A.; Steckelberg, J. M.; Osmon, D. R.; Cockerill, F. R.; Hanssen, A. D.; Patel, R. Advances in the Laboratory Diagnosis of Prosthetic Joint Infection: *Rev. Med. Microbiol.* 2003, *14* (1), 1–14. https://doi.org/10.1097/00013542-200301000-00001.

(15) Birlutiu, V. Diagnosis and Management of Orthopedic Implant-Associated Infection: A Comprehensive Review of the Literature. *Biomed Res* 2017, *28* (11), 11.

(16) Lenski, M.; Scherer, M. A. Diagnostic Potential of Inflammatory Markers in Septic Arthritis and Periprosthetic Joint Infections: A Clinical Study with 719 Patients. *Infect. Dis.* 2015, *47* (6), 399–409. https://doi.org/10.3109/00365548.2015.1006674.

(17) Treuhaft, P. S.; McCarty, D. J. Synovial Fluid PH, Lactate, Oxygen and Carbon Dioxide Partial Pressure in Various Joint Diseases. *Arthritis Rheum.* 1971, *14* (4), 475–484. https://doi.org/10.1002/art.1780140407.

(18) Brook, I.; Reza, M. J.; Bricknell, K. S.; Bluestone, R.; Finegold, S. M. Synovial Fluid Lactic Acid. a Diagnostic Aid in Septic Arthritis. *Arthritis Rheum.* 1978, *21* (7), 774–779. https://doi.org/10.1002/art.1780210706.

(19) Cummings, N. A.; Nordby, G. L. Measurement of Synovial Fluid PH in Normal and Arthritic Knees. *Arthritis Rheum.* 1966, *9* (1), 47–56. https://doi.org/10.1002/art.1780090106.

(20) De Vecchi, E.; Romanò, C. L.; De Grandi, R.; Cappelletti, L.; Villa, F.; Drago, L. Alpha Defensin, Leukocyte Esterase, C-Reactive Protein, and Leukocyte Count in Synovial Fluid for Pre-Operative Diagnosis of Periprosthetic Infection. *Int. J. Immunopathol. Pharmacol.* 2018, *32*, 1–6. https://doi.org/10.1177/2058738418806072.

(21) Parvizi, J.; Jacovides, C.; Adeli, B.; Jung, K. A.; Hozack, W. J. Mark B. Coventry Award: Synovial C-Reactive Protein: A Prospective Evaluation of a Molecular Marker for Periprosthetic Knee Joint Infection. *Clin. Orthop. Relat. Res.* 2012, *470* (1), 54–60. https://doi.org/10.1007/s11999-011-1991-y.

(22) Deirmengian, C.; Kardos, K.; Kilmartin, P.; Cameron, A.; Schiller, K.; Parvizi, J. Combined Measurement of Synovial Fluid &b.Alpha;-Defensin and C-Reactive Protein Levels: Highly Accurate for Diagnosing Periprosthetic Joint Infection: *J. Bone Jt. Surg.-Am. Vol.* 2014, *96* (17), 1439–1445. https://doi.org/10.2106/JBJS.M.01316.

(23) Lenski, M.; Scherer, M. A. Synovial IL-6 AS Inflammatory Marker in Periprosthetic Joint Infections. *J. Arthroplasty* 2014, *29* (6), 1105–1109. https://doi.org/10.1016/j.arth.2014.01.014.

(24) Gollwitzer, H.; Dombrowski, Y.; Prodinger, P. M.; Peric, M.; Summer, B.; Hapfelmeier, A.; Saldamli, B.; Pankow, F.; von Eisenhart-Rothe, R.; Imhoff, A. B.;

Schauber, J.; Thomas, P.; Burgkart, R.; Banke, I. J. Antimicrobial Peptides and Proinflammatory Cytokines in Periprosthetic Joint Infection. *J. Bone Jt. Surg.* 2013, *95* (7), 644–651. https://doi.org/10.2106/JBJS.L.00205.

(25) Chen, Y.; Kang, X.; Tao, J.; Zhang, Y.; Ying, C.; Lin, W. Reliability of Synovial Fluid Alpha-Defensin and Leukocyte Esterase in Diagnosing Periprosthetic Joint Infection (PJI): A Systematic Review and Meta-Analysis. *J. Orthop. Surg.* 2019, *14* (1), 453. https://doi.org/10.1186/s13018-019-1395-3.

(26) Deirmengian, C.; Kardos, K.; Kilmartin, P.; Cameron, A.; Schiller, K.; Booth, R. E.; Parvizi, J. The Alpha-Defensin Test for Periprosthetic Joint Infection Outperforms the Leukocyte Esterase Test Strip. *Clin. Orthop.* 2015, *473* (1), 198–203. https://doi.org/10.1007/s11999-014-3722-7.

(27) Bonanzinga, T.; Ferrari, M. C.; Tanzi, P.; Vandenbulcke, F.; Zahar, A.; Marcacci, M. The Role of Alpha Defensin in Prosthetic Joint Infection (PJI) Diagnosis: A Literature Review. *EFORT Open Rev.* 2019, *4* (1), 10–13. https://doi.org/10.1302/2058-5241.4.180029.

(28) Deirmengian, C.; Kardos, K.; Kilmartin, P.; Cameron, A.; Schiller, K.; Parvizi, J. Diagnosing Periprosthetic Joint Infection: Has the Era of the Biomarker Arrived? *Clin. Orthop. Relat. Res.* 2014, *472* (11), 3254–3262. https://doi.org/10.1007/s11999-014-3543-8.

(29) Shahi, A.; Parvizi, J. The Role of Biomarkers in the Diagnosis of Periprosthetic Joint Infection. *EFORT Open Rev.* 2016, *1* (7), 275–278. https://doi.org/10.1302/2058-5241.1.160019.

(30) Ward, T. T.; Steigbigel, R. T. Acidosis of Synovial Fluid Correlates with Synovial Fluid Leukocytosis. *Am. J. Med.* 1978, *64* (6), 933–936. https://doi.org/10.1016/0002-9343(78)90446-1.

(31) Park, S.-Y.; Kim, I.-S. Identification of Macrophage Genes Responsive to Extracellular Acidification. *Inflamm. Res.* 2013, *62* (4), 399–406. https://doi.org/10.1007/s00011-013-0591-6.

(32) Treuhaft, P. S.; McCarty, D. J. Synovial Fluid PH, Lactate, Oxygen and Carbon Dioxide Partial Pressure in Various Joint Diseases. *Arthritis Rheum.* 1971, *14* (4), 475–484. https://doi.org/10.1002/art.1780140407.

(33) Schinsky, M. F.; Della Valle, C. J.; Sporer, S. M.; Paprosky, W. G. Perioperative Testing for Joint Infection in Patients Undergoing Revision Total Hip Arthroplasty: *J. Bone Jt. Surg.-Am. Vol.* 2008, *90* (9), 1869–1875. https://doi.org/10.2106/JBJS.G.01255.

(34) Wang, F.; Raval, Y.; Chen, H.; Tzeng, T.-R. J.; DesJardins, J. D.; Anker, J. N. Development of Luminescent PH Sensor Films for Monitoring Bacterial Growth Through Tissue. *Adv. Healthc. Mater.* 2014, *3* (2), 197–204. https://doi.org/10.1002/adhm.201300101.

(35) Jones, E. M.; Cochrane, C. A.; Percival, S. L. The Effect of pH on the Extracellular Matrix and Biofilms. *Adv. Wound Care* 2015, *4* (7), 431–439. https://doi.org/10.1089/wound.2014.0538.

(36) Yee, D. K.; Chiu, K.; Yan, C.; Ng, F. Review Article: Joint Aspiration for Diagnosis of Periprosthetic Infection. *J. Orthop. Surg.* 2013, *21* (2), 236–240. https://doi.org/10.1177/230949901302100225.

(37) Brannan, S. R.; Jerrard, D. A. Synovial Fluid Analysis. *J. Emerg. Med.* 2006, *30* (3), 331–339. https://doi.org/10.1016/j.jemermed.2005.05.029.

(38) Deirmengian, C.; Feeley, S.; Kazarian, G. S.; Kardos, K. Synovial Fluid Aspirates Diluted with Saline or Blood Reduce the Sensitivity of Traditional and Contemporary Synovial Fluid Biomarkers. *Clin. Orthop.* 2020, *478* (8), 1805–1813. https://doi.org/10.1097/CORR.0000000000001188.

(39) Kerolus, G.; Clayburne, G.; Schumacher, H. R. Is It Mandatory to Examine Synovial Fluids Promptly after Arthrocentesis? *Arthritis Rheum.* 1989, *32* (3), 271–278. https://doi.org/10.1002/anr.1780320308.

(40) Cyteval, C.; Bourdon, A. Imaging Orthopedic Implant Infections. *Diagn. Interv. Imaging* 2012, *93* (6), 547–557. https://doi.org/10.1016/j.diii.2012.03.004.

(41) Potapova, I. Functional Imaging in Diagnostic of Orthopedic Implant-Associated Infections. *Diagnostics* 2013, *3* (4), 356–371. https://doi.org/10.3390/diagnostics3040356.

(42) Chen, H.; Rogalski, M. M.; Anker, J. N. Advances in Functional X-Ray Imaging Techniques and Contrast Agents. *Phys. Chem. Chem. Phys.* 2012, *14* (39), 13469. https://doi.org/10.1039/c2cp41858d.

(43) Uzair, U.; Benza, D.; Behrend, C. J.; Anker, J. N. Noninvasively Imaging pH at the Surface of Implanted Orthopedic Devices with X-Ray Excited Luminescence

Chemical Imaging. *ACS Sens.* 2019, *4* (9), 2367–2374. https://doi.org/10.1021/acssensors.9b00962.

(44) Philippova, O. E.; Hourdet, D.; Audebert, R.; Khokhlov, A. R. pH-Responsive Gels of Hydrophobically Modified Poly(Acrylic Acid). *Macromolecules* 1997, *30* (26), 8278–8285. https://doi.org/10.1021/ma970957v.

(45) Elliott, J. E.; Macdonald, M.; Nie, J.; Bowman, C. N. Structure and Swelling of Poly(Acrylic Acid) Hydrogels: Effect of PH, Ionic Strength, and Dilution on the Crosslinked Polymer Structure. *Polymer* 2004, *45* (5), 1503–1510. https://doi.org/10.1016/j.polymer.2003.12.040.

(46) Caló, E.; Khutoryanskiy, V. V. Biomedical Applications of Hydrogels: A Review of Patents and Commercial Products. *Eur. Polym. J.* 2015, *65*, 252–267. https://doi.org/10.1016/j.eurpolymj.2014.11.024.

(47) Ahmed, E. M. Hydrogel: Preparation, Characterization, and Applications: A Review. *J. Adv. Res.* 2015, *6* (2), 105–121. https://doi.org/10.1016/j.jare.2013.07.006.

(48) Koetting, M. C.; Peters, J. T.; Steichen, S. D.; Peppas, N. A. Stimulus-Responsive Hydrogels: Theory, Modern Advances, and Applications. *Mater. Sci. Eng. R Rep.* 2015, *93*, 1–49. https://doi.org/10.1016/j.mser.2015.04.001.

(49) Elliott, J. E.; Macdonald, M.; Nie, J.; Bowman, C. N. Structure and Swelling of Poly(Acrylic Acid) Hydrogels: Effect of PH, Ionic Strength, and Dilution on the Crosslinked Polymer Structure. *Polymer* 2004, *45* (5), 1503–1510. https://doi.org/10.1016/j.polymer.2003.12.040.

(50) Salomé Veiga, A.; Schneider, J. P. Antimicrobial Hydrogels for the Treatment of Infection: Antimicrobial Hydrogels for the Treatment of Infection. *Biopolymers* 2013, *100* (6), 637–644. https://doi.org/10.1002/bip.22412.

(51) Aswathy, S. H.; Narendrakumar, U.; Manjubala, I. Commercial Hydrogels for Biomedical Applications. *Heliyon* 2020, *6* (4), e03719. https://doi.org/10.1016/j.heliyon.2020.e03719.

(52) Luo Zheng, L.; Vanchinathan, V.; Dalal, R.; Noolandi, J.; Waters, D. J.; Hartmann, L.; Cochran, J. R.; Frank, C. W.; Yu, C. Q.; Ta, C. N. Biocompatibility of Poly(Ethylene Glycol) and Poly(Acrylic Acid) Interpenetrating Network Hydrogel by Intrastromal Implantation in Rabbit Cornea: Biocompatibility Of Poly(Ethylene Glycol) And Poly(Acrylic Acid). *J. Biomed. Mater. Res. A* 2015, *103* (10), 3157–3165. https://doi.org/10.1002/jbm.a.35453.

(53) De Giglio, E.; Cometa, S.; Cioffi, N.; Torsi, L.; Sabbatini, L. Analytical Investigations of Poly(Acrylic Acid) Coatings Electrodeposited on Titanium-Based Implants: A Versatile Approach to Biocompatibility Enhancement. *Anal. Bioanal. Chem.* 2007, *389* (7–8), 2055–2063. https://doi.org/10.1007/s00216-007-1299-7.

(54) Philippova, O. E.; Hourdet, D.; Audebert, R.; Khokhlov, A. R. Interaction of Hydrophobically Modified Poly(Acrylic Acid) Hydrogels with Ionic Surfactants. *Macromolecules* 1996, *29* (8), 2822–2830. https://doi.org/10.1021/ma951006p.

(55) Drozdov, A. D.; deClaville Christiansen, J. Modeling the Effects of PH and Ionic Strength on Swelling of Polyelectrolyte Gels. *J. Chem. Phys.* 2015, *142* (11), 114904. https://doi.org/10.1063/1.4914924.

(56) Arifuzzaman, Md.; Millhouse, P. W.; Raval, Y.; Pace, T. B.; Behrend, C. J.; Beladi Behbahani, S.; DesJardins, J. D.; Tzeng, T.-R. J.; Anker, J. N. An Implanted PH Sensor Read Using Radiography. *The Analyst* 2019, *144* (9), 2984–2993. https://doi.org/10.1039/C8AN02337A.

(57) Brannigan, R. P.; Dove, A. P. Synthesis, Properties and Biomedical Applications of Hydrolytically Degradable Materials Based on Aliphatic Polyesters and Polycarbonates. *Biomater. Sci.* 2017, *5* (1), 9–21. https://doi.org/10.1039/C6BM00584E.

(58) Weyers, R. E.; Blankenhorn, P. R.; Stover, L. R.; Kline, D. E. Effects of Sterilization Procedures on the Tensile Properties of Polycarbonate. *J. Appl. Polym. Sci.* 1978, *22* (7), 2019–2024. https://doi.org/10.1002/app.1978.070220722.

(59) Pelham, H.; Benza, D.; Millhouse, P. W.; Carrington, N.; Arifuzzaman, Md.; Behrend, C. J.; Anker, J. N.; DesJardins, J. D. Implantable Strain Sensor to Monitor Fracture Healing with Standard Radiography. *Sci. Rep.* 2017, *7* (1), 1489. https://doi.org/10.1038/s41598-017-01009-7.

(60) Carrington, N. T.; Milhouse, P. W.; Behrend, C. J.; Pace, T. B.; Anker, J. N.; DesJardins, J. D. *Measuring Intertrochanteric Fracture Stability with a Novel Strain-Sensing Sliding Hip Screw*; preprint; Orthopedics, 2020. https://doi.org/10.1101/2020.09.04.20183251.

(61) Rajamanthrilage, A. C.; Arifuzzaman, Md.; Millhouse, P. W.; Pace, T. B.; Behrend, C. J.; DesJardins, J. D.; Anker, J. N. *Measuring Orthopedic Plate Strain to Track*

Bone Healing Using a Fluidic Sensor Read via Plain Radiography; preprint; Bioengineering, 2020. https://doi.org/10.1101/2020.08.27.268169.

(62) Anker, J.; Behrend, C. J.; DesJardins, J. D. Radiographic Discernable Sensors and Orthopedic Applications for Same. US 10,667,745 B2, June 2, 2020.

(63) Kuo, C.-Y.; Don, T.-M.; Lin, Y.-T.; Hsu, S.-C.; Chiu, W.-Y. Synthesis of PH-Sensitive Sulfonamide-Based Hydrogels with Controllable Crosslinking Density by Post Thermo-Curing. *J. Polym. Res.* 2019, *26* (1), 18. https://doi.org/10.1007/s10965-018-1672-6.

(64) Guo, J.; Li, L.; Ti, Y.; Yhu, J. Synthesis and Properties of a Novel PH Sensitive Poly(N-Vinyl-Pyrrolidone-Co-Sulfadiazine) Hydrogel. *Express Polym. Lett.* 2007, *1* (3), 166–172. https://doi.org/10.3144/expresspolymlett.2007.26.

(65) Song, Z.; Borgwardt, L.; Høiby, N.; Wu, H.; Sørensen, T. S.; Borgwardt, A. Prosthesis Infections after Orthopedic Joint Replacement: The Possible Role of Bacterial Biofilms. *Orthop. Rev.* 2013, *5* (2), 14. https://doi.org/10.4081/or.2013.e14.

(66) Cochran, KW, D., J.; Mazur, M, D., KP. Acute Toxicity of Zirconium, Columbium, Strontium, Lanthanum, Cesium, Tantalum and Yttrium. *Arch Indusl Hyg. & Occupational Med.* 1950, *1* (6), 637–650.

(67) Cristea, D.; Ghiuță, I.; Munteanu, D. Tantalum Based Materials for Implants and Prostheses Applications. *Bull. Transilv. Univ. Bras.* 2015, *8* (2), 8.

(68) Namur, R. S.; Reyes, K. M.; Marino, C. E. B. Growth and Electrochemical Stability of Compact Tantalum Oxides Obtained in Different Electrolytes for Biomedical

Applications. *Mater. Res.* 2015, *18* (suppl 2), 91–97. https://doi.org/10.1590/1516-1439.348714.

(69) Eliaz, N. Corrosion of Metallic Biomaterials: A Review. *Materials* 2019, *12* (3), 407. https://doi.org/10.3390/ma12030407.

(70) Burke, G L. The Corrosion of Metals in Tissues; and an Introduction to Tantalum. *Can Med Assoc J.* 1940, *43* (2), 125–128.

(71) Hoffman, A. S. Hydrogels for Biomedical Applications. *Adv. Drug Deliv. Rev.* 2012, *64*, 18–23. https://doi.org/10.1016/j.addr.2012.09.010.

(72) Gaytán, I.; Burelo, M.; Loza-Tavera, H. Current Status on the Biodegradability of Acrylic Polymers: Microorganisms, Enzymes and Metabolic Pathways Involved. *Appl. Microbiol. Biotechnol.* 2021, *105* (3), 991–1006. https://doi.org/10.1007/s00253-020-11073-1.

(73) Larson, R. J.; Bookland, E. A.; Williams, R. T.; Yocom, K. M.; Saucy, D. A.; Freeman, M. B.; Swift, G. Biodegradation of Acrylic Acid Polymers and Oligomers by Mixed Microbial Communities in Activated Sludge. *J. Environ. Polym. Degrad.* 1997, *5* (1), 41–48.

(74) Lyu, S.; Untereker, D. Degradability of Polymers for Implantable Biomedical Devices. *Int. J. Mol. Sci.* 2009, *10* (9), 4033–4065. https://doi.org/10.3390/ijms10094033.

(75) Sennakesavan, G.; Mostakhdemin, M.; Dkhar, L. K.; Seyfoddin, A.; Fatihhi, S. J. Acrylic Acid/Acrylamide Based Hydrogels and Its Properties - A Review. *Polym.*

Degrad. Stab. 2020, *180*, 109308. https://doi.org/10.1016/j.polymdegradstab.2020.109308.

(76) Xu, J.; Lee, H. Anti-Biofouling Strategies for Long-Term Continuous Use of Implantable Biosensors. *Chemosensors* 2020, *8* (3), 66. https://doi.org/10.3390/chemosensors8030066.

(77) Gray, M.; Meehan, J.; Ward, C.; Langdon, S. P.; Kunkler, I. H.; Murray, A.; Argyle, D. Implantable Biosensors and Their Contribution to the Future of Precision Medicine. *Vet. J.* 2018, *239*, 21–29. https://doi.org/10.1016/j.tvjl.2018.07.011.

(78) Herber, S.; Bomer, J.; Olthuis, W.; Bergveld, P.; Berg, A. van den. A Miniaturized Carbon Dioxide Gas Sensor Based on Sensing of PH-Sensitive Hydrogel Swelling with a Pressure Sensor. *Biomed. Microdevices* 2005, *7* (3), 197–204. https://doi.org/10.1007/s10544-005-3026-5.

(79) Burke, C. S.; Markey, A.; Nooney, R. I.; Byrne, P.; McDonagh, C. Development of an Optical Sensor Probe for the Detection of Dissolved Carbon Dioxide. *Sens. Actuators B Chem.* 2006, *119* (1), 288–294. https://doi.org/10.1016/j.snb.2005.12.022.

(80) Sharifzadeh, G.; Hosseinkhani, H. Biomolecule-Responsive Hydrogels in Medicine. *Adv. Healthc. Mater.* 2017, *6* (24), 1700801. https://doi.org/10.1002/adhm.201700801.

(81) Miyata, T.; Hayashi, T.; Kuriu, Y.; Uragami, T. Responsive Behavior of Tumor-Marker-Imprinted Hydrogels Using Macromolecular Cross-Linkers: Tumor-

Marker-Imprinted Hydrogels Using Macromolecular Cross-Linkers. *J. Mol. Recognit.* 2012, *25* (6), 336–343. https://doi.org/10.1002/jmr.2190.

(82) Miyata, T.; Asami, N.; Uragami, T. Preparation of an Antigen-Sensitive Hydrogel Using Antigen−Antibody Bindings. *Macromolecules* 1999, *32* (6), 2082–2084. https://doi.org/10.1021/ma981659g.

(83) Herber, S.; Bomer, J.; Olthuis, W.; Bergveld, P.; Berg, A. van den. A Miniaturized Carbon Dioxide Gas Sensor Based on Sensing of PH-Sensitive Hydrogel Swelling with a Pressure Sensor. *Biomed. Microdevices* 2005, *7* (3), 197–204. https://doi.org/10.1007/s10544-005-3026-5.

(84) Brannan, S. R.; Jerrard, D. A. Synovial Fluid Analysis. *J. Emerg. Med.* 2006, *30* (3), 331–339. https://doi.org/10.1016/j.jemermed.2005.05.029.

CHAPTER THREE

X-RAY BASED SYNOVIAL FLUID CARBON DIOXIDE SENSOR FOR THE EARLY DETECTION OF PROSTHETIC HIP INFECTIONS

3.1. Abstract

Prosthetic hip infections are a common complication of hip surgeries and early diagnosis of these infections are extremely challenging. We developed a novel implantable carbon dioxide sensor for non-invasive early detection and monitoring of hip infections by measuring synovial fluid carbon dioxide levels, radiographically. The sensor is based on a pH responsive hydrogel as the sensing material covered with a carbon dioxide permeable membrane. At high carbon dioxide levels, the pH would decrease resulting in shrinking of the polyacrylic acid hydrogel. The length changes of the hydrogel can be monitored using plain radiography by measuring the movement of the tantalum bead with respect to the metal wire. It is expected for the sensor to have a longer lifetime compared to the pH sensor due to the encapsulation of the sensor and fluid in a carbon dioxide permeable membrane which is impermeable to aqueous molecules. The sensor shows a clear response in the range of 15-115 mm Hg carbon dioxide, independent of the external solution pH. In summary, the sensor is useful for noninvasive early detection of prosthetic hip infections by measuring carbon dioxide levels in synovial fluid.

3.2. Introduction

One of the leading causes of failure following joint replacement surgery are post-surgery infections with an incidence of about ~0.5-2% of total hip replacement surgeries.[1,2] The complications of post-surgery infections involve prolonged hospitalization, multiple operations, significant permanent deformity, or loss of the implant.[1,3,4] In the elderly, it may result in a higher incidence of mortality. Risk factors for infection include obesity, diabetes mellitus, rheumatoid arthritis, exogenous immunosuppressive medications, and malignancy.[2,5–7]

Infection associated with prosthetic joints are caused by microbial contamination which may occur during surgery or hematogenously due to microbial spread through bloodstream from a distant focus of infection.[8–10] Most cases of hip infections are caused by staphylococci species such as *Staphylococci aureus* and coagulase-negative staphylococcus species.[1,11–13] The prosthetic hip joint provides a surface for the attachment of microbial cells.[12,14] The microbes grow to form a monolayer, which later develops into a microcolony and eventually a biofilm is formed where the microbes are enclosed in a polymer matrix.[15–17] The biofilm protects the microbes from conventional antimicrobial agents and the host immune system, thus resulting in increased resistance to antibiotics and host immune responses.[18–20] Generally, due to low oxygen levels, anaerobic fermentation in the biofilm leads to local depletion of nutrients and accumulation of metabolic waste products such as lactic acid, citric acid, carbon dioxide, propionic acid, glycerol, ethanol, etc., within the biofilm (Figure 3.1a).[15,21,22] Studies of synovial membrane metabolism have been used to study the mechanism of lactic acid formation in the joints as reflected by

partial pressure of oxygen (pO_2), partial pressure of carbon dioxide (pCO_2), pH and lactic acid in synovial fluid effluents of septic joints from patients.[23–26] The studies showed a decrease in pO_2 was accompanied by a decrease in pH and an increase in pCO_2 and lactic acid concentrations.[24,27,28] In a study by Treuhaft and McCarty, a sharp rise in pCO_2 and lactate levels and decrease in pH was observed in samples with pO_2 levels lower than 27 mm Hg.[24] The correlation between pH and pCO_2 is shown in Figure 3.1b.[24] The rise in lactate may be due to the changeover of local tissues from mainly aerobic to anaerobic metabolism in anoxic conditions resulting in decrease in pH. An inverse relationship between synovial lactic acid levels and glucose was determined by Lund-Oleson[23] as a result of metabolism of glucose to pyruvic acid, followed by conversion to lactic acid under anaerobic conditions as shown in Figure 3.1a. Therefore, due to the poor removal of products, the pCO_2 levels would be higher during infection and can be used as a biomarker of infection.

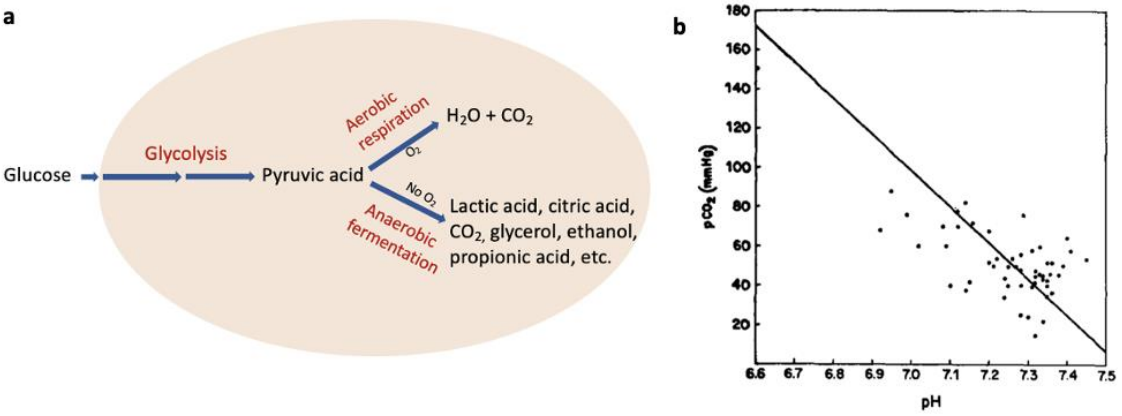

Figure 3.1: (a) Schematic diagram of cellular glucose metabolic pathways resulting in acidic metabolites. (b) Carbon dioxide partial pressure (pCO_2) of 55 joint fluids plotted

against pH values of the same fluid (reproduced with permission from Reference 24, Arthritis & Rheumatology, 1971).

Different methods of carbon dioxide sensing have been developed based mainly on optical methods. A common technique developed for sensing carbon dioxide include use of optodes (an optical fiber with a chemical sensing layer at tip), however it requires advanced readout equipment which can be expensive and may not be easily available in the medical settings.[29–33] Different types of solid electrolyte sensors for carbon dioxide detection have been developed which uses potentiometry, amperometry, and conductometry which are mostly suitable for measuring low pCO_2.[33–35] Carbon dioxide sensors have been developed that are based on the Severinghaus principle,[36] where carbon dioxide diffuses through a gas permeable membrane into an electrolyte solution resulting in a pH change which can be measured using various methods.[33] The pH measurements were originally carried out using glass electrode however it is not suitable for miniaturization, and other alternative methods including metal oxide electrodes, solvent polymeric membrane electrodes require reference electrodes which may suffer from drift.[33,37]

We are developing a carbon dioxide sensor for early detection of prosthetic joint infections based on a pH responsive hydrogel as the sensing material. Arthrocentesis (synovial fluid aspiration) is commonly used to detect/confirm infection when suspected from clinical examination and radiology.[38,39] However, the method is highly sensitive to conditions of fluid aspiration/storage, specifically, carbon dioxide may escape, resulting in pH drift.[40,41] While arthrocentesis is performed if infection is indicated, it is impractical or

contraindicated for screening or serial prosthetic joint infection measurements to monitor treatment because it is performed by a radiologist under fluoroscopy or ultrasound guidance which adds cost and scheduling issues; the procedure is painful, can induce tissue damage and allergic reaction to anesthetics or injected X-ray contrast agent used to confirm needle placement; complications are reported in 1-5% of cases; there is a very small but concerning risk of infecting a previously aseptic joint (with associated liability if test was not indicated).[42,43] Thus, noninvasive measurements of synovial fluid carbon dioxide measurements would be very helpful for early detection when more conservative treatments are often successful, and for monitoring treatment until eradication. Previously, we have developed a hydrogel-based pH sensor to measure pH of synovial fluid for the early detection of hip infections using X-ray imaging.[44] Even though no fouling effect on the sensor calibration curve, response rate or sensor degradation was observed in solutions of tryptic soy broth bacterial cell culture, bovine synovial fluid, bovine serum, highly oxidative hydrogen peroxide and copper ion medium, or storage in pH 7 buffer,[45] biofouling maybe a potential concern for an indwelling sensor. We have modified the pH sensor to determine carbon dioxide levels in synovial fluid with the added advantage of improved lifetime by encasing the sensor and fluid in a carbon dioxide permeable membrane which is impermeable to aqueous molecules.[46] The pH-sensitive hydrogel is placed in a sodium hydroxide solution enclosed by a carbon dioxide permeable membrane and exposed to different carbon dioxide concentrations. Higher carbon dioxide levels would result in decrease in pH of the solution, resulting in a change in size of the hydrogel,

which can be measured by X-ray radiography using the distance between the tantalum bead and the tungsten wire.[33,36] Schematic representation of the sensor is shown in Figure 3.2.

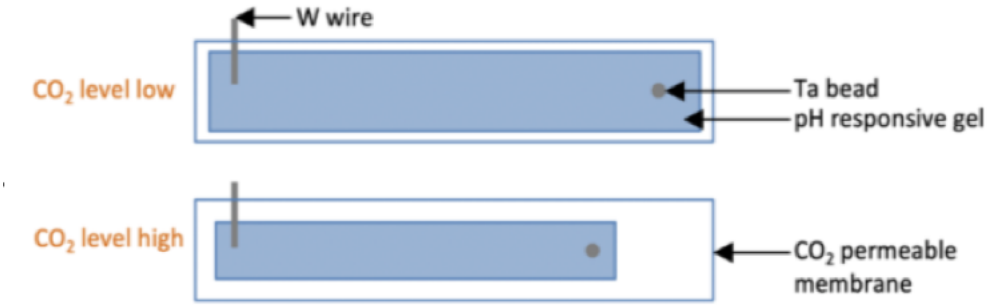

Figure 3.2: Schematic diagram of the hydrogel-based sensor to measure carbon dioxide levels.

3.2.1 Theory of synovial fluid carbon dioxide sensor

The sensor is covered with a gas-permeable membrane, which allows diffusion of CO_2 into the buffer solution without the interference of other liquids. The CO_2 that diffuses in will acidify water as represented in the following equilibria:

$$CO_{2(g)} + H_2O_{(l)} \rightleftharpoons H_2CO_{3(aq)} \qquad K_{CO2} = 3.38 \times 10^{-2}$$

$$H_2CO_{3(aq)} \rightleftharpoons H^+_{(aq)} + HCO_3^-{}_{(aq)} \qquad K_1 = 10^{-6.352}$$

$$HCO_3^-{}_{(aq)} \rightleftharpoons H^+_{(aq)} + CO_3^{2-}{}_{(aq)} \qquad K_2 = 10^{-10.329}$$

where K_{CO2} is the Henry's law constant and K_1 and K_2 is the first and second dissociation constants of H_2CO_3. The pH was calculated for different carbon dioxide levels (P_{CO2}) and plotted as shown in Figure 3.3 for distilled water and 1 mM NaOH. As seen in the graph

and according to Severinghaus et al., the addition of a base to water will double the pH response to CO_2. Therefore, the electrolyte solution used for the experiment is sodium hydroxide.

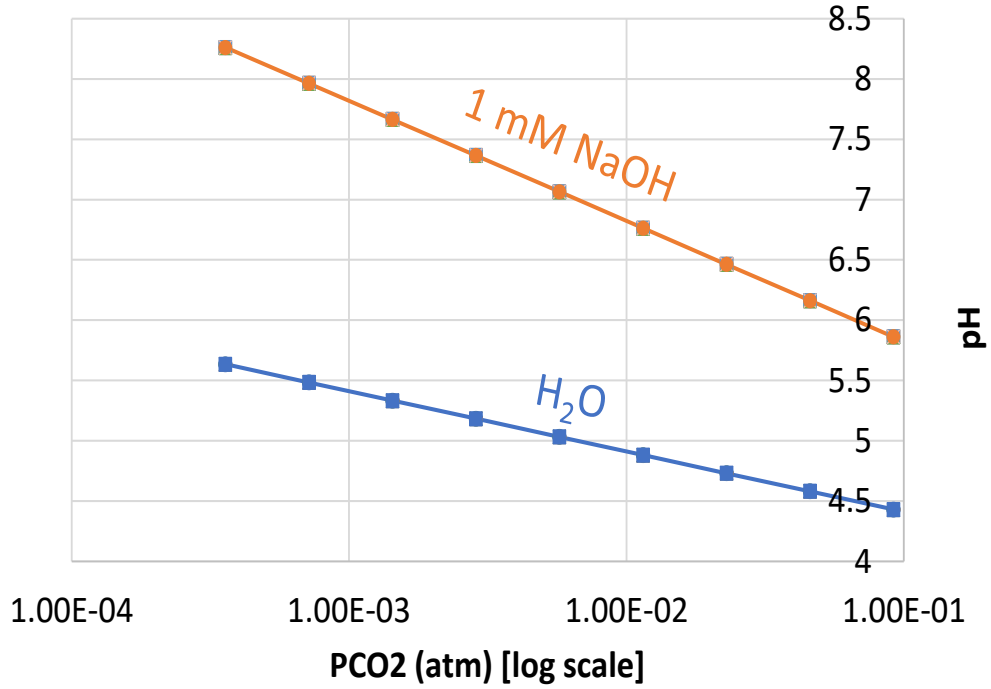

Figure 3.3: Calculated pH versus P_{CO2} in distilled water and 1 mM NaOH.

3.3. Materials and Methods

3.3.1. Materials

Acrylic acid 99% (Sigma, USA), n-octyl acrylate containing 400 ppm 4-methoxyphenol as inhibitor (Scientific Polymer Products, USA), anhydrous poly(ethylene glycol) diacrylate with average Mn 700 (Sigma, USA), 2-oxoglutaric acid (Wako Pure Chemical Industries Ltd, USA), N,N-dimethyl formamide (Sigma, USA), phosphate buffered saline (Sigma,

USA), reagent alcohol (Radnor, PA), reference standard pH buffers ranging from 2 to 11 (VWR Analytical, USA), Parafilm® M (Bemis Company, Inc., USA) were used as received. Sodium hydroxide (Ricca Chemical Company, Arlington, TX) and acetic acid (VWR Analytical, USA) was diluted as needed. Sodium hydrogen carbonate was purchased form VWR Chemicals BDH, West Chester, PA. Tantalum beads (0.394 mm diameter) were purchased from X-Medics, Frederiksberg, Denmark. Tungsten wire (diameter 0.26 mm) was purchased from McMaster-Carr, US. The polycarbonate casings for the sensor were machined by the Clemson University Machining and Technical Services.

3.3.2. Synthesis of pH sensing hydrogel

The hydrogel was prepared by free-radical co-polymerization of acrylic acid and n-octyl acrylate as the monomers, poly(ethylene glycol) diacrylate (M_n 700) as the crosslinker, and 2-oxoglutaric acid as the photoinitiator, with dimethylformamide as the solvent. The photo-polymerization reaction was performed under an inert nitrogen atmosphere using UV irradiation (365 nm) from both sides of the reaction cell at a temperature of approximately 45°C. The resulting polyacrylic acid-based hydrogel films were washed with 70% ethanol to remove any residual monomers, N,N-dimethyl formamide, and hydrate the hydrogel. The hydrogel was washed daily for at least 5 days to ensure the removal of unreacted monomers and initiators in the hydrogel film. Hydrogel samples of length ~10 mm was transferred to pH 7.4 phosphate-buffered saline (PBS).

3.3.3. Sensor response with time

For these experiments, the hydrogel was placed inside a tube open at both ends, one end was covered with parafilm and 0.1 mM NaOH was added to the tube and the other end was then sealed with parafilm. The tube was then immersed in a sodium bicarbonate solution corresponding to 15 mm Hg dissolved carbon dioxide (d_{CO2}) and allowed to equilibrate. Then it was transferred to a bicarbonate solution corresponding to 115 mm Hg d_{CO2} and images were taken, and the length of the hydrogels were measured using ImageJ software. Dissolved carbon dioxide standards were prepared by dissolving sodium hydrogen carbonate in deionized water to prepare a 1 M $NaHCO_3$ solution which was diluted to yield 15 mm Hg and 115 mm Hg dissolved CO_2 concentrations as given in Burke et al, 2006.[47]

3.3.4. Synovial fluid carbon dioxide sensor calibration

For these experiments, the hydrogel was placed inside a tube open at both ends, one end was covered with parafilm and 0.1 mM NaOH was added to the tube and the other end was then sealed with parafilm. Each tube was placed in a bicarbonate solution corresponding to 15, 30, 45, 60, 76, 91, and 115 mm Hg dissolved carbon dioxide (dCO_2) and images of the sensors were taken after 24 hours, and the length of the hydrogels were measured using ImageJ software. Dissolved CO_2 standards were prepared by dissolving sodium hydrogen carbonate in deionized water to prepare a 1 M $NaHCO_3$ solution which was diluted to yield the desired dissolved CO_2 concentrations as given in Burke et al, 2006.[47]

3.3.5. Fabrication of synovial fluid carbon dioxide sensor

The hydrogel was pinned at one end to a polycarbonate groove with a tungsten wire, and a radiodense tantalum bead (0.5 mm diameter) was embedded in the other end of the hydrogel. The groove was filled with 0.1 mM NaOH solution, and the groove was covered with parafilm at the top using commercially available adhesive (Loctite Superglue–Gel Control).

3.3.6. X-ray imaging of synovial fluid carbon dioxide sensor on hip implant

The synovial fluid carbon dioxide sensor was placed at the neck of the prosthesis and an X-ray image was taken (NEXT Equine DR II portable digital radiography system, Carlsbad, CA, with a battery powered veterinary X-ray generator, Oberhausen-Germany), and length measurements were analyzed using NIH ImageJ software.

3.4. Results and Discussion

3.4.1. Synthesis of pH sensing hydrogel and fabrication of injectable sensor

Hydrogels are networks of cross-linked hydrophilic polymers that can contain a large amount of water.[48–50] Hydrogels can undergo volume changes in response to changes in stimuli such as pH, temperature, light, ion concentration or electric field.[48,51] Hydrogels are widely used in the biomedical field in tissue engineering, drug delivery, self-healing materials, biosensors, and hemostasis bandages due to their increased biocompatibility, tunable biodegradability, properly mechanical strength, porous structure.[52–54] In addition,

hydrogels are used as sensors and actuators, where the stimulus-sensitive hydrogel acts as the sensing element and the transducer convert the swelling of the hydrogel to the optical or electrical domain.[55,56] Conductometric, amperometric, optical and mechanical methods have been explored to measure hydrogel swelling. Several studies by Herber et al. demonstrate the use of a pH responsive hydrogel as a sensing material and a pressure sensor as a transducer to design carbon dioxide pressure sensor in the diagnosis for gastrointestinal ischemia.[33,55,57] The sensor was miniaturized in his last study,[33] however, it does not discuss a method of detection of carbon dioxide levels in vivo in the developed sensor.

We developed a similar carbon dioxide sensor that is based on the swelling/ deswelling properties of polyacrylic acid-based hydrogel, where we will be measuring the length changes of the sensor in response to carbon dioxide levels, radiographically. Polyacrylic acid was selected as a well-suited pH responsive material reported to be stable, nontoxic, and non-inflammatory.[58–60] Polyacrylic acid polymer coatings have been previously studied for use in preventing corrosion on titanium and other metallic implants.[61] Polyethylene glycol (PEG) / polyacrylic acid devices have also been investigated in a rabbit model for use as corneal implants.[62] Polyacrylic acid hydrogels[63,64] are responsive to pH and swells at high pH and de-swell at low pH, around its effective acid dissociation constant (pK_a) of 5.56.[44] At high pH, the pendant carboxylic acid groups get deprotonated and become negatively charged carboxylate ions ($–COO^-$).[58,65] Due to increased electrostatic repulsions between bound charges on the polymer chains and increased osmotic pressure the hydrogel swells at high pH.[60,63] In contrast, at low pH the carboxylic acid groups in the polyacrylic acid chains of the network do not have any charges resulting in less repulsions

between the polymer chains and the hydrogel shrinks at low pH. Calibration of the pH hydrogel sensor shows a linear response between pH 4-8, and an acid dissociation constant (pK_a) of 5.56 when fitted to a modified Henderson-Hasselbalch equation with a factor (n=2.50) to account for a spread in hydrogel pK_a. Similar results were observed when the experiment was repeated in bovine synovial fluid in the physiologically relevant pH. The sensor response fit well to an exponential with a 30 min time constant, a linear response between pH 4-8, and 0.05 pH units interobserver agreement. Thus, we expect the length changes in the hydrogel resulting from the subsequent pH changes due to carbon dioxide variations in the synovial fluid can be detected using X-radiography using the developed sensor.

The polyacrylic acid hydrogel used in the sensor design was polymerized by free radical polymerization of the monomers, acrylic acid and n-octyl acrylate (n-OA); crosslinker, poly(ethylene glycol) diacrylate (M_n 700); photoinitiator, 2-oxoglutaric acid, with dimethylformamide (DMF) as the solvent. The photo-polymerization reaction was performed under an inert nitrogen atmosphere using UV irradiation (365 nm) from both sides of the reaction cell at a temperature of approximately 45 °C. The resulting polyacrylic acid-based hydrogel films were washed with 70% ethanol to remove any residual monomers, DMF and to hydrate the hydrogel. In the sensor design, for radiographic measurements, the pH-responsive hydrogel with an embedded tantalum bead is pinned on one end with a tungsten wire in a polycarbonate groove as shown in Figure 3.3. Polycarbonate is used in a wide range of biomedical applications such as in blood oxygenators and blood reservoirs in cardiac surgery products, filter cartridges for renal dialysis and surgical instruments due to its biocompatibility, glass like clarity, high

strength, and impact resistance.[66,67] The groove is then sealed with parafilm as the carbon dioxide permeable membrane in order to separate the hydrogel sensor from the external solution in the sensor design (Figure 3.4). Parafilm is a waterproof, semi-transparent, flexible film composed of a mixture of paraffin waxes and polyolefins which is permeable to gases like carbon dioxide and oxygen.[68] Recently, a study used drug loaded parafilm as a remote-controlled thermoresponsive patch for dermal drug delivery.[68] The gas permeability of parafilm for carbon dioxide is 1200 cc/m² d at 23 °C and 50% relative humidity. The carbon dioxide diffuses through the gas permeable membrane of parafilm into an electrolyte solution (0.1 mM NaOH) resulting in a change in pH (decrease in pH). Subsequently, in response to the pH change, the hydrogel which is in contact with the electrolyte solution decrease in size. Due to the presence of the radiopaque markers in the hydrogel, this change in length can be measured using X-ray radiography.

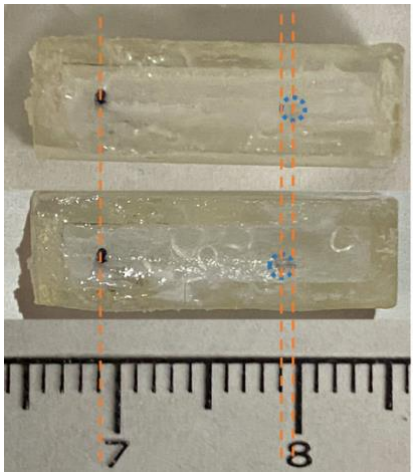

Figure 3. 4: Image of sensor at carbon dioxide percentages 60 mm Hg (top) and 76 mm Hg (bottom).

3.4.2. Sensor response with time

The sensor response with time was measured by first stabilizing the sensor exposed to P_{CO2} of 15 mm Hg and then transferring to a bicarbonate solution corresponding to P_{CO2} of 115 mm Hg, taking photographs of the sensor with time. Figure 3.5 shows the hydrogel length with time. It could be seen that the sensor started to stabilize around 10 hours.

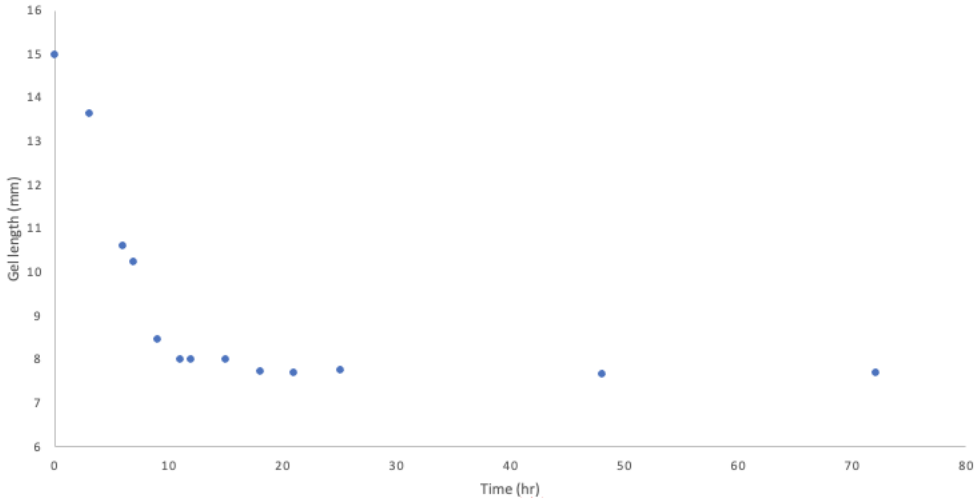

Figure 3.5: Hydrogel length vs time for the hydrogel-based carbon dioxide sensor.

3.4.3. Sensor calibration and selectivity

The hydrogel response to varying carbon dioxide levels is shown in Figure 3.6. The sensor was placed in bicarbonate solutions of varying CO_2 levels and the length of the hydrogel was measured. The change in length was calculated for each CO_2 level and normalized to the change in length at 15 mm Hg CO_2. As expected, the change in length increased when CO_2 levels increased from 15 to 115 mm Hg CO_2.

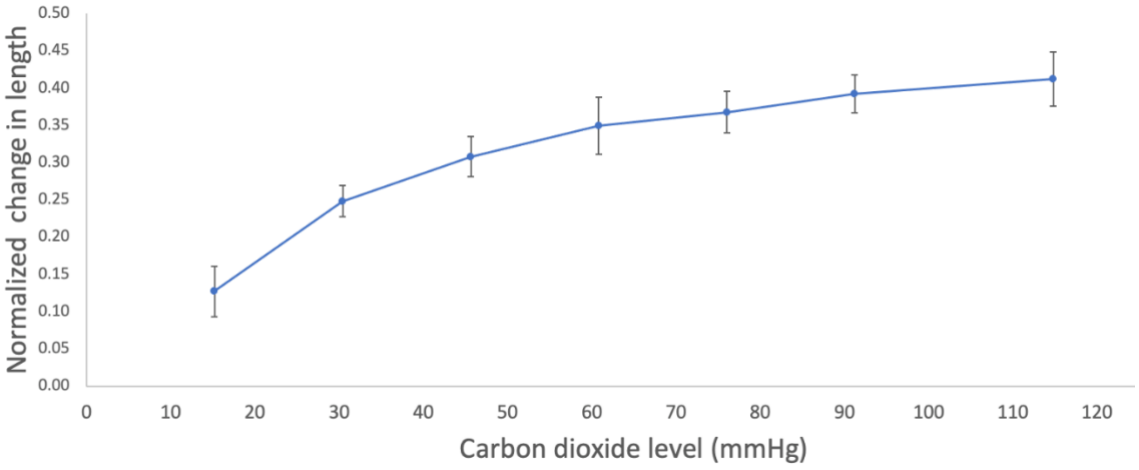

Figure 3.6: Calibration graph of hydrogel-based carbon dioxide sensor.

In order to test the selectivity of the sensor, initially the sensor (the hydrogel sensor with radiopaque markers encapsulated in parafilm) was placed in different external solutions of water, acetic acid, and sodium hydroxide and placed inside a cell incubator. The sensor showed a clear response that is independent of external fluid. Since the sensor is covered with a gas-permeable membrane, CO_2 can diffuse into the buffer solution without the interference of other liquids, whereas it is assumed that other gases present are inert. Therefore, the response of the sensor to changes in pH and salt concentration can only be attributed to the CO_2.

3.4.4. X-ray imaging of synovial fluid carbon dioxide sensor

The synovial fluid carbon dioxide (hydrogel with radiopaque markers in the polycarbonate casing covered with carbon dioxide permeable membrane) was allowed to

incubate at 76 mm Hg (10% CO_2) and 115 mm Hg (15% CO_2) carbon dioxide levels. The sensors were then imaged using X-ray radiography (Figure 3.7 a). The plain radiographs clearly showed the positions of the radiopaque markers.

The synovial fluid carbon dioxide sensor was then attached to the neck of the hip prosthetic implant (Figure 3.7b), so that the sensor would be in contact with synovial fluid but away from pressure bearing surfaces. The radiograph clearly showed the implant and the sensor position. The change in length of the sensor can be determined by measuring the distance between tantalum bead and pinning wire, which were clearly visible on the radiograph.

a

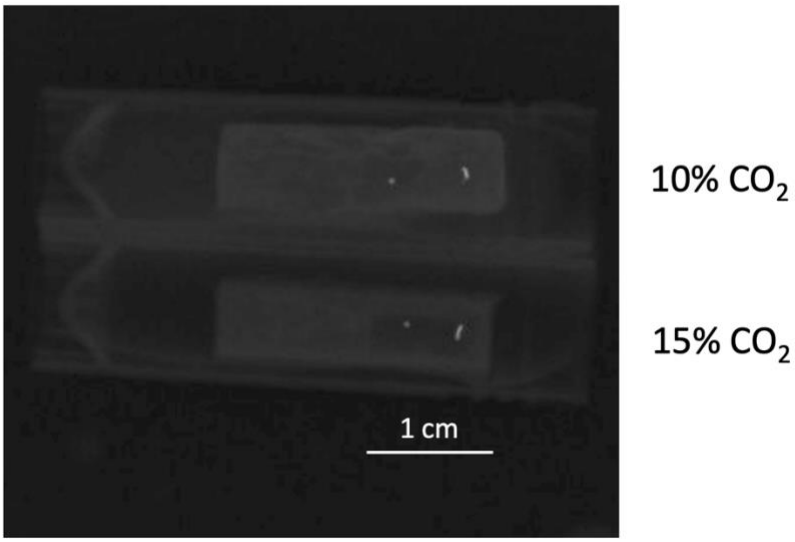

b

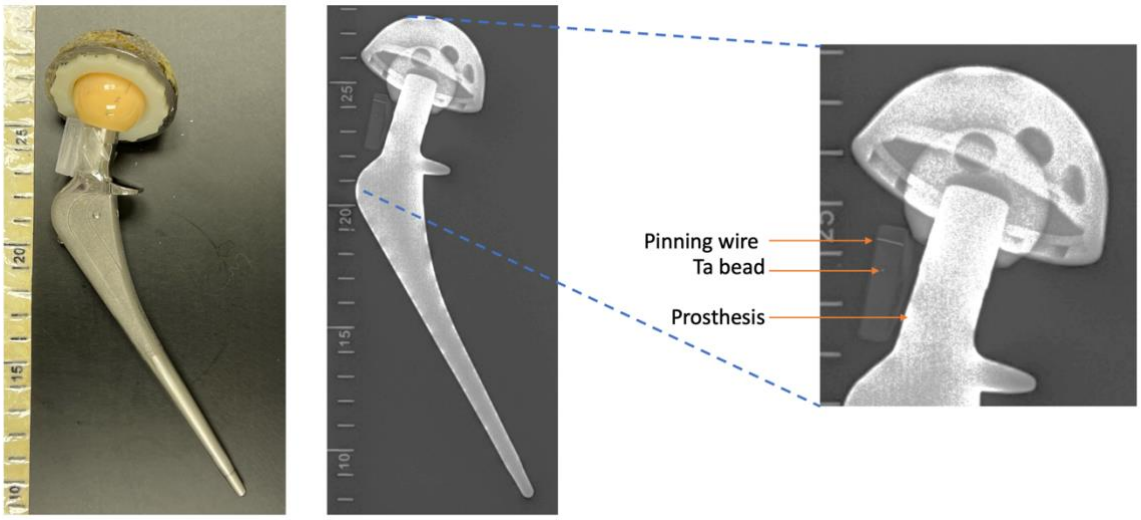

Figure 3.7: a) X-ray image of synovial fluid carbon dioxide sensor at two different carbon dioxide levels. b) Photograph of synovial fluid carbon dioxide sensor on hip prosthesis (left), X-ray image of synovial fluid carbon dioxide sensor on hip prosthesis (right), with the inset showing the zoomed image of the sensor with the radiopaque markers.

3.4.5. Limitations

With regard to clinical studies, the sensor performance needs to be determined ex vivo and in vivo. It is expected that the encasing would protect the hydrogel sensor from the pressure exerted by the surrounding tissue, thus having minimum effect on the performance of the sensor. Therefore, similar values to the in vitro results are expected in

the sensor performance in vivo, especially using a standing X-ray in place of a C-arm or portable unit (where prior results were acquired but these lack anti-scatter grids).

A potential concern regarding implantable sensors is their biocompatibility and stability in vivo. The materials used in the development of the sensor are biocompatible and have shown long term stability in vivo. The polyacrylic acid-based hydrogels are commonly used in drug delivery, biosensors, membrane and separation devices due to their biocompatibility and extended life-span.[54,59] They are expected to have very low degradation since the crosslinked polymer networks are expected to be highly resistant to degradation within the lifetime of the patient.[58,69] Tantalum has excellent anti-corrosive properties as a result of the stable tantalum oxide protective film formed on the surface of the metal.[70,71] Tantalum-based materials are widely used in clinical applications as radiopaque markers and medical implants with no adverse health effects.[70,72]

The pH hydrogel used in the development of the sensor is equilibrium-based and drift has not been observed after long term incubation in serum or even harsh oxidative environments. The difference between the pH sensor and the developed carbon dioxide sensor is that here the sensor is encapsulated with a carbon dioxide permeable membrane which would avoid interaction with large molecules, while allowing carbon dioxide to penetrate. It is expected this would dramatically improve sensor longevity in vivo. As an alternative to the parafilm, polydimethylsiloxane (PDMS) film or tubing can be used as a carbon dioxide permeable membrane. Compared to parafilm, PDMS is widely used as an optically clear, flexible, inert, non-toxic, biocompatible material, and routinely used as a biomedical implant material.[73]

3.5. Conclusions

A sensor with hydrogel composed of radiopaque markers sealed form the external environment by a carbon dioxide permeable membrane shows a clear response to carbon dioxide changes within a reasonable period of time. The hydrogel-based carbon dioxide sensor responds well in the medical interesting range between 2 and 15% carbon dioxide levels. The sensor was shown to be responsive selective to carbon dioxide due to the presence of the carbon dioxide permeable membrane, which only allows gas molecules to pass through. The sensor did not respond when exposed to acidic or basic external fluids, showing its selectivity of variation in carbon dioxide. The developed sensor can therefore be used for the measurement of carbon dioxide levels in synovial fluid.

3.6. References

(1) Del Pozo, J. L.; Patel, R. Infection Associated with Prosthetic Joints. *N. Engl. J. Med.* 2009, *361* (8), 787–794. https://doi.org/10.1056/NEJMcp0905029.

(2) Pulido, L.; Ghanem, E.; Joshi, A.; Purtill, J. J.; Parvizi, J. Periprosthetic Joint Infection: The Incidence, Timing, and Predisposing Factors. *Clin. Orthop.* 2008, *466* (7), 1710–1715. https://doi.org/10.1007/s11999-008-0209-4.

(3) Abad, C. L.; Haleem, A. Prosthetic Joint Infections: An Update. *Curr. Infect. Dis. Rep.* 2018, *20* (7), 15. https://doi.org/10.1007/s11908-018-0622-0.

(4) Birlutiu, V. Diagnosis and Management of Orthopedic Implant-Associated Infection: A Comprehensive Review of the Literature. *Biomed Res* 2017, *28* (11), 11.

(5) Berbari, E. F.; Hanssen, A. D.; Duffy, M. C.; Steckelberg, J. M.; Ilstrup, D. M.; Harmsen, W. S.; Osmon, D. R. Risk Factors for Prosthetic Joint Infection: Case-Control Study. *Clin. Infect. Dis.* 1998, *27* (5), 1247–1254. https://doi.org/10.1086/514991.

(6) Kurtz, S. M.; Lau, E. C.; Son, M.-S.; Chang, E. T.; Zimmerli, W.; Parvizi, J. Are We Winning or Losing the Battle With Periprosthetic Joint Infection: Trends in Periprosthetic Joint Infection and Mortality Risk for the Medicare Population. *J. Arthroplasty* 2018, *33* (10), 3238–3245. https://doi.org/10.1016/j.arth.2018.05.042.

(7) Marchant, M. H.; Viens, N. A.; Cook, C.; Vail, T. P.; Bolognesi, M. P. The Impact of Glycemic Control and Diabetes Mellitus on Perioperative Outcomes After Total Joint Arthroplasty: *J. Bone Jt. Surg.-Am. Vol.* 2009, *91* (7), 1621–1629. https://doi.org/10.2106/JBJS.H.00116.

(8) Akoh, J. A. Peritoneal Dialysis Associated Infections: An Update on Diagnosis and Management. *World J. Nephrol.* 2012, *1* (4), 106. https://doi.org/10.5527/wjn.v1.i4.106.

(9) Arciola, C. R.; Campoccia, D.; Montanaro, L. Implant Infections: Adhesion, Biofilm Formation and Immune Evasion. *Nat. Rev. Microbiol.* 2018, *16* (7), 397–409. https://doi.org/10.1038/s41579-018-0019-y.

(10) Esposito, S.; Leone, S. Prosthetic Joint Infections: Microbiology, Diagnosis, Management and Prevention. *Int. J. Antimicrob. Agents* 2008, *32* (4), 287–293. https://doi.org/10.1016/j.ijantimicag.2008.03.010.

(11) Tsukayama, D. T.; Estrada, R.; Gustilo, R. B. Infection after Total Hip Arthroplasty. A Study of the Treatment of One Hundred and Six Infections*: *J. Bone Jt. Surg.* 1996, *78* (4), 512–523. https://doi.org/10.2106/00004623-199604000-00005.

(12) Costerton, J. W.; Lewandowski, Z.; DeBeer, D.; Caldwell, D.; Korber, D.; James, G. Biofilms, the Customized Microniche. *J. Bacteriol.* 1994, *176* (8), 2137–2142. https://doi.org/10.1128/jb.176.8.2137-2142.1994.

(13) Molina-Manso, D.; del Prado, G.; Ortiz-Pérez, A.; Manrubia-Cobo, M.; Gómez-Barrena, E.; Cordero-Ampuero, J.; Esteban, J. In Vitro Susceptibility to Antibiotics of Staphylococci in Biofilms Isolated from Orthopaedic Infections. *Int. J. Antimicrob. Agents* 2013, *41* (6), 521–523. https://doi.org/10.1016/j.ijantimicag.2013.02.018.

(14) Dunne, W. M. Bacterial Adhesion: Seen Any Good Biofilms Lately? *Clin. Microbiol. Rev.* 2002, *15* (2), 155–166. https://doi.org/10.1128/CMR.15.2.155-166.2002.

(15) Costerton, J. W.; Montanaro, L.; Arciola, C. R. Biofilm in Implant Infections: Its Production and Regulation. *Int J Artif Organs* 2005, *28* (11), 1062–1068.

(16) Veerachamy, S.; Yarlagadda, T.; Manivasagam, G.; Yarlagadda, P. K. D. V. Bacterial Adherence and Biofilm Formation on Medical Implants: A Review. *Proc.*

Inst. Mech. Eng. [H] 2014, *228* (10), 1083–1099. https://doi.org/10.1177/0954411914556137.

(17) Hall-Stoodley, L.; Stoodley, P. Evolving Concepts in Biofilm Infections. *Cell. Microbiol.* 2009, *11* (7), 1034–1043. https://doi.org/10.1111/j.1462-5822.2009.01323.x.

(18) Stewart, E. J.; Payne, D. E.; Ma, T. M.; VanEpps, J. S.; Boles, B. R.; Younger, J. G.; Solomon, M. J. Effect of Antimicrobial and Physical Treatments on Growth of Multispecies Staphylococcal Biofilms. *Appl. Environ. Microbiol.* 2017, *83* (12). https://doi.org/10.1128/AEM.03483-16.

(19) Ciofu, O.; Rojo-Molinero, E.; Macià, M. D.; Oliver, A. Antibiotic Treatment of Biofilm Infections. *APMIS* 2017, *125* (4), 304–319. https://doi.org/10.1111/apm.12673.

(20) Campoccia, D.; Montanaro, L.; Arciola, C. R. The Significance of Infection Related to Orthopedic Devices and Issues of Antibiotic Resistance. *Biomaterials* 2006, *27* (11), 2331–2339. https://doi.org/10.1016/j.biomaterials.2005.11.044.

(21) Stewart, P. S.; Franklin, M. J. Physiological Heterogeneity in Biofilms. *Nat. Rev. Microbiol.* 2008, *6* (3), 199–210. https://doi.org/10.1038/nrmicro1838.

(22) Damgaard, L. R.; Nielsen, L. P.; Revsbech, N. P. Methane Microprofiles in a Sewage Biofilm Determined with a Microscale Biosensor. *Water Res.* 2001, *35* (6), 1379–1386. https://doi.org/10.1016/S0043-1354(00)00412-7.

(23) Lund-Olesen, K. Oxygen Tension in Synovial Fluids. *Arthritis Rheum.* 1970, *13* (6), 769–776. https://doi.org/10.1002/art.1780130606.

(24) Treuhaft, P. S.; McCarty, D. J. Synovial Fluid PH, Lactate, Oxygen and Carbon Dioxide Partial Pressure in Various Joint Diseases. *Arthritis Rheum.* 1971, *14* (4), 475–484. https://doi.org/10.1002/art.1780140407.

(25) Brook, I.; Reza, M. J.; Bricknell, K. S.; Bluestone, R.; Finegold, S. M. Synovial Fluid Lactic Acid. a Diagnostic Aid in Septic Arthritis. *Arthritis Rheum.* 1978, *21* (7), 774–779. https://doi.org/10.1002/art.1780210706.

(26) Tulamo, R.-M.; Bramlage, L. R.; Gabel, A. A. Sequential Clinical and Synovial Fluid Changes Associated with Acute Infectious Arthritis in the Horse. *Equine Vet. J.* 1989, *21* (5), 325–331. https://doi.org/10.1111/j.2042-3306.1989.tb02681.x.

(27) Stafford, G.; Akmal, M.; Mitchell-Hynd, C.; Skinner, J.; Bentley, G. Synovial Fluid PH as an Indicator of Infected Joint Arthroplasty. *Orthop. World Lit. Soc. J.* 2013.

(28) Behn, A. R.; Mathews, J. A.; Phillips, I. Lactate UV-System: A Rapid Method for Diagnosis of Septic Arthritis. *Ann. Rheum. Dis.* 1981, *40* (5), 489–492. https://doi.org/10.1136/ard.40.5.489.

(29) Marazuela, M. D.; Bondi, M. M.; Orellana, G. Marazuela, M. D., MC Moreno Bondi, and G. Orellana. "Enhanced Performance of a Fibre-Optic Luminescence CO2 Sensor Using Carbonic Anhydrase. *Sens. Actuators B Chem.* 1995, *29* (1–3), 126–131.

(30) Choi, M. F.; Hawkins, P. Novel Dye-Solvent Solutions for the Simultaneous Detection of Oxygen and Carbon Dioxide. *Anal. Chem.* 1995, *67* (21), 3897–3902.

(31) Orellana, G.; Moreno-Bondi, M. C.; Segovia, E.; Marazuela, M. D. Fiber-Optic Sensing of Carbon Dioxide Based on Excited-State Proton Transfer to a Luminescent Ruthenium (II) Complex. *Anal. Chem.* 1992, *64* (19), 2210–2215.

(32) Weigl, B. H.; Wolfbeis, O. S. Capillary Optical Sensors. *Anal. Chem.* 1994, *66* (20), 3323–3327.

(33) Herber, S.; Bomer, J.; Olthuis, W.; Bergveld, P.; Berg, A. van den. A Miniaturized Carbon Dioxide Gas Sensor Based on Sensing of PH-Sensitive Hydrogel Swelling with a Pressure Sensor. *Biomed. Microdevices* 2005, *7* (3), 197–204. https://doi.org/10.1007/s10544-005-3026-5.

(34) Miyachi, Y.; Sakai, G.; Shimanoe, K.; Yamazoe, N. Fabrication of CO2 Sensor Using NASICON Thick Film. *Sens. Actuators B Chem.* 2003, *93* (1–3), 250–256.

(35) Haeusler, A.; Meyer, J. U. A Novel Thick Film Conductive Type CO2 Sensor. *Sens. Actuators B Chem.* 1996, *34* (1–3), 388–395.

(36) Severinghaus, J. W.; Freeman, A. Electrodes for Blood PO2, and PC02 Determination. *J. Appl. Physiol.* 1958, *13* (3), 515–520.

(37) Suzuki, H.; Arakawa, H.; Sasaki, S.; Karube, I. Micromachined Severinghaus-Type Carbon Dioxide Electrode. *Anal. Chem.* 1999, *71* (9), 1737–1743. https://doi.org/10.1021/ac9811468.

(38) Fink, B.; Makowiak, C.; Fuerst, M.; Berger, I.; Schäfer, P.; Frommelt, L. The Value of Synovial Biopsy, Joint Aspiration and C-Reactive Protein in the Diagnosis of Late Peri-Prosthetic Infection of Total Knee Replacements. *J. Bone Joint Surg. Br.* 2008, *90-B* (7), 874–878. https://doi.org/10.1302/0301-620X.90B7.20417.

(39) Yee, D. K.; Chiu, K.; Yan, C.; Ng, F. Review Article: Joint Aspiration for Diagnosis of Periprosthetic Infection. *J. Orthop. Surg.* 2013, *21* (2), 236–240. https://doi.org/10.1177/230949901302100225.

(40) Deirmengian, C.; Feeley, S.; Kazarian, G. S.; Kardos, K. Synovial Fluid Aspirates Diluted with Saline or Blood Reduce the Sensitivity of Traditional and Contemporary Synovial Fluid Biomarkers. *Clin. Orthop.* 2020, *478* (8), 1805–1813. https://doi.org/10.1097/CORR.0000000000001188.

(41) Kerolus, G.; Clayburne, G.; Schumacher, H. R. Is It Mandatory to Examine Synovial Fluids Promptly after Arthrocentesis? *Arthritis Rheum.* 1989, *32* (3), 271–278. https://doi.org/10.1002/anr.1780320308.

(42) Brannan, S. R.; Jerrard, D. A. Synovial Fluid Analysis. *J. Emerg. Med.* 2006, *30* (3), 331–339. https://doi.org/10.1016/j.jemermed.2005.05.029.

(43) Porrino, J.; Wang, A.; Moats, A.; Mulcahy, H.; Kani, K. Prosthetic Joint Infections: Diagnosis, Management, and Complications of the Two-Stage Replacement Arthroplasty. *Skeletal Radiol.* 2020, *49* (6), 847–859. https://doi.org/10.1007/s00256-020-03389-w.

(44) Wijayaratna, U. N.; Kiridena, S. D.; Adams, J. D.; Behrend, C. J.; Anker, J. N. Synovial Fluid PH Sensor for Early Detection of Prosthetic Hip Infections. *Adv. Funct. Mater.* 2021, *31* (37), 2104124. https://doi.org/10.1002/adfm.202104124.

(45) Arifuzzaman, Md.; Millhouse, P. W.; Raval, Y.; Pace, T. B.; Behrend, C. J.; Beladi Behbahani, S.; DesJardins, J. D.; Tzeng, T.-R. J.; Anker, J. N. An Implanted PH

Sensor Read Using Radiography. *The Analyst* 2019, *144* (9), 2984–2993. https://doi.org/10.1039/C8AN02337A.

(46) Xu, J.; Lee, H. Anti-Biofouling Strategies for Long-Term Continuous Use of Implantable Biosensors. *Chemosensors* 2020, *8* (3), 66. https://doi.org/10.3390/chemosensors8030066.

(47) Burke, C. S.; Markey, A.; Nooney, R. I.; Byrne, P.; McDonagh, C. Development of an Optical Sensor Probe for the Detection of Dissolved Carbon Dioxide. *Sens. Actuators B Chem.* 2006, *119* (1), 288–294. https://doi.org/10.1016/j.snb.2005.12.022.

(48) Ahmed, E. M. Hydrogel: Preparation, Characterization, and Applications: A Review. *J. Adv. Res.* 2015, *6* (2), 105–121. https://doi.org/10.1016/j.jare.2013.07.006.

(49) Bahram, M.; Mohseni, N.; Moghtader, M. An Introduction to Hydrogels and Some Recent Applications. In *Emerging Concepts in Analysis and Applications of Hydrogels*; Majee, S. B., Ed.; InTech, 2016. https://doi.org/10.5772/64301.

(50) Gyles, D. A.; Castro, L. D.; Silva, J. O. C.; Ribeiro-Costa, R. M. A Review of the Designs and Prominent Biomedical Advances of Natural and Synthetic Hydrogel Formulations. *Eur. Polym. J.* 2017, *88*, 373–392. https://doi.org/10.1016/j.eurpolymj.2017.01.027.

(51) Lee, B. K.; Kim, J.-R.; Park, K.; Cho, Y. W. Environment-Responsive Hydrogels for Drug Delivery. *Drug Des.* 22.

(52) Chai, Q.; Jiao, Y.; Yu, X. Hydrogels for Biomedical Applications: Their Characteristics and the Mechanisms behind Them. *Gels* 2017, *3* (1), 6. https://doi.org/10.3390/gels3010006.

(53) Aswathy, S. H.; Narendrakumar, U.; Manjubala, I. Commercial Hydrogels for Biomedical Applications. *Heliyon* 2020, *6* (4), e03719. https://doi.org/10.1016/j.heliyon.2020.e03719.

(54) Caló, E.; Khutoryanskiy, V. V. Biomedical Applications of Hydrogels: A Review of Patents and Commercial Products. *Eur. Polym. J.* 2015, *65*, 252–267. https://doi.org/10.1016/j.eurpolymj.2014.11.024.

(55) Herber, S.; Olthuis, W.; Bergveld, P.; van den Berg, A. Exploitation of a PH-Sensitive Hydrogel Disk for CO2 Detection. *Sens. Actuators B Chem.* 2004, *103* (1–2), 284–289. https://doi.org/10.1016/j.snb.2004.04.113.

(56) van der Linden, H. J.; Herber, S.; Olthuis, W.; Bergveld, P. Stimulus-Sensitive Hydrogels and Their Applications in Chemical (Micro)Analysis. *The Analyst* 2003, *128* (4), 325–331. https://doi.org/10.1039/b210140h.

(57) Herber, S.; Olthuis, W.; Bergveld, P. A Swelling Hydrogel-Based PCO2 Sensor. *Sens. Actuators B Chem.* 2003, *91* (1–3), 378–382. https://doi.org/10.1016/S0925-4005(03)00121-7.

(58) Sennakesavan, G.; Mostakhdemin, M.; Dkhar, L. K.; Seyfoddin, A.; Fatihhi, S. J. Acrylic Acid/Acrylamide Based Hydrogels and Its Properties - A Review. *Polym. Degrad. Stab.* 2020, *180*, 109308. https://doi.org/10.1016/j.polymdegradstab.2020.109308.

(59) Hoffman, A. S. Hydrogels for Biomedical Applications. *Adv. Drug Deliv. Rev.* 2012, *64*, 18–23. https://doi.org/10.1016/j.addr.2012.09.010.

(60) Koetting, M. C.; Peters, J. T.; Steichen, S. D.; Peppas, N. A. Stimulus-Responsive Hydrogels: Theory, Modern Advances, and Applications. *Mater. Sci. Eng. R Rep.* 2015, *93*, 1–49. https://doi.org/10.1016/j.mser.2015.04.001.

(61) De Giglio, E.; Cometa, S.; Cioffi, N.; Torsi, L.; Sabbatini, L. Analytical Investigations of Poly(Acrylic Acid) Coatings Electrodeposited on Titanium-Based Implants: A Versatile Approach to Biocompatibility Enhancement. *Anal. Bioanal. Chem.* 2007, *389* (7–8), 2055–2063. https://doi.org/10.1007/s00216-007-1299-7.

(62) Luo Zheng, L.; Vanchinathan, V.; Dalal, R.; Noolandi, J.; Waters, D. J.; Hartmann, L.; Cochran, J. R.; Frank, C. W.; Yu, C. Q.; Ta, C. N. Biocompatibility of Poly(Ethylene Glycol) and Poly(Acrylic Acid) Interpenetrating Network Hydrogel by Intrastromal Implantation in Rabbit Cornea: Biocompatibility of Poly(Ethylene Glycol) and Poly(Acrylic Acid). *J. Biomed. Mater. Res. A* 2015, *103* (10), 3157–3165. https://doi.org/10.1002/jbm.a.35453.

(63) Philippova, O. E.; Hourdet, D.; Audebert, R.; Khokhlov, A. R. PH-Responsive Gels of Hydrophobically Modified Poly(Acrylic Acid). *Macromolecules* 1997, *30* (26), 8278–8285. https://doi.org/10.1021/ma970957v.

(64) Philippova, O. E.; Hourdet, D.; Audebert, R.; Khokhlov, A. R. Interaction of Hydrophobically Modified Poly(Acrylic Acid) Hydrogels with Ionic Surfactants. *Macromolecules* 1996, *29* (8), 2822–2830. https://doi.org/10.1021/ma951006p.

(65) Elliott, J. E.; Macdonald, M.; Nie, J.; Bowman, C. N. Structure and Swelling of Poly(Acrylic Acid) Hydrogels: Effect of PH, Ionic Strength, and Dilution on the Crosslinked Polymer Structure. *Polymer* 2004, *45* (5), 1503–1510. https://doi.org/10.1016/j.polymer.2003.12.040.

(66) Brannigan, R. P.; Dove, A. P. Synthesis, Properties and Biomedical Applications of Hydrolytically Degradable Materials Based on Aliphatic Polyesters and Polycarbonates. *Biomater. Sci.* 2017, *5* (1), 9–21. https://doi.org/10.1039/C6BM00584E.

(67) Weyers, R. E.; Blankenhorn, P. R.; Stover, L. R.; Kline, D. E. Effects of Sterilization Procedures on the Tensile Properties of Polycarbonate. *J. Appl. Polym. Sci.* 1978, *22* (7), 2019–2024. https://doi.org/10.1002/app.1978.070220722.

(68) Akash, S. Z.; Lucky, F. Y.; Hossain, M.; Bepari, A. K.; Rahman, G. M. S.; Reza, H. M.; Sharker, S. Md. Remote Temperature-Responsive Parafilm Dermal Patch for On-Demand Topical Drug Delivery. *Micromachines* 2021, *12* (8), 975. https://doi.org/10.3390/mi12080975.

(69) Lyu, S.; Untereker, D. Degradability of Polymers for Implantable Biomedical Devices. *Int. J. Mol. Sci.* 2009, *10* (9), 4033–4065. https://doi.org/10.3390/ijms10094033.

(70) Cristea, D.; Ghiuță, I.; Munteanu, D. Tantalum Based Materials for Implants and Prostheses Applications. *Bull. Transilv. Univ. Bras.* 2015, *8* (2), 8.

(71) Namur, R. S.; Reyes, K. M.; Marino, C. E. B. Growth and Electrochemical Stability of Compact Tantalum Oxides Obtained in Different Electrolytes for Biomedical

Applications. *Mater. Res.* 2015, *18* (suppl 2), 91–97. https://doi.org/10.1590/1516-1439.348714.

(72) Eliaz, N. Corrosion of Metallic Biomaterials: A Review. *Materials* 2019, *12* (3), 407. https://doi.org/10.3390/ma12030407.

(73) Miranda, I.; Souza, A.; Sousa, P.; Ribeiro, J.; Castanheira, E. M. S.; Lima, R.; Minas, G. Properties and Applications of PDMS for Biomedical Engineering: A Review. *J. Funct. Biomater.* 2021, *13* (1), 2. https://doi.org/10.3390/jfb13010002.

CHAPTER FOUR

AN X-RAY INTERROGATED FALLING BEAD SYNOVIAL FLUID VISCOSITY SENSOR FOR EARLY DETECTION OF PROSTHETIC JOINT INFECTIONS

4.1. Abstract

Prosthetic joint infections are a major complication for patients undergoing joint surgery. Available diagnostic tests are nonspecific to prosthetic joint infections and based on serum or synovial biomarkers or culture methods which have their own disadvantages. Synovial fluid viscosity is one of the parameters defining the rheology properties of synovial fluid. during infection, the viscosity of synovial fluid decreases and it may be useful as a diagnostic tool for prosthetic joint infections and may provide complementary information regarding prosthetic joint infections. A falling bead synovial fluid viscosity sensor was developed with the aim of using X-ray radiography to determine the rate at which the bead falls which would be indicative of infection. The sensor consists of a radiopaque bead moving in synovial fluid in a plastic tube with a scale and the rate of movement of the bead can be measured by taking a series of X-ray images. Several strategies for the viscosity sensor are discussed. A reference fluid containing fluid relevant to clinically determined viscosity threshold was important way to compare and improve viscosity resolution. The moving bead synovial fluid viscosity sensor has the potential to be an important diagnostic tool noninvasive measurements of synovial fluid viscosity measurements would be helpful in detection of prosthetic joint infections, early.

4.2. Introduction

Prosthetic joint infections are infections involving the joint prosthesis and adjacent tissue. Periprosthetic joint infection accounts for 25% of failed knee arthroplasties and 15% of failed hip arthroplasties.[1–3] Prosthetic joint infections remain a challenging complication due to difficulties in diagnosis, unpredictability of occurrence, frequent need for prolonged antimicrobial therapy and multiple surgeries.[2,4,5] When infections are detected early (within 3 weeks of symptoms or 30 days of surgery), they can often be treated via antibiotics along with surgical irrigation and debridement.[2,6,7] After this time, however, treatment usually requires implant removal followed by reinsertion of the implant after the infection is eradicated. These revisions carry significant risks for patient mobility, other morbidities, and mortality (5% 2-month mortality following prosthetic joint infection in 2015)[8] as well as staggering hospital costs. Direct costs of prosthetic joint infection treatment are around $100,000 per episode,[9] and lifetime treatment cost for a 65-year-old is an estimated $390,806.[10] Therefore, the ability to easily detect and monitor early infection during healing would be key to reducing the need for costly revision surgeries.

Diagnosis of prosthetic joint infections is based upon a combination of clinical findings, laboratory results from peripheral blood and synovial fluid, microbiological data, histological evaluation of periprosthetic tissue, intraoperative inspection, and, in some cases, radiographic results.[4,11,12] There is no one test or finding that is 100% accurate for prosthetic joint infection diagnosis. A set of clinical guidelines have being published by the Musculoskeletal Infection Society (MSIS) for prosthetic joint infections which have been useful in the diagnosis.[13,14] The tests based on serum biomarkers currently in use are

highly sensitive such as erythrocyte sedimentation rate (ESR), C-reactive protein levels (CRP), and serum white cell counts (WBC),[15–17] however they are less specific to prosthetic joint infections since these markers are elevated in any type of inflammation or infection.[18] Microbiological cultures require time and are not always successful in isolating the infecting organisms and may result in false positive results.[14] Molecular imaging approaches like positron emission tomography (PET), single-photon emission computed tomography (SPECT), or sophisticated magnetic resonance imaging (MRI) can detect some relevant disease features but are expensive and not available everywhere.[19–21] Polymerase chain reaction (PCR) and gene sequencing also show promise but are not routine at present.[2,6,22] Radiographs are also routinely used in preclinical research and is useful to screen for prosthetic loosening and fracture[20] but lacks sensitivity and specificity to detect prosthetic joint infections.

Since systemic blood biomarkers of infection are often absent at early stages of joint infections when the infection is nascent and localized, arthrocentesis (synovial fluid aspiration) is commonly used to detect and confirm infection when suspected from clinical examination and radiology.[23–25] Aspirated synovial fluid samples are submitted for WBC count and differential, crystal analysis, Gram stain, and bacterial culture cultures. The methods suffer from low specificity (WBC count), or less sensitivity (Gram stain) long analysis time (bacterial culture).[12,22,26] Recently, there has been increasing interest in potential use of synovial fluid biomarkers to achieve rapid diagnosis of joint infections.[1,26–28] The most frequently studied synovial fluid markers with high diagnostic utility in the diagnosis of joint infections are synovial fluid C-reactive protein,[25,29,30] leukocyte

esterase,[31–33] interleukins,[17,34,35] and alpha-defensin.[36–39] Currently, some biomarkers used for prosthetic infection diagnosis include leukocyte esterase (using colorimetric test strips)[33,40] and alpha defensin (laboratory-based ELISA alpha-defensin test and the commercially available Synovasure™ test kit).[33,41,42] The immunoassay of aspirated joint fluid for alpha-defensin molecules was shown to have high sensitivity and specificity for diagnosing periprosthetic infection.[28] However, a drawback of these tests for biomarkers is that they can be performed only after synovial fluid is collected via arthrocentesis, which is not practical for routine screening or serial monitoring during treatment due to high cost of fluoroscopy and/or ultrasound guidance by radiologist, possible tissue damage or allergic reaction from anesthetics or injected X-ray contrast agent, and possible potential risk of infecting a previously aseptic joint.[23,24] In addition, substantial dilution of synovial fluid with saline or blood during collection (caused by the presence of a hemarthrosis or a dry tap), results in poor quality synovial fluid specimens with diluted biomarkers, decreasing the sensitivity of the laboratory testing.[43,44] Thus, noninvasive screening of the implantation site for detection of early infection is needed.

We are developing a synovial fluid sensor that can be attached to implants that will enable measurement of synovial fluid viscosity in vivo using X-ray imaging technique. Viscosity (a measure of a fluid's resistance to flow) is one of the parameters defining the rheology properties of synovial fluid. Viscosity of synovial fluid can be checked by observing the length of the string formed as the syringe is pulled away from the slide where normal fluid will form a string 5 to 8 cm in length before breaking.[23,45] The main constituents of human synovial fluid are proteins, lipids, and hyaluronic acid, which can

have a significant effect on the rheological properties.[46–48] Hyaluronic acid is the macromolecule which provides synovial fluid with its viscoelastic properties.[47,49] It has been shown that the concentration of hyaluronic acid in synovial fluid is in a close relationship with synovial fluid viscosity.[50] They showed that the synovial fluid acts as an effective lubricant for the synovium membrane if it contains hyaluronic acid with an intrinsic viscosity of about 4,000 mL/g or higher, and a concentration of greater than 0.5 mL/g. Studies show viscosity was lowered with low hyaluronic acid,[51] and a negative correlation was observed between total protein concentration and synovial fluid viscosity properties.[46,52]

Previously, few studies have been done on using synovial fluid as a diagnostic marker of prosthetic joint infections. Galandakova et al. found that synovial fluid viscosity of patients with aseptic loosening differed from patients with osteoarthritis[53] and a study by Fu et al.[46] reported significantly lower viscosity in patients with prosthetic joint infection (7.93 mPas, range 3.0-15.0) compared to the aseptic failure (13.11 mPas, range 6.3-20.4) as shown in Figure 4.1.[46] They determined the optimal threshold value for synovial fluid viscosity for the diagnosis of prosthetic joint infections to be 11.80 mPas, and in their study synovial fluid viscosity outperformed CRP, ESR, and plasma D-dimer, with a sensitivity of 93.33% and a specificity of 66.67%.[46] The decrease in viscosity of the fluid during infection may be due to degradation of hyaluronic acid in the synovial fluid by proteolytic action of lysozymes released by polymorphonuclear cells or bacteria.[45,46] Therefore, synovial fluid viscosity can be considered as a promising marker for the diagnosis of prosthetic joint infections.

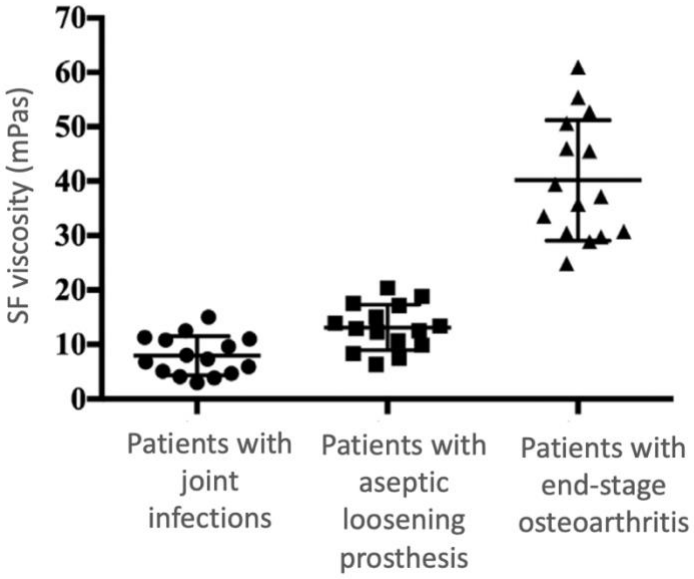

Figure 4.1: Synovial fluid viscosity levels among patients with prosthetic joint infections, aseptic loosening, and end stage osteoarthritis (reproduced with permission from Reference 46, The Journal of Arthroplasty, 2019).

The synovial fluid viscosity sensor we are developing is based on the time it takes for a radiopaque bead to move through the fluid in a tube (test sensor) and will be compared with movement of a bead in reference tube with normal synovial fluid viscosity (reference). Schematic representation is shown in Figure 4.2. The movement of the bead will be visualized using a series of X-ray images in order to determine time. Radiology is used as the preferred mode of visualization since it provides a rapid, noninvasive imaging technique, available in almost all medical settings. During infection, due to lowering of the viscosity of synovial fluid than normal, it is expected for the bead to fall faster in the test sensor compared to the reference.[46,54] Several sensor design approaches are discussed in slowing down the dense radiopaque beads in order to obtain radiographs within a

measurable time and making use of wall effects from angle-dependent rolling on the tube walls. The use of a reference fluid in a separate tube was also an important way to improve viscosity resolution, especially near clinically determined viscosity thresholds. Thus, noninvasive measurements of synovial fluid viscosity measurements would be helpful in detection of prosthetic joint infections, early.

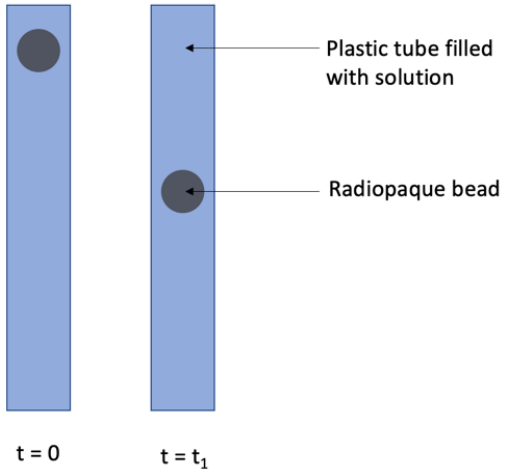

Figure 4.2: Schematic of falling bead synovial fluid viscosity sensor.

4.3. Materials and Methods

4.3.1. Materials

Glycerol was purchased from VWR Chemicals BDH®, West Chester, PA, polyethylene glycol (PEG) with molecular weight 1000 and paraffin wax beads were purchased from Spectrum Chemical Mfg. Corp, Gardena, CA. Plastic polyolefin tubes were purchased from Sopby on Amazon.com, Inc. Tantalum beads (0.394 mm diameter) were purchased

from X-Medics, Frederiksberg, Denmark. Tungsten microparticles were purchased from. Bovine synovial fluid was obtained from Lampire Biological Labs, Pipersville, PA.

4.3.2. Preparation of glycerol and polyethylene glycol solutions of different viscosities

The glycerol/ water and polyethylene glycol/ water solutions of varying viscosities corresponding to the physiological relevant values (~1-20 mPas) were prepared based on literature. Glycerol solutions were prepared between 10, 30. 60, 70 weight % glycerol/water for viscosities of 1.31, 2.50, 10.80 and 22.50 mPas, respectively based on previously reported values.[55,56] Polyethylene glycol (PEG) with molecular weight 1000 was used for the experiments with PEG and the solutions were prepared based on PEG viscosity measurements by Gonzalez-Tello et al.[57] The PEG/ water solutions used for the experiments were between 10, 20, 30, 40, 50 weight % for viscosities of 5.2, 6.7, 9.2, 13.2, and 24.4 mPas, respectively.

4.3.3. X-ray interrogated falling bead synovial fluid viscosity sensor based on radiopaque tantalum bead

Glycerol solution (60 weight %) was prepared which correspond to viscosity of 10.8 mPas, which is the average viscosity relevant to synovial fluid. A plastic tube (1.5 mm diameter) sealed at one end with a binder clip was filled with the 60 weight % glycerol solution and placed on a vertical surface with a scale attached to it. A tantalum bead (diameter: 0.394 mm) was allowed to freely fall through the solution and the time taken for the bead to fall was determined by taking a video at 30 frames per second.

In order to slow down the tantalum bead, a piece of Styrofoam was attached to the tantalum bead using a small amount of commercially available adhesive (Loctite Superglue Gel Control, Rocky Hill, CT). The bead was then allowed to freely fall through the glycerol solution (60 weight %) solution and the time taken for the bead to fall was determined by taking a video at 30 frames per second.

4.3.4. Angle dependence of tantalum bead movement in glycerol and bovine synovial fluid

A plastic tube sealed at one end was filled with the 60 weight % glycerol solution (corresponding to ~10 mPas viscosity), a tantalum bead was added to it and the tube was sealed at the open end (reference sensor). Another sensor was prepared by filling another plastic tube with bovine synovial fluid, a tantalum bead was added to it and the tube was sealed (test sensor). The sensor was attached to an inclinometer, which gives a measure of the angle. The movement of the bead was measured at different angles in both the test and reference sensor by taking videos for each at 30 frames per second.

4.3.5. X-ray interrogated falling bead synovial fluid viscosity sensor based on tungsten microparticle encapsulated paraffin wax bead

A bead containing tungsten microparticles in paraffin wax was prepared as another strategy to obtain a bead with the desired speed in viscosity relevant to synovial fluid. The bead was prepared by encapsulating tungsten microparticles in melted paraffin wax and allowed to cool. The bead was then allowed to freely fall through the glycerol solution (60 weight %) solution and the time taken for the bead to fall was determined by taking a video at 30

frames per second. In order to study the velocity of the bead at different viscosities, the velocity of the bead was studied at physiologically relevant viscosities between ~1 and 20 mPas in both glycerol and PEG solutions. Solutions of glycerol were prepared between 10-70 weight % glycerol/ water (corresponding to viscosities between 1.31 and 22.50 mPas, respectively). Solutions of PEG were prepared between 10-50 weight% glycerol/ water (corresponding to viscosities between 5.2 and 24.4 mPas, respectively). The bead was allowed to freely fall through each solution and the time taken for the bead to fall was determined by taking a video at 30 frames per second for each.

4.3.6. Testing the falling bead synovial viscosity sensor in an arm

The sensor was prepared by filling a plastic tube with 60 weight % glycerol solution (corresponding viscosity 10.8 mPas). The tungsten microparticle encapsulated paraffin wax bead added to the tube. The tube was then sealed on the open end and taped to a ruler and the whole set up was taped to the arm to resemble the sensor in the elbow joint. The arm was allowed to rest on a horizontal surface and the arm was moved by 45 degrees and 90 degrees and a video (at 30 frames per second) of the sensor was recorded for each. The time taken for the bead to fall was determined from the video.

4.4. Results and Discussion

Synovial fluid is a viscous, straw colored, transparent fluid secreted into joint cavity by the inner membrane of synovial joint (synovial membrane) and provides shock

absorption, lubrication, and nutrition to adjacent articular cartridge.[23,49] Hyaluronic acid, high-molecular-weight polymerized glycosaminoglycan, in synovial fluid is responsible for its unique consistency and high viscosity of synovial fluid.[47,50] Synovial fluid in animals and humans is non-Newtonian with shear thinning properties (fluid whose viscosity decreases with increasing shear rate).[45,54] It is also elastic and thixotropic showing a yield stress and in conditions of inflammation or infection, the flow properties of synovial fluid changes. The fluid becomes less viscous, behaves more like a Newtonian fluid, and loses its elasticity and thixotropy. The reason for decrease in viscosity during inflammation/ infection may be due to fragmentation of hyaluronate by the proteolytic action of lysozymes released by polymorphonuclear cells resulting in decreased concentration of hyaluronic acid and low viscosity of synovial fluid.[47,58]

The falling bead synovial fluid viscosity sensor aims to measures the rate/ time of a falling bead in synovial fluid using X-ray radiography. The bead movement in a fluid is based on Stokes' Law, the drag force (*f*) on the metal sphere is proportional to the viscosity of the fluid η, the radius *r* of the sphere, and the velocity (or speed) *v* of the sphere as:

$$f = 6\pi\eta r v \tag{4.1}$$

The ball approaches its terminal velocity through an exponential decay and then it falls with a constant velocity when the gravitational force is equal to the buoyant force. As shown in Equation 4.2, where ρ_b is the density of the bead, ρ_l is the density of the fluid and *g* is acceleration due to gravity.

$$v_f = \frac{2r^2 (\rho_b - \rho_l) g}{9\,\eta} \tag{4.2}$$

From the Equation 4.2, it can be derived that the terminal velocity of the bead is indirectly proportional to viscosity of the fluid. For typical ball size and mass as used in this sensor design, the time constant to reach terminal velocity is negligibly small) and can be safely ignored. Other factors may affect the terminal velocity such as the object falling near a boundary (like the wall of the container) moves more slowly than an object falling far from a wall.[59,60] Therefore, since there is a decrease in viscosity of synovial fluid during infections, the bead would move at a slower rate during infections when compared to normal and by the use of a radiopaque bead this movement can be visualized using X-ray imaging. In the design of the falling bead synovial fluid viscosity sensor, the sensor needs to able to see difference in viscosities 7 mPas or less since the clinically relevant values are between 3.0-15.0 mPas.[46] The sensor will be attached to prosthesis and the patient can be asked to move the joint by 45 degrees or could roll patient lying on one side to the other side. There should be at least 10 s between raising leg and taking X-ray (expect operator to be +/- 1 s or more). Therefore, the bead velocity needs to be a minimum of 1 mm/s at 10 mPas for reliable measurements using X-ray.

4.4.1. X-ray interrogated falling bead synovial fluid viscosity sensor based on radiopaque tantalum bead

For X-ray imaging of sensor, the bead needs to be radiopaque, or a radiopaque marker should be attached to it. A sensor was prepared by filling a plastic tube with glycerol adjusted to 10 mPas to mimic synovial fluid average viscosity (Figure 4.3a) and the time

taken for a tantalum bead (diameter: 0.394 mm, density: 16654 kg m^{-3}) was measured. The time was too fast to be used for the measurements, therefore several strategies were used to slow down the bead. Another sensor was prepared where a small piece of Styrofoam was attached to the to the tantalum bead (diameter: 0.394 mm, density: 16654 kg m^{-3}) (Figure 4.3b) and its velocity in 10 mPas glycerol solution was measured. The attachment of a less dense material like Styrofoam slowed the movement of the tantalum bead by about 0.67 cm/s.

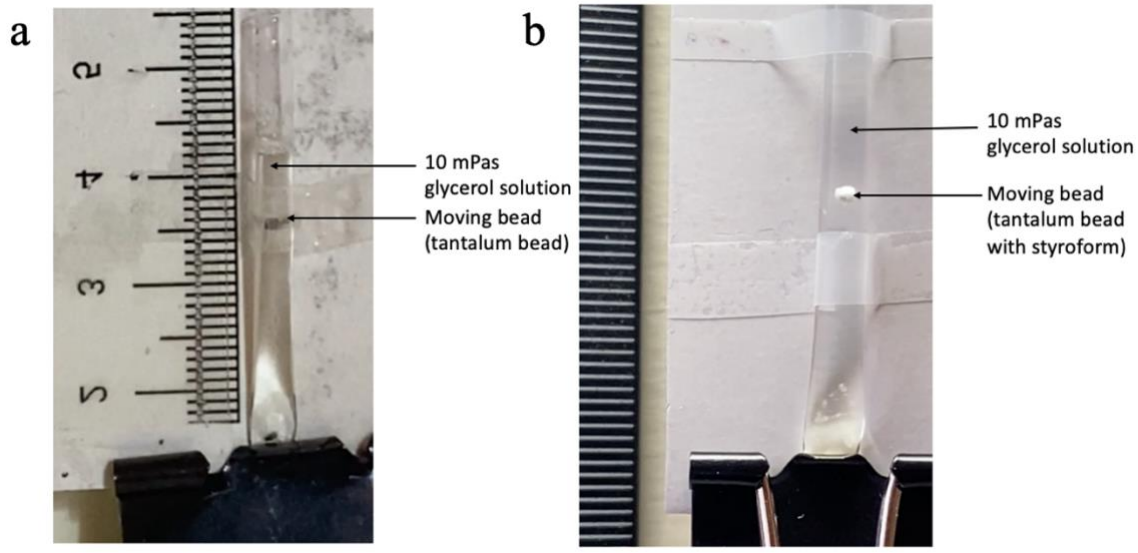

Figure 4.3: (a) Tantalum bead (0.394 mm) moving inside a plastic tube in 10 mPas glycerol solution, (b) Tantalum bead (0.394 mm) attached to Styrofoam moving inside a plastic tube in 10 mPas glycerol solution.

4.4.2. Angle dependence of tantalum bead movement in glycerol and bovine synovial fluid

The beads need to be slowed down so that at 10 mPas, it would need to travel 1 cm in about at least 10 seconds (velocity of 1 mm/s). Another way to slow down would be to measure the time taken for the bead to fall at different angles. For this, experiments were carried out to determine the angle dependence on the velocity of the tantalum bead (0.394 mm diameter). The tantalum bead was allowed to fall through a bovine synovial fluid in one tube, and a glycerol solution of 10 mPas viscosity in another tube (which acts as the reference) at different angles using an inclinometer as shown in Figure 4.4.

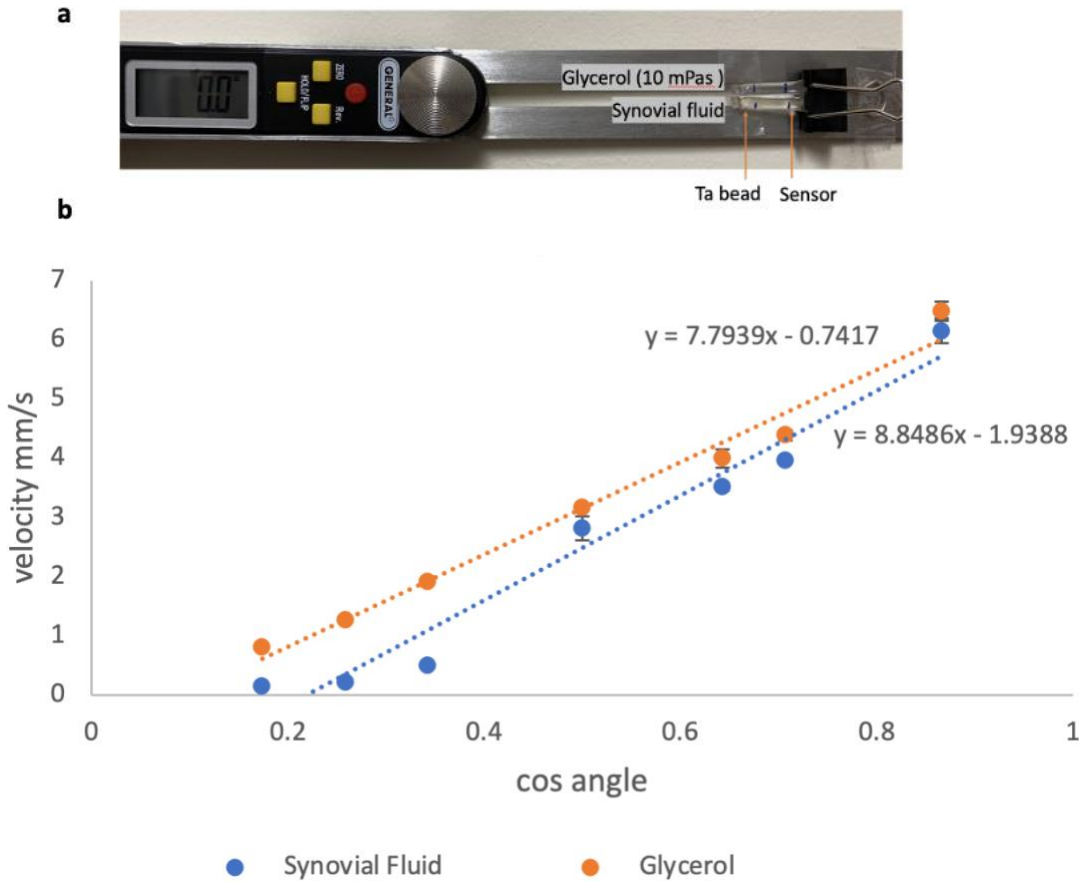

Figure 4.4: (a) Setup used to measure the angle dependence of the viscosity sensor showing the tube with glycerol adjusted to 10 mPas and tube with bovine synovial fluid, each containing a tantalum bead (0.394 mm diameter), (b) Velocity versus cosine angle for the movement of tantalum bead in glycerol (10 mPas) and synovial fluid.

4.4.3. X-ray interrogated falling bead synovial fluid viscosity sensor based on tungsten microparticles embedded in paraffin wax

Another strategy was to embed tungsten microparticles in paraffin wax (density of ~0.9 g/cm^2) to make a bead (Figure 4.5a) and the velocity was measured. Results showed adding paraffin works to slow down the velocity of the bead. A calibration graph was prepared for the movement of the bead in both glycerol and polyethylene glycol (PEG) (Figure 4.5b). The results showed a good linear curve of time vs. viscosity in both PEG and glycerol solutions. However, viscosities by PEG or glycerol should completely overlap and pass through the intercept, which can only be seen for PEG (glycerol about 0.1 seconds high). A problem encountered was that when the bead was slowed down, at higher viscosities the density comes into effect, and it started to float.

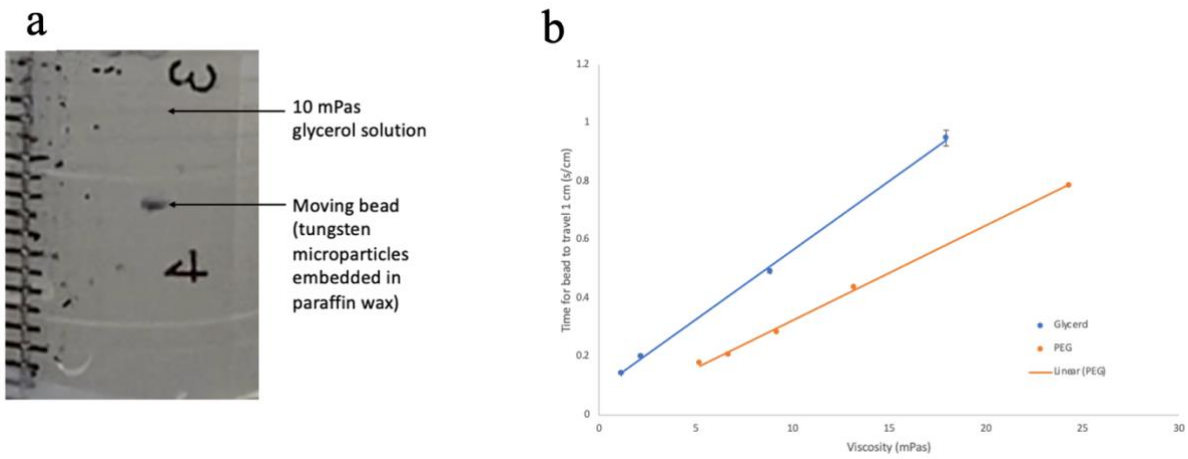

Figure 4.5: (a) Bead made of tungsten microparticles embedded in paraffin wax moving inside a heat shrink tube in 10 mPas glycerol solution, (b) Time for bead to travel 1 cm versus viscosity for the tungsten particles in wax bead in glycerol and PEG adjusted to the relevant viscosity.

4.4.4. Testing the falling bead synovial viscosity sensor in an arm

In order to show the proof of concept, the sensor was attached to arm and time measurements for the bead to fall after moving the arm by 45 degrees and 90 degrees was measured as shown in Figure 4.6. The sensor was prepared by filling a plastic tube with glycerol adjusted to 10 mPas. The tube was then sealed on the open end and taped to a ruler and the whole set up was taped to the arm to resemble the sensor in the elbow joint.

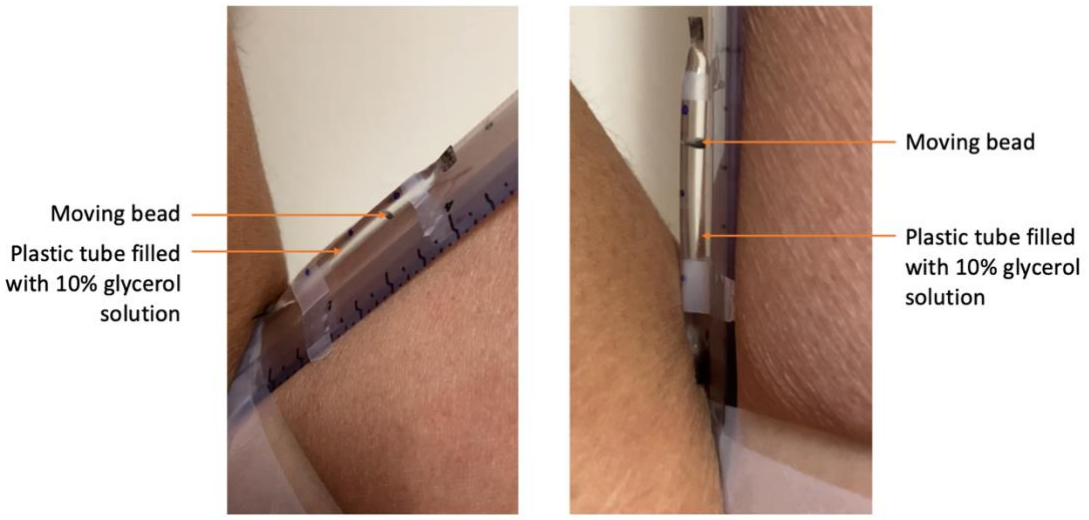

Figure 4.6: The proof of concept of falling bead synovial fluid viscosity sensor attached to an arm. The images show the movement of the bead after moving the arm by 45 degrees (left) and after moving the arm by 90 degrees (right).

4.4.5. Limitations

Since the goal is to visualize the sensor radiographically, it is critical for the moving bead to be radiopaque or have a radiopaque marker. Radiopaque materials have high density, therefor ethe challenge is to slow the movement of the bead in order to be able to take at least two X-ray images. Ideally, the bead travelling at a velocity of 1 mm/s in a 10 mPas viscous solution will enable us to obtain X-ray images and determine the time taken for the movement of the bead. The tube needs to be made porous in order for the diffusion of external synovial fluid. The sensor will need to be tested in different external solutions to determine its selectivity and effect of surrounding medium.

4.5. Conclusions

A falling bead synovial fluid viscosity sensor was developed to determine infections early during prosthetic joint infections by X-ray radiography. The sensor consists of a radiopaque bead in synovial fluid inside a plastic tube with a scale and the rate of movement of the bead can be measured by taking a series of X-ray images. A change in rate/ time taken for the bead to fall will be an indication of infections due to decrease in viscosity during infections. The tube with a reference fluid adjusted to the viscosity of the normal synovial fluid will provide a way of comparing the viscosity, in vivo. Improvements need to be made with regard to making the sensor be slow enough to enable X-ray imaging. The moving bead synovial fluid viscosity sensor has the potential to provide noninvasive measurements of synovial fluid viscosity measurements in detection of prosthetic joint infections, early.

4.6. References

(1) Deirmengian, C.; Kardos, K.; Kilmartin, P.; Cameron, A.; Schiller, K.; Parvizi, J. Diagnosing Periprosthetic Joint Infection: Has the Era of the Biomarker Arrived? *Clin. Orthop. Relat. Res.* 2014, *472* (11), 3254–3262. https://doi.org/10.1007/s11999-014-3543-8.

(2) Abad, C. L.; Haleem, A. Prosthetic Joint Infections: An Update. *Curr. Infect. Dis. Rep.* 2018, *20* (7), 15. https://doi.org/10.1007/s11908-018-0622-0.

(3) Del Pozo, J. L.; Patel, R. Infection Associated with Prosthetic Joints. *N. Engl. J. Med.* 2009, *361* (8), 787–794. https://doi.org/10.1056/NEJMcp0905029.

(4) Esposito, S.; Leone, S. Prosthetic Joint Infections: Microbiology, Diagnosis, Management and Prevention. *Int. J. Antimicrob. Agents* 2008, *32* (4), 287–293. https://doi.org/10.1016/j.ijantimicag.2008.03.010.

(5) Berbari, E. F.; Hanssen, A. D.; Duffy, M. C.; Steckelberg, J. M.; Ilstrup, D. M.; Harmsen, W. S.; Osmon, D. R. Risk Factors for Prosthetic Joint Infection: Case-Control Study. *Clin. Infect. Dis.* 1998, *27* (5), 1247–1254. https://doi.org/10.1086/514991.

(6) Ricciardi, B. F.; Muthukrishnan, G.; Masters, E. A.; Kaplan, N.; Daiss, J. L.; Schwarz, E. M. New Developments and Future Challenges in Prevention, Diagnosis, and Treatment of Prosthetic Joint Infection. *J. Orthop. Res.* 2020, *38* (7), 1423–1435. https://doi.org/10.1002/jor.24595.

(7) Betsch, B. Y.; Eggli, S.; Siebenrock, K. A.; Täuber, M. G.; Mühlemann, K. Treatment of Joint Prosthesis Infection in Accordance with Current Recommendations Improves Outcome. *Clin. Infect. Dis.* 2008, *46* (8), 1221–1226. https://doi.org/10.1086/529436.

(8) Kurtz, S. M.; Lau, E. C.; Son, M.-S.; Chang, E. T.; Zimmerli, W.; Parvizi, J. Are We Winning or Losing the Battle With Periprosthetic Joint Infection: Trends in Periprosthetic Joint Infection and Mortality Risk for the Medicare Population. *J. Arthroplasty* 2018, *33* (10), 3238–3245. https://doi.org/10.1016/j.arth.2018.05.042.

(9) Garfield, K.; Noble, S.; Lenguerrand, E.; Whitehouse, M. R.; Sayers, A.; Reed, M. R.; Blom, A. W. What Are the Inpatient and Day Case Costs Following Primary Total Hip Replacement of Patients Treated for Prosthetic Joint Infection: A Matched Cohort Study Using Linked Data from the National Joint Registry and Hospital Episode Statistics. *BMC Med.* 2020, *18* (1), 335. https://doi.org/10.1186/s12916-020-01803-7.

(10) Svensson, K. Diagnosis and Management of Periprosthetic Joint Infections. 2020.

(11) Akoh, J. A. Peritoneal Dialysis Associated Infections: An Update on Diagnosis and Management. *World J. Nephrol.* 2012, *1* (4), 106. https://doi.org/10.5527/wjn.v1.i4.106.

(12) Porrino, J.; Wang, A.; Moats, A.; Mulcahy, H.; Kani, K. Prosthetic Joint Infections: Diagnosis, Management, and Complications of the Two-Stage Replacement Arthroplasty. *Skeletal Radiol.* 2020, *49* (6), 847–859. https://doi.org/10.1007/s00256-020-03389-w.

(13) Parvizi, J.; Zmistowski, B.; Berbari, E. F.; Bauer, T. W.; Springer, B. D.; Della Valle, C. J.; Garvin, K. L.; Mont, M. A.; Wongworawat, M. D.; Zalavras, C. G. New Definition for Periprosthetic Joint Infection: From the Workgroup of the Musculoskeletal Infection Society. *Clin. Orthop.* 2011, *469* (11), 2992–2994. https://doi.org/10.1007/s11999-011-2102-9.

(14) Alijanipour, P.; Bakhshi, H.; Parvizi, J. Diagnosis of Periprosthetic Joint Infection: The Threshold for Serological Markers. *Clin. Orthop. Relat. Res.* 2013, *471* (10), 3186–3195. https://doi.org/10.1007/s11999-013-3070-z.

(15) Garcia-Tsao, G.; Conn, H. O.; Lerner, E. The Diagnosis of Bacterial Peritonitis: Comparison of PH, Lactate Concentration and Leukocyte Count. *Hepatology* 1985, *5* (1), 91–96. https://doi.org/10.1002/hep.1840050119.

(16) Keemu, H.; Vaura, F.; Maksimow, A.; Maksimow, M.; Jokela, A.; Hollmén, M.; Mäkelä, K. Novel Biomarkers for Diagnosing Periprosthetic Joint Infection from Synovial Fluid and Serum. *JBJS Open Access* 2021, *6* (2). https://doi.org/10.2106/JBJS.OA.20.00067.

(17) Saleh, A.; George, J.; Faour, M.; Klika, A. K.; Higuera, C. A. Serum Biomarkers in Periprosthetic Joint Infections. *Bone Jt. Res.* 2018, *7* (1), 85–93. https://doi.org/10.1302/2046-3758.71.BJR-2017-0323.

(18) Shahi, A.; Parvizi, J. The Role of Biomarkers in the Diagnosis of Periprosthetic Joint Infection. *EFORT Open Rev.* 2016, *1* (7), 275–278. https://doi.org/10.1302/2058-5241.1.160019.

(19) Cyteval, C.; Bourdon, A. Imaging Orthopedic Implant Infections. *Diagn. Interv. Imaging* 2012, *93* (6), 547–557. https://doi.org/10.1016/j.diii.2012.03.004.

(20) Potapova, I. Functional Imaging in Diagnostic of Orthopedic Implant-Associated Infections. *Diagnostics* 2013, *3* (4), 356–371. https://doi.org/10.3390/diagnostics3040356.

(21) Odekerken, J. C. E.; Brans, B. T.; Welting, T. J. M.; Walenkamp, G. H. I. M. ^{18}F-FDG MicroPET Imaging Differentiates between Septic and Aseptic Wound Healing after Orthopedic Implant Placement: A Longitudinal Study of an Implant

Osteomyelitis in the Rabbit Tibia. *Acta Orthop.* 2014, *85* (3), 305–313. https://doi.org/10.3109/17453674.2014.900894.

(22) Jacovides, C. L.; Parvizi, J.; Adeli, B.; Jung, K. A. Molecular Markers for Diagnosis of Periprosthetic Joint Infection. *J. Arthroplasty* 2011, *26* (6), 99-103.e1. https://doi.org/10.1016/j.arth.2011.03.025.

(23) Brannan, S. R.; Jerrard, D. A. Synovial Fluid Analysis. *J. Emerg. Med.* 2006, *30* (3), 331–339. https://doi.org/10.1016/j.jemermed.2005.05.029.

(24) Guenther, L. E.; Pyle, B. W.; Turgeon, T. R.; Bohm, E. R.; Wyss, U. P.; Schmidt, T. A.; Brandt, J.-M. Biochemical Analyses of Human Osteoarthritic and Periprosthetic Synovial Fluid. *Proc. Inst. Mech. Eng. [H]* 2014, *228* (2), 127–139. https://doi.org/10.1177/0954411913517880.

(25) Fink, B.; Makowiak, C.; Fuerst, M.; Berger, I.; Schäfer, P.; Frommelt, L. The Value of Synovial Biopsy, Joint Aspiration and C-Reactive Protein in the Diagnosis of Late Peri-Prosthetic Infection of Total Knee Replacements. *J. Bone Joint Surg. Br.* 2008, *90-B* (7), 874–878. https://doi.org/10.1302/0301-620X.90B7.20417.

(26) Lee, Y. S.; Koo, K.-H.; Kim, H. J.; Tian, S.; Kim, T.-Y.; Maltenfort, M. G.; Chen, A. F. Synovial Fluid Biomarkers for the Diagnosis of Periprosthetic Joint Infection: A Systematic Review and Meta-Analysis. *J. Bone Jt. Surg.* 2017, *99* (24), 2077–2084. https://doi.org/10.2106/JBJS.17.00123.

(27) Deirmengian, C.; Hallab, N.; Tarabishy, A.; Della Valle, C.; Jacobs, J. J.; Lonner, J.; Booth, R. E. Synovial Fluid Biomarkers for Periprosthetic Infection. *Clin.*

Orthop. Relat. Res. 2010, *468* (8), 2017–2023. https://doi.org/10.1007/s11999-010-1298-4.

(28) Figueiredo, A.; Ferreira, R.; Alegre, C.; Judas, F.; Fonseca, F. Diagnosis of Periprosthetic Joint Infection from from Novel Synovial Fluid Biomarkers to Identification of the Etiological Agent. *Bone Res.* 2018, *2* (4), 555594.

(29) Parvizi, J.; McKenzie, J. C.; Cashman, J. P. Diagnosis of Periprosthetic Joint Infection Using Synovial C-Reactive Protein. *J. Arthroplasty* 2012, *27* (8), 12–16. https://doi.org/10.1016/j.arth.2012.03.018.

(30) Parvizi, J.; Jacovides, C.; Adeli, B.; Jung, K. A.; Hozack, W. J. Mark B. Coventry Award: Synovial C-Reactive Protein: A Prospective Evaluation of a Molecular Marker for Periprosthetic Knee Joint Infection. *Clin. Orthop. Relat. Res.* 2012, *470* (1), 54–60. https://doi.org/10.1007/s11999-011-1991-y.

(31) De Vecchi, E.; Romanò, C. L.; De Grandi, R.; Cappelletti, L.; Villa, F.; Drago, L. Alpha Defensin, Leukocyte Esterase, C-Reactive Protein, and Leukocyte Count in Synovial Fluid for Pre-Operative Diagnosis of Periprosthetic Infection. *Int. J. Immunopathol. Pharmacol.* 2018, *32*, 1–6. https://doi.org/10.1177/2058738418806072.

(32) Wyatt, M. C.; Beswick, A. D.; Kunutsor, S. K.; Wilson, M. J.; Whitehouse, M. R.; Blom, A. W. The Alpha-Defensin Immunoassay and Leukocyte Esterase Colorimetric Strip Test for the Diagnosis of Periprosthetic Infection: A Systematic Review and Meta-Analysis. *J. Bone Jt. Surg.* 2016, *98* (12), 992–1000. https://doi.org/10.2106/JBJS.15.01142.

(33) Chen, Y.; Kang, X.; Tao, J.; Zhang, Y.; Ying, C.; Lin, W. Reliability of Synovial Fluid Alpha-Defensin and Leukocyte Esterase in Diagnosing Periprosthetic Joint Infection (PJI): A Systematic Review and Meta-Analysis. *J. Orthop. Surg.* 2019, *14* (1), 453. https://doi.org/10.1186/s13018-019-1395-3.

(34) Gollwitzer, H.; Dombrowski, Y.; Prodinger, P. M.; Peric, M.; Summer, B.; Hapfelmeier, A.; Saldamli, B.; Pankow, F.; von Eisenhart-Rothe, R.; Imhoff, A. B.; Schauber, J.; Thomas, P.; Burgkart, R.; Banke, I. J. Antimicrobial Peptides and Proinflammatory Cytokines in Periprosthetic Joint Infection. *J. Bone Jt. Surg.* 2013, *95* (7), 644–651. https://doi.org/10.2106/JBJS.L.00205.

(35) Lenski, M.; Scherer, M. A. Synovial IL-6 AS Inflammatory Marker in Periprosthetic Joint Infections. *J. Arthroplasty* 2014, *29* (6), 1105–1109. https://doi.org/10.1016/j.arth.2014.01.014.

(36) Berger, P.; Van Cauter, M.; Driesen, R.; Neyt, J.; Cornu, O.; Bellemans, J. Diagnosis of Prosthetic Joint Infection with Alpha-Defensin Using a Lateral Flow Device: A Multicentre Study. *Bone Jt. J.* 2017, *99-B* (9), 1176–1182. https://doi.org/10.1302/0301-620X.99B9.BJJ-2016-1345.R2.

(37) Bingham, J.; Clarke, H.; Spangehl, M.; Schwartz, A.; Beauchamp, C.; Goldberg, B. The Alpha Defensin-1 Biomarker Assay Can Be Used to Evaluate the Potentially Infected Total Joint Arthroplasty. *Clin. Orthop. Relat. Res.* 2014, *472* (12), 4006–4009. https://doi.org/10.1007/s11999-014-3900-7.

(38) Bonanzinga, T.; Zahar, A.; Dütsch, M.; Lausmann, C.; Kendoff, D.; Gehrke, T. How Reliable Is the Alpha-Defensin Immunoassay Test for Diagnosing Periprosthetic

Joint Infection? A Prospective Study. *Clin. Orthop.* 2017, *475* (2), 408–415. https://doi.org/10.1007/s11999-016-4906-0.

(39) Stone, W. Z.; Gray, C. F.; Parvataneni, H. K.; Al-Rashid, M.; Vlasak, R. G.; Horodyski, M.; Prieto, H. A. Clinical Evaluation of Synovial Alpha Defensin and Synovial C-Reactive Protein in the Diagnosis of Periprosthetic Joint Infection. *J. Bone Jt. Surg.* 2018, *100* (14), 1184–1190. https://doi.org/10.2106/JBJS.17.00556.

(40) Deirmengian, C.; Kardos, K.; Kilmartin, P.; Cameron, A.; Schiller, K.; Booth, R. E.; Parvizi, J. The Alpha-Defensin Test for Periprosthetic Joint Infection Outperforms the Leukocyte Esterase Test Strip. *Clin. Orthop.* 2015, *473* (1), 198–203. https://doi.org/10.1007/s11999-014-3722-7.

(41) Ahmad, S. S.; Hirschmann, M. T.; Becker, R.; Shaker, A.; Ateschrang, A.; Keel, M. J. B.; Albers, C. E.; Buetikofer, L.; Maqungo, S.; Stöckle, U.; Kohl, S. A Meta-Analysis of Synovial Biomarkers in Periprosthetic Joint Infection: Synovasure™ Is Less Effective than the ELISA-Based Alpha-Defensin Test. *Knee Surg. Sports Traumatol. Arthrosc.* 2018, *26* (10), 3039–3047. https://doi.org/10.1007/s00167-018-4904-8.

(42) Deirmengian, C.; Kardos, K.; Kilmartin, P.; Gulati, S.; Citrano, P.; Booth, R. E. The Alpha-Defensin Test for Periprosthetic Joint Infection Responds to a Wide Spectrum of Organisms. *Clin. Orthop.* 2015, *473* (7), 2229–2235. https://doi.org/10.1007/s11999-015-4152-x.

(43) Deirmengian, C.; Feeley, S.; Kazarian, G. S.; Kardos, K. Synovial Fluid Aspirates Diluted with Saline or Blood Reduce the Sensitivity of Traditional and

Contemporary Synovial Fluid Biomarkers. *Clin. Orthop.* 2020, *478* (8), 1805–1813. https://doi.org/10.1097/CORR.0000000000001188.

(44) Kerolus, G.; Clayburne, G.; Schumacher, H. R. Is It Mandatory to Examine Synovial Fluids Promptly after Arthrocentesis? *Arthritis Rheum.* 1989, *32* (3), 271–278. https://doi.org/10.1002/anr.1780320308.

(45) Barnett, C. H. Measurement and Interpretation of Synovial Fluid Viscosities. *Ann. Rheum. Dis.* 1958, *17* (2), 229–233. https://doi.org/10.1136/ard.17.2.229.

(46) Fu, J.; Ni, M.; Chai, W.; Li, X.; Hao, L.; Chen, J. Synovial Fluid Viscosity Test Is Promising for the Diagnosis of Periprosthetic Joint Infection. *J. Arthroplasty* 2019, *34* (6), 1197–1200. https://doi.org/10.1016/j.arth.2019.02.009.

(47) Ogston, A. G.; Stanier, J. E. The Physiological Function of Hyaluronic Acid in Synovial Fluid; Viscous, Elastic and Lubricant Properties. *J. Physiol.* 1953, *119* (2–3), 244–252. https://doi.org/10.1113/jphysiol.1953.sp004842.

(48) Tamer, T. M. Hyaluronan and Synovial Joint: Function, Distribution and Healing. *Interdiscip. Toxicol.* 2013, *6* (3), 111–125. https://doi.org/10.2478/intox-2013-0019.

(49) Ropes, M. W.; Bennett, G. A.; Bauer, W. The Origin and Nature of Normal Synovial Fluid. *J. Clin. Invest.* 1939, *18* (3), 351–372. https://doi.org/10.1172/JCI101050.

(50) Swann, D. A.; Radin, E. L.; Nazimiec, M.; Weisser, P. A.; Curran, N.; Lewinnek, G. Role of Hyaluronic Acid in Joint Lubrication. *Ann. Rheum. Dis.* 1974, *33* (4), 318–326. https://doi.org/10.1136/ard.33.4.318.

(51) Mazzucco, D. Variation in Joint Fluid Composition and Its Effect on the Tribology of Replacement Joint Articulation. 286.

(52) Myant, C.; Underwood, R.; Fan, J.; Cann, P. M. Lubrication of Metal-on-Metal Hip Joints: The Effect of Protein Content and Load on Film Formation and Wear. *J. Mech. Behav. Biomed. Mater.* 2012, *6*, 30–40. https://doi.org/10.1016/j.jmbbm.2011.09.008.

(53) Galandáková, A.; Ulrichová, J.; Langová, K.; Hanáková, A.; Vrbka, M.; Hartl, M.; Gallo, J. Characteristics of Synovial Fluid Required for Optimization of Lubrication Fluid for Biotribological Experiments. *J. Biomed. Mater. Res. B Appl. Biomater.* 2017, *105* (6), 1422–1431. https://doi.org/10.1002/jbm.b.33663.

(54) Sundblad, L. The Chemistry of Synovial Fluid with Special Regard to Hyaluronic Acid. *Acta Orthop. Scand.* 1950, *20* (2), 105–113. https://doi.org/10.3109/17453675009043408.

(55) Sheely, M. L. Glycerol Viscosity Tables. *Ind. Eng. Chem.* 1932, *24* (9), 1060–1064. https://doi.org/10.1021/ie50273a022.

(56) Segur, J. B.; Oberstar, H. E. Viscosity of Glycerol and Its Aqueous Solutions. *Ind. Eng. Chem.* 1951, *43* (9), 2117–2120.

(57) Gonzalez-Tello, P.; Camacho, F.; Blazquez, G. Density and Viscosity of Concentrated Aqueous Solutions of Polyethylene Glycol. *J. Chem. Eng. Data* 1994, *39* (3), 611–614. https://doi.org/10.1021/je00015a050.

(58) Jebens, E. H.; Monk-Jones, M. E. On the Viscosity and PH of Synovial Fluid and the PH of Blood. *J. Bone Joint Surg. Br.* 1959, *41* (2), 388–400.

(59) Francis, A. W. Wall Effect in Falling Ball Method for Viscosity. *Physics* 1933, *4* (11), 403–406. https://doi.org/10.1063/1.1745151.

(60) Brizard, M.; Megharfi, M.; Mahé, E.; Verdier, C. Design of a High Precision Falling-Ball Viscometer. *Rev. Sci. Instrum.* 2005, *76* (2), 025109. https://doi.org/10.1063/1.1851471.

CHAPTER FIVE

CONCLUSIONS AND FUTURE WORK

5.1. Conclusions

A new generation of implantable chemical sensors that gives physicians the ability to measure local chemical concentrations from routine radiographs is developed. The approach is especially promising for detecting and monitoring implant-associated infections. The applications of the sensor presented in this dissertation are focused on prosthetic joint infections and aim to develop the first implantable sensors that can be read directly through X-ray imaging for early, non-invasive determination of prosthetic joint infections. The goal is to functionalize X-ray imaging which is a widely available, indispensable tool for detecting and monitoring disease conditions, however, cannot provide any biochemical information.[1,2] The sensors developed here are based on a pH-responsive hydrogel with radiopaque markers in order to enable length measurements using X-ray imaging. The sensors are small enough for integration into a prosthesis and enable local biochemical measurements at the site of the infection itself by X-ray radiography. The sensors use a robust, passive mechanism based on hydrogel swelling chemical equilibrium with minimum effects from the matrix and less susceptible to drift from aging and biofouling and do not require frequent recalibration, or implantation of new sensor devices with time.

Both the synovial fluid pH and carbon dioxide sensors are based on the length changes of polyacrylic acid-based hydrogel in response to pH. The performance of the

hydrogel in vitro in buffer, bovine serum, bovine synovial fluid, human peritoneal fluid shows good linearity and reversibility with minimal effects from the matrix. Previous studies on the performance of the pH-responsive hydrogel in culture media and incubation in highly oxidative environments for a month containing hydrogen peroxide and copper ions also showed similar results, with minimal matrix effects.[3] X-ray images of the synovial pH and carbon dioxide sensor on a hip prosthesis show that the markers are clearly seen in the radiographs. Studies of the sensor in an in vivo model in a rat peritoneal infection study showed the sensor location in the rat clearly and a pH drop was observed during infection not observed in the control. In addition, postmortem measurements showed that the sensors had not drifted or changed calibration after implantation for two weeks. While these results are in a peritoneal cavity rather than a prosthetic hip, they are consistent with in vitro results showing minimal effect from varying the matrices. The carbon dioxide sensor has the additional advantage of the hydrogel being separated from the external environment by a gas-permeable membrane which will significantly reduce the potential for biofouling. Preliminary studies show the potential to use both sensors together in a prosthesis as a dual sensor which will enable simultaneous measurement of both synovial fluid pH and carbon dioxide levels which will be important in the diagnosis of infections and improve reliability of the sensor.

The falling bead synovial fluid viscosity sensor provides a simple way to determine prosthetic joint infections early by X-ray radiography by measuring the change in rate/ time taken for the bead to fall will be an indication of infections due to a decrease in viscosity during infections. The use of a reference fluid in a separate tube was also an important way

to improve viscosity resolution, especially near clinically determined viscosity thresholds. The sensor has the potential to be developed to provide noninvasive measurements of synovial fluid viscosity measurements in the detection of prosthetic joint infections, early.

The main advantage of the developed sensors is that they can be easily implemented in already available clinical settings, avoid the use of electronics or other complex instrumentation, and do not require special personnel for analyzing the data. The sensors can be attached easily to the prosthesis prior to implantation without any additional modifications to the already available commercial prosthesis. For hip infections, the pH and carbon dioxide sensor can be attached to the neck of the prosthesis so that the sensor will be in contact with synovial fluid. For the other joints, the sensor casing can be slightly modified to fit into the prosthesis joint. In the case of the viscosity sensor, sensor design can be modified to fit the joint of interest which would enable X-ray imaging of the sensor. Other advantages of the radiographic sensor approaches discussed in the dissertation include simplicity, speed (radiographs already routinely acquired), more reliable immersion in synovial fluid with no risk of dilution or drift between fluid removal and analysis, and easier repeated analysis compared to other methods of synovial fluid analysis.

In summary, the designed sensors are simple, easy to develop, manufacture, and integrate into clinical settings. Such an X-ray visualized synovial sensor has not been developed before and it has the potential to be expanded for other types of biomarkers as well by using a different stimuli-responsive hydrogel. The sensors functionalize plain radiography which will greatly facilitate clinical adoption with potentially transformative orthopedic applications for detecting, monitoring, and studying implant infections.

5.2. Future Work

Future work with regard to clinical applications, both the pH sensor and carbon dioxide sensor performance needs to be tested ex vivo and in vivo. The effect of tissue and bone on X-ray contrast in a patient can be determined by ex vivo imaging of sensor using human cadavers and similar results to the in vitro model are expected. Using the Hawkin's Surgical Innovation center, the sensor will be tested ex vivo in two human cadaver specimens to show that the measurements can be performed using a standard X-ray unit. The sensor will be attached to a prosthetic hip and implanted in a human cadaver. Via synovial capsule injections, the pH will be cycled from 6.9 to 7.4 and back, while X-ray images are acquired every 5 minutes. The two cadaver specimens will be radiographed sequentially. To measure interobserver variation, multiple physicians will report the position of a random selection of the images. Measurements can be made based on both the scale position and, more precisely, using a DICOM viewer. In a related cadaver study with a prototype pH sensor on a tibial plate;[4] the sensor accurately responded over a pH 4-8 range with less sensitivity around pH 7; nonetheless, it had a 30 min reversible response time and inter-observer variation corresponding to 0.1 units. Similar to the pH sensor, the interobserver reliability of the carbon dioxide sensor will be measured by determining the position of the tantalum bead from the X-ray images by multiple observers.

The sensor performance in vivo can be determined by implanting the sensors in a sheep infection model. The sensors can be designed so that both sensors will fit the neck of the prosthesis so that they will be in contact with the synovial fluid and simultaneous measurements of pH and carbon dioxide levels can be determined and compared. A

prepilot study will be used to validate the ability of the sensors to detect and report synovial fluid pH and carbon dioxide levels surrounding the neck of a hip prosthesis and confirm that the readings correspond to infection in vivo. Arthrocentesis will be carried out periodically during the study, to test the aspirated synovial fluid for pH (pH electrode), carbon dioxide (gas analyzer), for biomarkers of infection such as C-reactive protein (blood analyzer machine).

The animal use protocol for the pH sensor is already approved for testing the sensor performance in a sheep model. Various animal species have been used as models of human orthopedic pathologic conditions, including non-human primates, dogs, cats, pigs, cattle, horses, sheep, goats, rabbits, guinea pigs, rats, and mice.[5] Even though rats and mice are commonly used, due to their small size, they can only be used for studies involving basic orthopedics and require special instrumentation and surgical techniques.[5] Out of the other available animal models, sheep are commonly used in vivo experimental models in orthopedic research applications.[5–8] Domestic sheep are placid animals and allows dor easy handling during experiments. Their body weight similar to humans and sufficiently large to allow serial sampling and multiple experimental procedures. These features allow researchers to conduct a proper evaluation of orthopedic implants produced with dimensions for use in humans.[5,7]

For the pre-pilot study to ensure proper surgical placement and imaging and sensor performance in vitro, two sheep will be used, one as the control and the other infected. The sheep will be acquired from an appropriate vendor and housed at Godley-Snell Research Center (GSRC). Hip radiographs will be taken of each sheep before purchase to ensure the

sheep are able to accommodate the hip implant. Each sheep will undergo a complete physical examination including a radiographic assessment to ensure the femur can accommodate the prosthetic hip implant. The sheep will be acclimated for 10 days during which they will be trained on the measurement technique (standing radiographs taken on scale or pressure mat). Sheep will be weighed on the day of surgery to establish baseline and once per week thereafter and will be monitored for normal activity, food and water consumption and fecal and urine output. The sheep will be randomly treated unilaterally with a total hip replacement using a hip implant (Biomedtrix, USA) with the pH sensor and/or carbon dioxide sensor attached to it.[6] For one of the sheep, the implant with sensor will be inoculated in a region with *Staphylococcus aureus* (5000 cfu) before closing the incision. Post-surgery, standing X-ray images will be taken weekly for 10 weeks. Radiographs acquired to ensure proper implant positioning and integration using either the table-top or portable X-ray system. If necessary, the animal will be imaged under light anesthesia. Each week, arthrocentesis will be performed using aseptic technique, under anesthesia previously described, to collect synovial fluid samples (1 mL) and compare the sensor response to synovial fluid pH, CO_2 level, viscosity. After 10 weeks, sheep will be euthanized with commercial euthanasia solution and a terminal 10 ml blood sample obtained. We will analyze the blood for toxicity and/or inflammatory markers such as cytokines, C-reactive protein (CRP), and/or leukocyte count to inform us in the event of an infection or an inflammatory response. Synovial fluid will be drawn to analyze for infection biomarkers and pH. The sensors will be extracted and checked for sensor performance (accuracy, precision, reversibility, and response rate in alternating pH 7.5/6.5 buffers).

The 21-day pilot study will be performed with six sheep with 3 infected and 3 aseptic surgeries. In each sheep, a Biomedtrix prosthetic hip implant with the pH sensor and/or carbon dioxide sensor attached will be surgically implanted. Postoperatively, radiographic pH readings will be acquired, along with measurement of core temperature, serum CRP and ESR levels, synovial fluid WBC, and alpha defensin. In postmortem specimens, the histology and local chemical environment, and sensor performance will be analyzed. Based on prior literature, an initial pH drop of ~ 0.5 pH units in synovial fluid within 24 hours and continuing throughout the 3 weeks is expected. A 21-day trial was selected because most implant infections occur early, and the cut-off point for early infection is generally less than two weeks. The 3-week pilot study will allow us to observe restoration of pH after the initial acute inflammatory phase in week one but is not long enough for the infection to clear.

Periodic collection of blood samples from the sheep can be analyzed for serum non-specific markers of inflammation such as CRP levels and erythrocyte sedimentation rate (ESR), and arthrocentesis can be performed to aspirate synovial fluid samples which can be analyzed for synovial fluid pH, lactate and alpha-defensin to compare the levels in control and infected sheep. Postmortem, the pH near the implant will be compared with the radiographic measurements, and three sensors in each group will be incubated in pH 7.4 and 6.9 buffers to verify the calibration curve and measure the response rate. Histology will be performed to observe evidence for tissue growth, chronic inflammatory response, and/or infection.

For the falling bead synovial fluid viscosity sensor, the movement of the bead needs to be slowed down enough (a velocity of 1 mm/s in a 10 mPas viscous solution) for the determination of the position of the bead from X-ray images. The sensor design needs to be modified by using a porous tube in order for the diffusion of external synovial fluid. In vitro tests regarding the specificity of the sensor for viscosity and effect of surrounding external environment need to be assessed. In vitro studies need to be performed for the sensor using X-ray imaging. Following in vitro tests, the sensor will be attached to a prosthesis and X-ray images will be taken ex vivo in a cadaver model and in vivo in a sheep model.

5.2.1. CRP sensor

The pH sensor can be modified by replacing the pH-responsive hydrogel with an antigen responsive hydrogel that responds to the presence of a particular biomarker in synovial fluid. As a preliminary study, a C-Reactive protein (CRP) hydrogel was developed. C-reactive protein (CRP) is an acute-phase plasma protein and increases at sites of infection or inflammation.[9–11] CRP is produced as a homopentameric protein, which can irreversibly dissociate into five separate monomers at sites of infection or inflammation.[9,10] It is synthesized mainly in liver hepatocytes, and also by smooth muscle cells, macrophages, endothelial cells, lymphocytes, and adipocytes.[10,12] It is normally found at concentrations less than 10 mg/L in the blood.[10,11] During infectious or inflammatory disease states, CRP levels rise rapidly and peak at levels of up to 350–400 mg/L after 48 hours. Even though serum CRP levels are routinely analyzed for prosthetic joint infection

diagnosis,[13–15] they lack specificity for joint infections. Studies have shown local CRP levels in synovial fluid are a better biomarker of prosthetic joint infections, however, analysis is only possible by aspirating synovial fluid by arthrocentesis.[16–18] Therefore, a sensor to measure local CRP levels at the site of the infection itself using routinely available X-ray imaging will be useful in the diagnosis of prosthetic joint infections.

A biomolecule-responsive hydrogel with reversible swelling previously reported method by Miyata et al. will be used to design the CRP hydrogel.[19–21] Miyata *et al.* developed a bioconjugated semi-interpenetrating network (semi-IPN) hydrogel that could be actuated by antigen-antibody complexion between the rabbit immunoglobulin G (IgG) antigen and goat anti-rabbit IgG (GAR IgG) antibody. In this approach, an antigen-antibody semi-interpenetrating network hydrogel was synthesized consisting of polymer networks with antigens and linear polymers with antibodies. In design of the CRP responsive hydrogel, the rabbit immunoglobulin G (IgG) antigen was replaced with CRP, and goat anti-rabbit IgG (GAR IgG) antibody was replaced with CRP antibody.

In the preparation of the CRP sesnitive hydrogel, the antibody (Anti-CRP) was chemically modified by coupling it with N-succinimidyl acrylate (NSA) in phosphate buffer solution. NSA (0.4 mg) was added to a phosphate buffer solution (0.02 M, pH 7.4) containing Anti-CRP (100 mg), and the reaction mixture was incubated at 36 ˚C for one hour to introduce the vinyl groups into the Anti-CRP. The resultant vinyl(Anti-CRP) (570 mg) was added to acrylamide (AAm) (30 mg), with 0.01 mL of 0.1 M aqueous ammonium persulphate (APS) and 0.01 mL of 0.8 M aqueous N,N,N',N'-tetramethylethylenediamine (TEMED) as redox initiators. The copolymerization was performed at 25 ˚C for 3 h to

synthesize the polymerized Anti-CRP. Similarly, vinyl(CRP) was synthesized by modifying CRP (100 mg) with NSA (0.4 mg) in PBS (0.02 M, pH 7.4) and incubated at 36 ˚C for 1 hour. The resultant vinyl(CRP) (2.46 mg), AAm (82 mg) and N,N'-methylenebisacrylamide (MBAA) (0.1 weight% relative to AAm) as a crosslinker were dissolved in 600 mg of PBS containing the polymerized Anti-CRP. As soon as aqueous APS (0.01 mL, 0.1 M) and aqueous TEMED (0.01 mL, 0.8 M) were added into the mixture as redox initiators, the solution was injected into a reaction cell and polymerized at 25 ˚C for 3 h. After the polymerization, the resultant hydrogels were immersed in phosphate buffer to remove any residual chemicals and unreacted monomers. Polyacrylamide (PAAm) hydrogel was also prepared as a control by the redox copolymerization of AAm and MBAA in the presence of redox initiators.

Preliminary results of the CRP hydrogel showed swelling and deswelling in the presence and absence of antigen (Figure 5.1). The sensor will need to be optimized for clinically relevant response range and test its long-term stability in synovial fluid. The synovial fluid CRP sensor design would be similar to X-ray based discussed in the dissertation, with the responsive hydrogel with embedded radiopaque bead enclosed in a casing and attached to a hip prosthesis. After characterization of the sensor in vitro, X-ray imaging of sensor in cadaveric model will be carried out. In vivo studies to determine sensor performance will be performed in a sheep model.

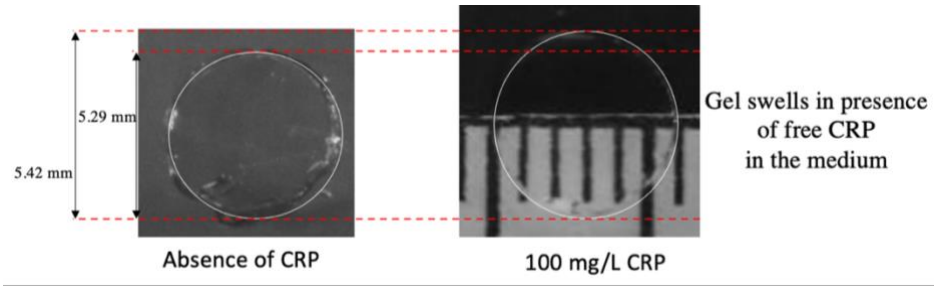

Figure 5.1: Preliminary results of response of CRP responsive hydrogel to external solutions of CRP.

5.2.2. Glucose sensor

A preliminary study was conducted to extend the hydrogel pH sensor to detect synovial fluid glucose by incorporating enzymes glucose oxidase and catalase. Normally, synovial fluid glucose levels are less than 10 mg/dL lower than serum levels.[23,24] Joint disorders that are classified as infectious demonstrate large decreases in synovial fluid glucose and can be as much as 20–100 mg/dL less than serum levels. The hydrogel will be modified by incorporating glucose oxidase and catalase enzymes. It is expected that due to oxidation of glucose to gluconic acid by glucose oxidase enzyme, there would be a decrease in the pH of the solution. Catalase enzyme is added to remove the produced hydrogen peroxide.

In the preparation of the glucose responsive hydrogel, since glucose oxidase and catalase enzymes did not dissolve in dimethylformamide (DMF), 70% ethanol was used to prepare the hydrogel. Glucose oxidase (3 mg) and catalase (3 mg) were dissolved first in 100 µL of water:DMF (70:30) solution. In a separate vial, the reagents for the preparation the polyacrylic acid hydrogel were mixed (10% acrylic acid, 5% n-octyl acrylate, 1%

polyethyleneglycol diacrylate, 0.1 % 2-oxoglutaric acid in DMF). The enzyme mix was then added dropwise to the hydrogel mix and a pale-yellow solution was obtained. The mixture was polymerized in a reaction cell, in a nitrogen atmosphere in a glove box under UV irradiation. The resultant hydrogels were washed with 70% ethanol.

In order to measure the response of the hydrogel to different glucose solutions, hydrogel disks were placed in different glucose concentrations and placed in an incubator at 37 ˚C. The preliminary results show that there is a change in the size of the hydrogel (0.562 mm) upon leaving the gels in a solution of glucose (Figure 5.2). This shows that the pH sensitive hydrogel could be improved by incorporating different molecular recognition elements to be specific to a particular biomarker for the detection, treatment, and progress of diseases. Incorporation of different molecular recognition elements to the pH sensitive hydrogel to sense multiple biomarkers that are useful in diagnosis of diseases.

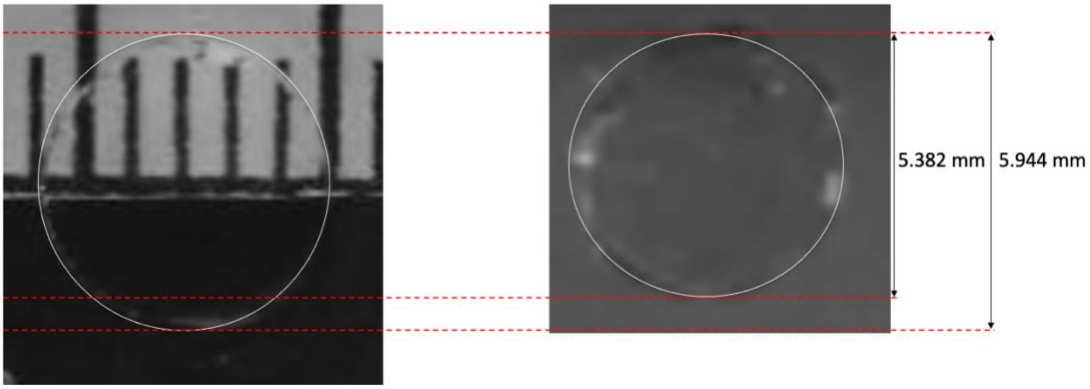

Figure 5.2: Polyacrylic acid hydrogel containing glucose oxidase and catalase, initial (left) and after leaving in glucose solution (right).

In summary, we developed and validated implantable sensors to radiographically measure various biomarkers of infection for early detection of prosthetic joint infections. The designed sensors are simple, easy to read and not limited to a particular disease condition and can be modifies to detect a broad range of diseases. The sensor is easily modified to any specific biomarker of interest for a particular disease condition. The approach promises to functionalize plain film radiography, providing local chemical analysis using ubiquitous infrastructure and standard of care procedures.

5.3. References

(1) Chen, H.; Rogalski, M. M.; Anker, J. N. Advances in Functional X-Ray Imaging Techniques and Contrast Agents. *Phys. Chem. Chem. Phys.* 2012, *14* (39), 13469. https://doi.org/10.1039/c2cp41858d.

(2) Gureyev, T. E.; Mayo, S. C.; Myers, D. E.; Nesterets, Ya.; Paganin, D. M.; Pogany, A.; Stevenson, A. W.; Wilkins, S. W. Refracting Röntgen's Rays: Propagation-Based x-Ray Phase Contrast for Biomedical Imaging. *J. Appl. Phys.* 2009, *105* (10), 102005. https://doi.org/10.1063/1.3115402.

(3) Arifuzzaman, Md.; Millhouse, P. W.; Raval, Y.; Pace, T. B.; Behrend, C. J.; Beladi Behbahani, S.; DesJardins, J. D.; Tzeng, T.-R. J.; Anker, J. N. An Implanted PH Sensor Read Using Radiography. *The Analyst* 2019, *144* (9), 2984–2993. https://doi.org/10.1039/C8AN02337A.

(4) Pelham, H.; Benza, D.; Millhouse, P. W.; Carrington, N.; Arifuzzaman, Md.; Behrend, C. J.; Anker, J. N.; DesJardins, J. D. Implantable Strain Sensor to Monitor

Fracture Healing with Standard Radiography. *Sci. Rep.* 2017, *7* (1), 1489. https://doi.org/10.1038/s41598-017-01009-7.

(5) Martini, L.; Fini, M.; Giavaresi, G.; Giardino, R. Sheep Model in Orthopedic Research: A Literature Review. *Comp. Med.* 2001, *51* (4), 8.

(6) El-Warrak, A. O.; Olmstead, M.; Schneider, R.; Meinel, L.; Bettschart-Wolfisberger, R.; Akens, M. K.; Auer, J.; von Rechenberg, B. An Experimental Animal Model of Aseptic Loosening of Hip Prostheses in Sheep to Study Early Biochemical Changes at the Interface Membrane. *BMC Musculoskelet. Disord.* 2004, *5* (1), 7. https://doi.org/10.1186/1471-2474-5-7.

(7) Potes, J. C.; Reis, J.; Capela e Silva, F.; Relvas, C.; Cabrita, A. S.; Simões. The Sheep as an Animal Model in Orthopaedic Research. *Exp. Pathol. Health Sci.* 2008, *2* (1), 29–32.

(8) Jakobsen, T.; Kold, S.; Baas, J.; Søballe, K.; Rahbek, O. Sheep Hip Arthroplasty Model of Failed Implant Osseointegration. *Open Orthop. J.* 2015, *9* (1), 525–529. https://doi.org/10.2174/1874325001509010525.

(9) Du Clos, T. W.; Mold, C. C-Reactive Protein: An Activator of Innate Immunity and a Modulator of Adaptive Immunity. *Immunol. Res.* 2004, *30* (3), 261–278. https://doi.org/10.1385/IR:30:3:261.

(10) Pepys, M. B.; Hirschfield, G. M. C-Reactive Protein: A Critical Update. *J. Clin. Invest.* 2003, *111* (12), 1805–1812. https://doi.org/10.1172/JCI200318921.

(11) Vashist, S. K.; Venkatesh, A. G.; Marion Schneider, E.; Beaudoin, C.; Luppa, P. B.; Luong, J. H. T. Bioanalytical Advances in Assays for C-Reactive Protein. *Biotechnol. Adv.* 2016, *34* (3), 272–290. https://doi.org/10.1016/j.biotechadv.2015.12.010.

(12) Salvo, P.; Dini, V.; Kirchhain, A.; Janowska, A.; Oranges, T.; Chiricozzi, A.; Lomonaco, T.; Di Francesco, F.; Romanelli, M. Sensors and Biosensors for C-Reactive Protein, Temperature and PH, and Their Applications for Monitoring Wound Healing: A Review. *Sensors* 2017, *17* (12), 2952. https://doi.org/10.3390/s17122952.

(13) Abad, C. L.; Haleem, A. Prosthetic Joint Infections: An Update. *Curr. Infect. Dis. Rep.* 2018, *20* (7), 15. https://doi.org/10.1007/s11908-018-0622-0.

(14) Osmon, D. R.; Berbari, E. F.; Berendt, A. R.; Lew, D.; Zimmerli, W.; Steckelberg, J. M.; Rao, N.; Hanssen, A.; Wilson, W. R. Diagnosis and Management of Prosthetic Joint Infection: Clinical Practice Guidelines by the Infectious Diseases Society of America. *Clin. Infect. Dis.* 2013, *56* (1), e1–e25. https://doi.org/10.1093/cid/cis803.

(15) Alijanipour, P.; Bakhshi, H.; Parvizi, J. Diagnosis of Periprosthetic Joint Infection: The Threshold for Serological Markers. *Clin. Orthop. Relat. Res.* 2013, *471* (10), 3186–3195. https://doi.org/10.1007/s11999-013-3070-z.

(16) Fink, B.; Makowiak, C.; Fuerst, M.; Berger, I.; Schäfer, P.; Frommelt, L. The Value of Synovial Biopsy, Joint Aspiration and C-Reactive Protein in the Diagnosis of Late Peri-Prosthetic Infection of Total Knee Replacements. *J. Bone Joint Surg. Br.* 2008, *90-B* (7), 874–878. https://doi.org/10.1302/0301-620X.90B7.20417.

(17) Deirmengian, C.; Hallab, N.; Tarabishy, A.; Della Valle, C.; Jacobs, J. J.; Lonner, J.; Booth, R. E. Synovial Fluid Biomarkers for Periprosthetic Infection. *Clin. Orthop. Relat. Res.* 2010, *468* (8), 2017–2023. https://doi.org/10.1007/s11999-010-1298-4.

(18) Stone, W. Z.; Gray, C. F.; Parvataneni, H. K.; Al-Rashid, M.; Vlasak, R. G.; Horodyski, M.; Prieto, H. A. Clinical Evaluation of Synovial Alpha Defensin and Synovial C-Reactive Protein in the Diagnosis of Periprosthetic Joint Infection. *J. Bone Jt. Surg.* 2018, *100* (14), 1184–1190. https://doi.org/10.2106/JBJS.17.00556.

(19) Miyata, T.; Asami, N.; Uragami, T. Preparation of an Antigen-Sensitive Hydrogel Using Antigen−Antibody Bindings. *Macromolecules* 1999, *32* (6), 2082–2084. https://doi.org/10.1021/ma981659g.

(20) Miyata, T.; Asami, N.; Uragami, T. A Reversibly Antigen-Responsive Hydrogel. *Nature* 1999, *399* (6738), 766–769. https://doi.org/10.1038/21619.

(21) Miyata, T.; Asami, N.; Uragami, T. Structural Design of Stimuli-Responsive Bioconjugated Hydrogels That Respond to a Target Antigen. *J. Polym. Sci. Part B Polym. Phys.* 2009, *47* (21), 2144–2157. https://doi.org/10.1002/polb.21812.

(22) Miyata, T.; Asami, N.; Uragami, T. A Reversibly Antigen-Responsive Hydrogel. *Nature* 1999, *399* (6738), 766–769. https://doi.org/10.1038/21619.

(23) Brannan, S. R.; Jerrard, D. A. Synovial Fluid Analysis. *J. Emerg. Med.* 2006, *30* (3), 331–339. https://doi.org/10.1016/j.jemermed.2005.05.029.

(24) Guenther, L. E.; Pyle, B. W.; Turgeon, T. R.; Bohm, E. R.; Wyss, U. P.; Schmidt, T. A.; Brandt, J.-M. Biochemical Analyses of Human Osteoarthritic and Periprosthetic

Synovial Fluid. *Proc. Inst. Mech. Eng. [H]* 2014, *228* (2), 127–139. https://doi.org/10.1177/0954411913517880.